Mathematical Modelling of Spread of Vector Borne Disease In Germany

DISSERTATION

zur Erlangung des akademischen Grades doctor rerum naturalium
(Dr. rer. nat.) im Fach Physik, Spezialisierung:
Theoretische Physik

eingereicht an der
Mathematisch-Naturwissenschaftlichen Fakultät
Humboldt-Universität zu Berlin

von
MS Suman Bhowmick

Präsident (komm.) der Humboldt-Universität zu Berlin
Prof. Dr. Peter Frensch

Dekan der Mathematisch-Naturwissenschaftlichen Fakultät
Prof. Dr. Caren Tischendorf

Gutachter
1. Prof. Dr. I. M. Sokolov, Humboldt-Universität zu Berlin
2. Prof. Dr. B. Lindner, Humboldt-Universität zu Berlin
3. Prof. Dr. B. Blasius, Carl von Ossietzky Universität, Oldenburg

Tag der mündlichen Prüfung: 14.03.2022

असतो मा साद गमय, तमसो मा ज्योतिर् गमय, मृत्योर मा अमृतम् गमय

DOI:https://doi.org/10.18452/25782

HUMBOLDT UNIVERSITY

Abstract

Faculty of Mathematics and Natural Sciences
Department of Physics

Dr. rer. nat.

Mathematical Modelling of Spread of Vector Borne Disease In Germany

by Suman Bhowmick

The objective of this thesis is to develop the necessary mathematical model to assess the potential spread of *West Nile Virus* (WNV) in Germany and employ the developed tool to analyse another tick-borne disease *Crimean-Congo Hemorrhagic Fever* (CCHFV).

Given the backdrop of global warming and the climate change, increasing temperature has benefitted the vector population. The increase in the temperature has a positive influence in the life cycle of the vector and the increase in its activities. In this thesis, we have developed an Ordinary Differential Equation (ODE) model system to understand the influence of the periodic introduction of infectious agents into the local susceptible population while taking account of influence of temperature. As results, we have found an analytic expression of the basic reproduction number (R_0) and its interplay with the temperature. The sensitivity analysis shows us the importance of the ratio between the susceptible mosquitoes to the local host population. As a central result we have extrapolated the temperature trend under different IPCC conditions and found the condition under which the circulation of West Nile Virus will be permanent in Germany.

The transmission of WNV is a spatiotemporal dynamic process. Different factors have an immense influence on the spatial spread. The movement of the interacting species is one of the key factors that facilitates the potential spread of the disease dissemination in new places. We have introduced a metapopulation model including both the vector and host movements. Our results have shown that it is necessary to include the vector movement as the vector movement speeds up the disease transmission process in the local host population. We have analysed the movement matrices of the vector-host population and mathematically derived the R_0 of the patchy model. Mathematically we have developed different control methods. We have simulated the possible geo-spatial spread of WNV on a map.

Furthermore, we have utilised the developed mathematical models to examine different scenarios under which CCHFV can potentially establish in a naive population along with we mathematically derived different control scenarios to manage the burden of tick infection.

Keywords: ODE, Epidemiology, Network, Metapopulation Model, Sensitivity Analysis

HUMBOLDT UNIVERSITY

Zusammenfassung

Faculty of Mathematics and Natural Sciences
Department of Physics

Dr. rer. nat.

Mathematical Modelling of Spread of Vector Borne Disease In Germany

von Suman Bhowmick

Ziel dieser Doktorarbeit ist ein mathematisches Modell zu entwickeln, um eine mögliche Ausbreitung des West-Nil-Virus (WNV) in Deutschland zu simulieren und zu bewerten. Das entwickelte Werkzeug soll auch auf eine weitere, durch Zecken übertragene Krankheit, dem Krim-Kongo-Hämorrhagischen Fieber (CCHFV) angewendet werden.

Die durch den Klimawandel verursachte globalen Erwärmung unterstützt auch die Verbreitung und Entwicklung verschiedener Vektorpopulationen. Dabei hat eine Temperaturerhöhung einen positiven Einfluss auf den Lebenszyklus des Vektors und die Zunahme der Vektoraktivität. In dieser Arbeit haben wir ein Differentialgleichungsmodell (ODE) entwickelt, um den Einfluss eines regelmäßigen Eintrags von Infektionserregern auf die empfängliche Population unter Berücksichtigung des Temperatureinflusses zu verstehen. Als Ergebnis haben wir einen analytischen Ausdruck der Basisreproduktionszahl (R_0) und deren Wechselwirkung mit der Temperatur gefunden. Eine Sensitivitätsanalyse zeigt, wie wichtig das Verhältnis der anfälligen Mücken zur lokalen Wirtspopulation ist. Als ein zentrales Ergebnis haben wir den zukünftigen Temperaturverlauf auf Basis der Modellergebnisse des IPCC in unser Modell integriert und Bedingungen gefunden, unter denen es zu einer dauerhaften Etablierung des West-Nil-Virus in Deutschland kommt.

Die Übertragung des WNV ist ein räumlich-zeitlicher dynamischer Prozess. Verschiedene Faktoren haben einen wesentlichen Einfluss auf die räumliche Ausbreitung. Die räumliche Bewegung der an der Infektionskette beteiligten Arten ist einer der Schlüsselfaktoren, welche eine räumliche Ausbreitung des Virus ermöglicht und erleichtert. Wir haben ein Metapopulationsmodell entwickelt, welches sowohl die Vektor- als auch die Wirtsbewegungen umfasst. Unsere Ergebnisse haben gezeigt, dass es notwendig ist, die Vektorbewegung einzubeziehen, da die Vektorbewegung den Krankheitsübertragungsprozess in der lokalen Wirtspopulation beschleunigt. Dazu haben wir unser Modell um ein sogenanntes Patchy-Modell erweitert, die Bewegungsmatrizen der Vektor-Wirt-Population analysiert und den R_0 Wert Modells mathematisch abgeleitet. Wir haben auf mathematische Art verschiedene Kontrollstrategien überprüft und haben die räumliche Verbreitung von WNV auf einer Karte dargestellt. Darüber hinaus haben wir die entwickelten mathematischen Modelle verwendet, um verschiedene Szenarien zu untersuchen, unter denen sich CCHFV möglicherweise in einer naiven Population etablieren kann, und wir haben verschiedene Kontrollszenarien

mathematisch abgeleitet, um die Belastung von einer Infektion durch Zecken zu bewältigen.

Schlagwörter: ODE, Epidemiologie, Netzwerk, Metapopulationsmodell, Sensitivitätsanalyse

Acknowledgements

First of all, I would like to thank Prof. Franz J. Conraths, Dr. Jörn M. Gethmann and Dr. Hartmut H. K. Lentz for their endless support and for providing me with the opportunity to work independently on a compelling topic. Additionally, I would like to thank Prof. Igor M. Sokolov for providing numerous progenitive ideas and discussions, in pertinent with the predictions of establishment West Nile Virus in Germany and spatial extension of our mathematical model.

The muse of this thesis originates in two different places: Humboldt-University of Berlin and the Friedrich-Loeffler-Institute (FLI) in Insel Riems, Greifswald. Concerning my working schedule in the FLI, I am indebted to Jörn for his constant encouragement and providing explanations in the fields of epidemiology and disease dynamics. He has always been a pillar of support while I'm having doubts to understand the basic biology and entomology. I would like to convey my special gratitude towards Hartmut who taught me how to develop the critical thoughts about the modelling hypothesis and development, while introducing me to the field of network science and spatial models. His never ending skepticism has helped me to improve my coding skill significantly. I thank Franz for his endless support and enthusiasm to explore beyond the problem of mosquito-borne disease and endorsing the fruitful discussions with Cornelia Silaghi to develop the models for tick-borne diseases. I would like to acknowledge the gratification that I received while having the discussion with the colleagues from FLI, especially Christoph, Patrick, Nikolai, Thorstein, Carolina, Carola and Ronald. Ronald and Patrick made sure that I remain sane to be productive enough to understand the GIS and enjoy the beauty of *Norddeutschland*. The interaction with Thorstein beyond the topics of epidemiology has always been cherishable. Amicable interactions and the much needed help have always been a hallmark of our secretary Sonja. My travel-mate Filip has been an awesome argumentative colleague to deal with along with Irene who brought the Spanish flavour to the FLI. All those days away from home as well as the routine mornings and evenings in the *grandpa* bus and through the *schaden straße* to the FLI could not have been the same without the CuliFo project members. Thanks to Niko, Chris, Nils who kept me engaged in the BBQ on the weekends. Much kudos to Pedro for keeping me focussed. Thanks to Naeem, Faruk, Saiful for the weekend cricket, even in the midst of winter and Ali for interesting conversation and discussion.

During my PhD I had the opportunity to travel to various conferences, workshops and to interact and exchange ideas with many experts and leaders in the field of network science. In particular, I thank Ralf Wieland, Philipp Hövel, Dirk Brockmann, Gina Polo. All afternoons spent at TU Physics group have been also a lot of fun, thanks to Andreas, Jason and Philipp. Gym sessions after the long brainstorming sessions were really enjoyable.

All the time spent at HU Physics has been great fun particularly thanks to Robert and Flavio. I also sincerely thank Prof. Igor Sokolov for teaching me how to think like a physicist rather than a mathematical biologist. During numerous zoom calls, he construed the topics ranging from anomalous diffusion to metapopulation-network models. Thanks to his experience and wiseness I was able to learn independently the skills necessary to make all the work that culminated in this thesis.

I have been lucky to have many mentors in my life who have led me down the path to pursue science. Rana D. Parshad, Kathleen Kavanagh, Erik M. Bollt and Joseph Skufca, Tom A. Langen taught me about the complex system, mathematical modelling, and biology when I was a student at Clarkson. I would like to express my gratitude to Rana who has always been an inspirational figure to introduce me to the field of mathematical biology and epidemiology. I would like to thank Emmanuel, Aladdin and John for being patient and helpful towards me. Donald family will remain close to my heart, especially Jacob who has been a great brother to me. I will appreciate your effort Thomas, you have been a phenomenal person to me. Matthew and Mike had been true mates to me. Thanks Garegin for bringing little Armenia with you.

My previous mentors Swaroop Nandan Bora, K. V. Srikanth, Shrihari Sridharan, Ritumoni Sarma who taught me PDE, applied analysis in IIT Guwahati that directed me toward mathematical modelling later on. I would like to appreciate the effort Pushpendu Jana took to teach me the basics of coding and applied mathematics in Scottish Church College.

I would like to thank Ramu aka "Samvar", Lasoon, Maalik for being so generous with me and providing me constant encouragement to understand the mathematics behind every details.

Finally, I want to thank my parents, especially my sisters who have been the reason who I am and where I am. I would like to acknowledge my thankfulness to Olga who has provided the necessary company to continue this journey in an entirely new country without knowing the local language. Thank you Maryna for sustaining my tantrums and still being patient with me, I really appreciate that. Thank you Germany.

Contents

List of Figures

List of Tables

List of Abbreviations

ODE	**O**rdinary **D**ifferential **E**quation
PDE	**P**artial **D**ifferential **E**quation
WNV	**W**est **N**ile **V**irus
WNF	**W**est **N**ile **F**ever
CCHF	**C**rimean **C**ongo **H**emorrhagic **F**ever
CCHFV	**C**rimean **C**ongo **H**emorrhagic **F**ever **V**irus
MBD	**M**osquito **B**ourne **D**isease
TBD	**T**ick **B**ourne **D**isease
IE	**I**ntegral **E**quation
GIS	**G**eographical **I**nformation **S**ystem
SI	**S**usceptible **I**nfected
SIR	**S**usceptible **I**nfected **R**ecovered
SEIR	**S**usceptible **E**xposed **I**nfected **R**ecovered
DFE	**D**isease **F**ree **E**quilibrium
SSIM	**S**tructural **S**imilarity **I**ndex
DFE	**D**isease **F**ree **E**quilibrium
NGM	**N**ext **G**eneration **M**atrix

Dedicated to those teachers who taught me how to think

CHAPTER 1

Introduction

1.1 Epidemics and Modelling

Disease is an important aspect of one specie's evolution. It paves the way to make sure the survival of the fittest. In the ancient time, the Hindus, the Israelites had dealt with the life threatening plagues ("Plague in Ancient India" 1899; Zias, 1991). Throughout history, people from different civilisations believed that epidemics carry ethereal messages. Epidemic has always touched people's life. Often it paved its way towards a serious issue for societies and therefore, the comprehension and hence to predict its clutch in the society became a research subject of paramount interest.

In the medieval time, the spread of black death from Asia throughout Europe in waves is estimated to have caused the death of around one-third of the population of Europe and later it was followed by Great Plague of London in 1665–1666 (Brauer, 2017). Although the work presented (Noble, 1974) is comparatively simpler in the current modelling framework, but it was indeed an influential effort. The initial attempts to give a mathematical form to the potential spread of smallpox by D. Bernoulli in 1760 is well documented in the works of (Hethcote, 2000) .

The early 20^{th} century witnessed the inception of modern mathematical advancement in modelling the epidemics (Serfling, 1952). In 1906 (Hamer, 1906), a discrete-time model was developed and then in 1911 a continuous ordinary differential equation (ODE) (Ross, 1911) model was constructed to understand the spread of Malaria in India. The seminal works conducted by Kermack and McKendrick (Kermack, McKendrick, and Walker, 1927), See Tillett (Tillett, 1992), for the discussion on mathematical models that combine epidemiological data and other data and the usefulness of such an analytic framework for the evaluation of public health strategies. In (Kermack, McKendrick, and Walker, 1927), the authors first derived the existence of an epidemic threshold i.e. a disease requires a crucial infection rate beyond which the disease can spread. Modelling of infectious disease became a primary scientific research ground after the release of the influential book of Bailey, 1957. With the passage of time, the modelling efforts in the spread of infectious agents incorporate different aspects like demographic structures, age structures, disease-vectors and quarantine (Hethcote, 2000). Additionally, the usage of game theory in the vaccine strategies is commendable (Bauch and Earn, 2004). Using Partial Differential Equations (PDE) to model the dissemination of epidemics is a useful modelling technique to

understand the spread of disease in the space (Capasso, 2008). The availability of the accessible contact data of the host in recent years has brought in higher resolution to understand the mixing patterns (Mossong et al., 2008). Network analysis and metapopulation analysis have become necessary tools to retrieve the adequate information on the spread of disease (Wasserman and Faust, 1994). Well known mathematical concepts ranging from Graph theory (Bollobás, Saito, and Wormald, 1985) to cellular automata (Fu and Milne, 2003) are being applied to the disease modelling as there has been a link amongst the individuals who are associated with their capacity for the spread of epidemic (Keeling and Eames, 2005).

In the midst of growing population, the demand for the foods also have increased multifold and this has caused the rapid growth of industrialised animal, poultry farming. Livestock and the poultry epidemics are the major economic losses in the modern day economy. For example, the foot-and-mouth disease in the UK had brought severe economic losses and problems (Kitching, Hutber, and Thrusfield, 2005). In order to deal with the infectious diseases in the poultry and the livestock, various mathematical methods from the human epidemiology have been utilised. Network analysis also has been successfully employed to monitor the possible outbreaks and to mitigate the outbreaks while accounting the livestock trade movement data (Christley et al., 2005; Kao et al., 2006; Dubé et al., 2011; Bakran-Lebl et al., 2016). Metapopulation models which exhibit the analogy with the different farms or habitat patches can ideally be the appropriate choices for the modelling attempt (Hess, 1996; Keeling et al., 2010a). These collective modelling endeavours can provide necessary tools to support for the proper planning of surveillance and vaccination strategies in livestock disease management.

The modelling endeavours in epidemiology can be divided into two categories: data driven predictive-forecast models and the conjectural models with the bolster from the theoretical aspects. Predictive models amalgamate the necessary information pertaining to the disease for the purpose of forecasting, whereas the conjectural models are being utilised in the context to apprehend the basic principles, characteristics of the spreading mechanism. Lucidly speaking, these models try to capture the know-how of the dissemination process in the population. In this kind of modelling effort, often the modeller makes use of elementary assumptions to construct the local dynamics and aims for the macroscopic picture of the process. Conjectural-theoretical models are akin to the models in mathematical physics or theoretical physics for the purpose of perusal of the proposed problem aligned with certain conjectures or assumptions. However, during the course of such modelling attempt, often many details of the real problem- such as individual behaviour, infection pathways etc are being approximated with proper reasons for the purpose of constructing a mathematically tractable and feasible model.

In this effort, we have utilised the conjectural models in combinations with the real weather data in order to gain the necessary insights of course of a disease outbreak in Germany.

1.2 Building Blocks of Epidemic Modelling

Modelling attempt through Ordinary Differential Equation (ODE) has grown into a crucial factor in epidemiology, where the ODE models are employed to facsimile the interactions amongst the individuals of a homogenous or stratified population. Besides, working as a building block in epidemiological modelling, ODEs can imitate the transiting health status of populations which change continuously. A complex model of an epidemic dissemination combines multiple operational aspects of disease transmission. ODE based complex systems of models are flexible; virtually any number or type of operational compartments can be combined into one single model system. Modern ODE based models are quite ubiquitous and elementary in nature and often employed to construct more complex models of systems. As an analogy, we can often perceive the local ODE equations as a brick of a house which is a complex model system. Reviews on such modelling effort can be found in (Keeling and Rohani, 2008; Diekmann and Heesterbeek, 2000).

The mathematical roots of continuous ODE based model go back to (Kermack, McKendrick, and Walker, 1927; Kermack, McKendrick, and Walker, 1932; Kermack, McKendrick, and Walker, 1933). These works had built the modern day foundations of mathematical modelling endeavours based on ODE model systems. These works had an immense influence on the development of mathematical models of disease spread and still applicable. In these seminal works, the main assumptions are that population remain constant and disease induced death is being included. This is compatible with the course of an epidemic being brief compared with the life time of an individual. Compartmental models for the disease transmission have turned out to be a helpful tool to predict the disease progression and the potential to evaluate the public health policies and interventions. Commonly speaking, compartmental models describe the disease dissemination through a population of concern by identifying the rates of progression of a populace from susceptible to, infected with and recovered from the disease. There might be some intermediate stages too. The authors in (Capasso and Paveri-Fontana, 1979) developed a simple deterministic mathematic model to decipher the spread of Cholera in a town and it gave some good suggestions like sanitation, hygiene practices for the public health policies.

The transition rate from the susceptible state to the infected state is often termed as the force of infection or incidence rate and the transition rate from the state of infected to recovered from disease is termed as the recovery rate (Liu, Hethcote, and Levin, 1987). Usually the incidence rate is often considered as a bilinear term but there has been a significant explorative work regarding alternative nonlinear incidence rates. These alternative forms of incidence rates are usually expanded to characterise the behaviour, such as crowding of infected individuals or avoidance or the saturations (Liu, Hethcote, and Levin, 1987; Ruan and Wang, 2003; Alexander and Moghadas, 2005; Driessche and Watmough, 2000) or to include the multi-stage infections (Krylova and Earn, 2013).

The potential and the confirmed role played by the environmental variables and climatic conditions in shaping the course and the progress of an epidemic is well understood. Infectious disease can be influenced by the climatic conditions through their effects on abundance of the vectors such as mosquitoes (Rogers and Randolph, 2006) and ticks or the survival of

pathogens outside the host (Lowen et al., 2007). Thereupon, the global warming, changes in the climate due to the anthropogenic reasons affect the burden of infectious diseases (Metcalf et al., 2017; McMichael, Woodruff, and Hales, 2006). So, it is of utmost important to accommodate such weather driven factors into the modelling efforts to understand potential and the confirmed shape of the epidemics.

The heterogenous influence of climate shift on temperature and precipitation may have readily effect on the spread of various disease, especially the disease like West Nile Fever, Dengue etc. Temperature influences on the temporal changes in vector development, vector activity (Mulatti et al., 2014; Hartley et al., 2012; Spanoudis et al., 2018; Lalubin et al., 2013). Consequently, the risk of mosquito-borne diseases such West Nile Fever (WNF) also follows a seasonal pattern that correlates with temperature. WNV is is a neurotropic mosquito-borne virus which belongs to the Flavivirus genus (Colpitts et al., 2012). WNV is maintained by an enzootic cycle which includes birds and ornithophilic mosquitoes of the Culex genus and the Culex pipiens complex from the same genus is considered the most important vectors in Europe (Kramer, Li, and Shi, 2007; Zeller and Schuffenecker, 2004). Some birds are among the most competent amplifier hosts as they develop enough serum viremia to infect efficiently feeding mosquitoes (Dohm, O'Guinn, and Turell, 2002). In the backdrop of global warming and the current climatic situation, it appears that WNV is expanding its geographical range in Europe, while triggering an increase in the numbers of epidemics or sporadic cases in birds, humans and equines (Semenza and Suk, 2018; Veronesi et al., 2018; Barrett, 2018).

The impact of the temperature and the other climatic factors have been studied at the continental level and for selective countries in Europe (Morin and Comrie, 2013; Harrigan et al., 2014; Marini et al., 2018; Rubel et al., 2008; Abdelrazec and Gumel, 2017;). However, at the country level the effect of rising temperature and coupling of seasonality are not analysed systematically. Moreover, it is evident that the directed and periodic spread of WNV into a naive population can possibly be described by the feasible roles of a transporting agent (e.g. migratory birds) which introduces the WNV into that population. The following unanswered questions remain:

- What is the impact of rising temperature on the potential infection dynamics?
- What is the impact of migrating birds on the infection dynamics in the concerned places?

We address these questions in Chapter 2, where we derive a model for infection dynamics of WNV incorporating the potential role of the migratory birds in Germany.

There have been significant eco-epidemiological and public health-related questions pertaining to infectious disease transmission where the spatial component is very important. In that situation, a simple mechanistic model can not possibly explain the spatial features of disease dissemination. Although the ODE models discussed above while including the environmental factors provide a powerful tool to understand and predict the course of epidemics locally (Mordecai et al., 2017; A. Rvachev and Longini, 1985; Kraay et al., 2018; Heffernan, Smith, and Wahl, 2005; Kioutsioukis and Stilianakis, 2019;

Ewing et al., 2016; Yu, Madras, and Zhu, 2018; Bhowmick et al., 2020; Cailly et al., 2012; Eikenberry and Gumel, 2018; Tien and Earn, 2010; Lessler and Cummings, 2016), these models often can not bring the necessary information related to the potential spread or the influx of the infection from the surrounding habitat patches. During the spread of an epidemic, often the propagation reveals that the effect of influx of infected population from one habitat patch to another one is very significant. Therefore, the analysis of spatial spread of epidemic has drawn a significant attention during the last years. It is quite essential to represent the locale of hosts and the course of transmission while taking account of spatially heterogenous interventions. In few occasions, the location of the host (plants) is well defined but for the animals and humans, it is better to average the mobility. Fundamental works on spatial models can be found in (Tuite et al., 2011; Bengtsson et al., 2015; Murray, Stanley, and Brown, 1986; Murray and Seward, 1992; Keeling and Grenfell, 1998; Capasso and Maddalena, 1981; Viboud et al., 2006; Thieme, 1977; Gilarranz, 2020; Riley et al., 2015).

There are different classes of deterministic spatial models that can be described according to different modes of infection spread, host-vector distributions, and their interactions. Distinct models can be called upon as an individual-based model, metapopulation model, or network-based model. Individual-based models (Espíndola et al., 2011; Perez and Dragicevic, 2009) explicitly represent every individual host while governed by some set of rules and simulation algorithm and usually computationally heavy. Through metapopulation models one can track the number of the interacting populations at different locations according to their health status. Often, in this modelling effort, the underlying assumption is that each location is connected to some or all other patches (Keeling et al., 2010a; Watts et al., 2005; Keeling and Gilligan, 2000; Gog, Woodroffe, and Swinton, 2002; Colizza and Vespignani, 2008; Colizza et al., 2006; Juher, Ripoll, and Saldaña, 2009). In case of network based model, commonly each node can be defined as an individual host and is connected to a small subset of other hosts (Keeling, 2005; Volz and Meyers, 2009; Barabási and Albert, 1999a; Bajardi et al., 2011; Kiss, Miller, and Simon, 2017; Pastor-Satorras et al., 2015).

It is often difficult to analyse the data from those ODE based models that don't include the spatial aspect and then it is challenging to find the aggregated spatial attributes of epidemic transmission such as wave. Additionally, with the advent of modern day technologies and available high spatial resolution data, it is generally required to include the spatial spread to plausibly explain the observed data.

For this reason, a significant amount of modelling work has been done to understand the spread of the epidemic has taken the refuge of spatial modelling approaches. In the first instance, nonlinear Integral Equations (IE) were used to describe the final state of the epidemic in a spatial model and it was a generalisation of D. G. Kendall's pandemic threshold theorem (1957). Different types of spatial models including the metapopulation models formulated as a set of simple ODEs or Stochastic Differential Equations (SDEs) or IEs are employed to investigate the geographical spread of disease (Thieme, 1977; Marcati and Pozio, 1980; Mockus, 1998).

It is to be noted that the previously mentioned deterministic modelling efforts do not necessarily make disjoint sets of efforts. We can represent each

habitat patch as a node and the connecting strength is being governed by some algorithm.

What is still missing in the context of spatial spread of WNV in Germany is the closed mathematical framework to accommodate the multi-species model. As a central element, this framework must include the spatial structure and ability to predict the potential probable cases of WNV in Germany.

Main questions in this context are the following:

- What might be the possible course of WNV transmission in Germany?
- How can we formally represent the spatial features of the potential spread of WNV in Germany?
- What could possibly be the mitigation strategies?

We address these questions in Chapter 4, after introducing a spatial deterministic metapopulation model formulated as a set of locally temperature driven ODE model in Chapter 2 while including the network features.

The model is able to answer the above posed questions. We believe that providing such a model contributes a key element to construct other various mathematical models.

Beyond the mosquito-borne diseases (MBD), there is an effort to utilise the same deterministic modelling approach to understand the tick-borne diseases (TBD). It is to be noted that while modelling MBD and TBD, mathematical approaches and formal modelling paths are similar with the exception of the TBD. In TBD, the modelling effort is more challenging due to the presence of multiple transmission routes (Hoch, Breton, and Vatansever, 2018; Hoch et al., 2016; Matser et al., 2009). Another aspect that utilises one assumption is that ticks are capable to infect their potential hosts in their lifecycle. With the purpose to model the transmission dynamics of the ticks, it is often assumed that various life stages of the ticks will delay the transmission but the qualitatively speaking the potential transmission dynamics will remain the same in the equilibrium (Rosà and Pugliese, 2007).

As a key factor, this framework must incorporate the modelling assumptions and the necessary tools to include the different transmission routes.

Fundamental queries in this subject are the following:

- What are the sensitive parameters for the potential spread of disease (CCHFV in our case)?
- What are the control measurements for the different geographical regions?
- What is the burden of various transmission routes in different countries?

We put on an effort to answer to the above said queries in Chapter 5. It is our understanding that the modelling effort can potentially be exploited to expand and to include the environmental variables and different age structures.

CHAPTER 2

Mathematical Theory

In this chapter, we recapitulate the mathematical formalism that is being employed to model infectious disease and metapopulation-network models. We describe the mathematical framework to analyse the epidemics, metapopulation-network models and put an effort to draw the outline of several relevant results of earlier research. We address these models in Sections 2.2 and in Section 2.3. These sections give an overview over some important results of modern metapopulation-network theory.

2.1 Mathematical Models in Epidemiology

In prior to the formulation of the models for the spread of epidemic, we shall distinguish between conjectural-theoretical and forecasting-predictive data driven models. Conjectural-theoretical models are utilised to accommodate conceptual findings such as the threshold values or testing theories or to get the insight of the disease mechanism whereas the predictive models are employed to understand different facets of the disease transmission that contribute to predict the certain spreading process. These kinds of models can be utterly complex and computationally heavy and beyond of this thesis, hence we concentrate in the usage of theoretical models. In the following sections we briefly report some basic mathematical properties of different epidemic models.

2.2 Deterministic Mathematical Models

The main objective of this section is to give a prelude on the basics of deterministic compartmental modelling through implementation. Here, we reformulate some well known models and try to derive their solutions. The population is subdivided according to their health status and the subdivided populations are termed as *compartments*. We discuss about the employment of such compartments to describe the fundamental models in the field of epidemiology.

2.2.1 SI

Let us assume a population of N individuals. In the simplest setting, the health status of each individual is either susceptible (S) or infected (I).

Birth or death in the population is neglected. Susceptible individuals get infected, if they are in contact with an infected individual. Here, the classes susceptible and infected are termed as compartments as described before and the increase in the infected compartment follows the local reaction scheme:

$$S + I \mapsto 2I$$

Assuming that α is the infected rate through which new susceptible become infected, we obtain the corresponding differential equation model

$$\begin{aligned} \frac{dS}{dt} &= -\alpha SI \\ \frac{dI}{dt} &= \alpha SI \end{aligned} \tag{2.1}$$

where S and I are the numbers of susceptible and infected individuals respectively. The model Eq. (2.1) is called SI-model. The total population is $N = S + I$. Therefore, Eq. (2.1) can be reformulated as:

$$\frac{dI}{dt} = \alpha(N - I)I, \tag{2.2}$$

i.e. a logistic differential equation. Hence, in the limit $t \to \infty$ the whole population is infected ($I(\infty) = N$) eventually. A solution of the model system Eq. (2.1) is shown in the Fig. 2.1

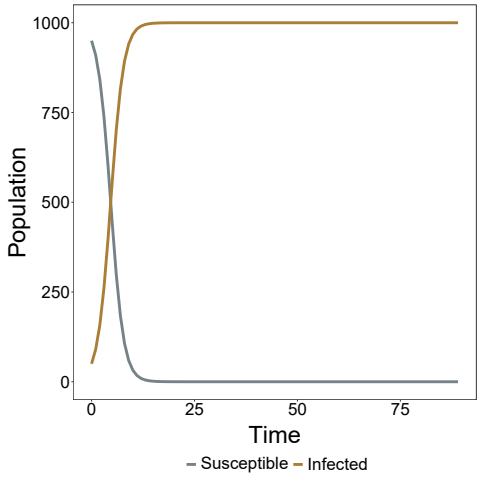

FIGURE 2.1: Solution of the susceptible-infected (SI) model Eq. (2.1). Parameters: $\alpha = 0.1$, $N = 1000$, $S(0) = 950$, $I(0) = 50$.

2.2.2 SIR

In contrast to the infection mechanism introduced in the previous section, many epidemics actually accommodate an immunised state, where these immunised individuals have no contribution in the disease spread. Such examples can be found in (Kermack, McKendrick, and Walker, 1927; Kermack, McKendrick, and Walker, 1932; Kermack, McKendrick, and Walker, 1933). In such situation, individuals recover from the disease after being infected for a certain period of time. This characteristic is modelled by

introducing an additional compartment for the recovered population. The infection scheme is then extended to include the recovered compartment as susceptible-infected-recovered (SIR) and the model system can be formulated as:

$$\begin{aligned} \frac{dS}{dt} &= -\alpha SI \\ \frac{dI}{dt} &= \alpha SI - \gamma I \\ \frac{dR}{dt} &= \gamma I \end{aligned} \tag{2.3}$$

where S, I and R are the numbers of susceptible, infected and recovered individuals respectively. The model Eq. (2.3) is called SIR-model and α is the infection rate and γ is the recovery rate. A typical solution of Eq. (2.3) is shown in the Fig. 2.2.

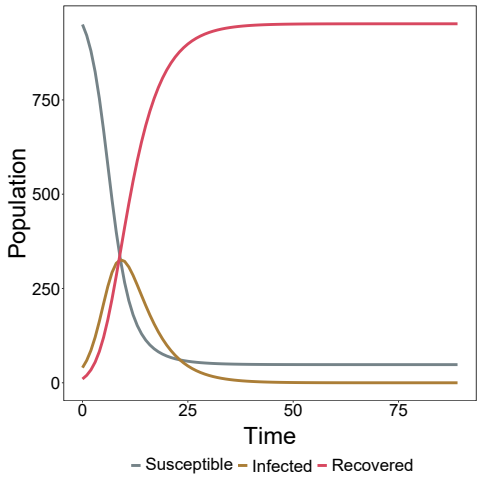

FIGURE 2.2: Solution of the susceptible-infected-recovered (SIR) model Eq. (2.3). Parameters: $\alpha = 0.1$, $\gamma = 0.02$, $N = 1000$, $S(0) = 950$, $I(0) = 50$, $R(0) = 0$.

There is no closed form solution for the system Eq. (2.3), but some fundamental conclusions can be obtained analytically.

This SIR model Eq. (2.3) show more complex features compared to the SI model Eq. (2.1). Let us assume $(S(0), I(0), R(0))$ is the initial condition. We first analyse the fixed points of the system, i.e. (S^*, I^*, R^*) where

$$\frac{dS^*}{dt} = -\alpha S^* I^* = 0, \quad \frac{dI^*}{dt} = \alpha S^* I^* - \gamma I^* = 0, \quad \frac{dR^*}{dt} = \gamma I^* = 0 \tag{2.4}$$

It follows from the last equation that $I^* = 0$ at the fixed point, where the values of S^* and R^* should follow this relationship $S^* + R^* = N$. Therefore, $(S^*, 0, R^*)$ is a fixed point. In the early phase of an infection, the stability of the fixed point can be analysed in the following manner. All the individuals are susceptible in the inception and consequently $I^* = N - S^*$. An outbreak can occur, iff $dI/dt > 0$, i.e.

$$\frac{dI}{dt} = \alpha S^*(N - S^*) - \gamma(N - S^*) = (N - S^*)(\alpha S^* - \gamma) > 0. \tag{2.5}$$

It readily follows from Eq. (2.5) that the number of infected grows, if

$$\alpha S^*/\gamma > 1. \tag{2.6}$$

Eq. (2.6) is crucial in epidemiology as it describes a threshold for the potential spread of an infection. This dimensionless metric is called the *Basic Reproduction Number* R_0. Recall that $S \approx N$ in the fixed point in the beginning of the epidemic. Thus, it follows that the condition for an outbreak is

$$R_0 = N\frac{\alpha}{\gamma} > 1. \tag{2.7}$$

A dimensionless quantity of central importance in the field of epidemiology is the so-called basic reproduction number, R_0, which is the expected number of new infections engendered by a single infected individual introduced into a fully susceptible population. One of the main goals in epidemiology to curtail the magnitude of R_0 under the critical value $R_0 = 1$. It can readily be observed that from Eq. (2.7) that this can be achieved through reducing the infection rate α or by increasing the recovery rate γ through proper treatment.

When we analyse the late phase of the SIR dynamics, we can observe the difference between the SI model described in Section 2.2.1 with the SIR model. In case of an SIR like outbreak does not necessarily infect the whole population, even if $R_0 > 1$. The reasoning can be attributed to the fact that there is a critical mass of susceptible individuals in order to keep an infection alive Eq. (2.6). The accumulated number of infected individuals in an infection process is disposed of the number of recovered at the end of the infection as every recovered has to be in the infected state in the first place. An important measure throughout this work is therefore the *outbreak size* R_∞.

To compute the outbreak size, we deal with the second fixed point of Eq. (2.3), i.e. the fixed point for $t \to \infty$. At this stage of the infection, there are no infected and a fraction of the population is recovered. So, the fixed point is given by $(N - R_\infty, 0, R_\infty)$. A straightforward way to obtain the outbreak size R_∞ is to use the model equations in Eq. (2.3) and compute the following differential

$$\frac{dS}{dR} = -\frac{\alpha}{\gamma}S$$

and separate the variables This gives us the following integrals

$$\int_{S^*}^{N-R_\infty} \frac{dS}{S} = -\frac{\alpha}{\gamma}\int_{R^*}^{R_\infty} dR.$$

We integrate from the initial condition at $t = 0$ to the final condition at $t \to \infty$, where $S_\infty = N - R_\infty$. Using that $R^* = 0$ at $t = 0$ gives

$$R_\infty = S^* - Se^{-\frac{\alpha}{\gamma}R_\infty} \tag{2.8}$$

This transcendental equation can be solved numerically using a Newton-Raphson technique.

Additionally, if $S(0) = N$, then $N - S(\infty)$ is the final size of the outbreak and the fraction ultimately infected is $f = \frac{R(\infty)}{N} = 1 - \frac{S(\infty)}{N}$. In terms of the

latter, we get

$$R_0 = -\frac{\log(1-f)}{f} \tag{2.9}$$

The following shows the relationship between final size and R_0:

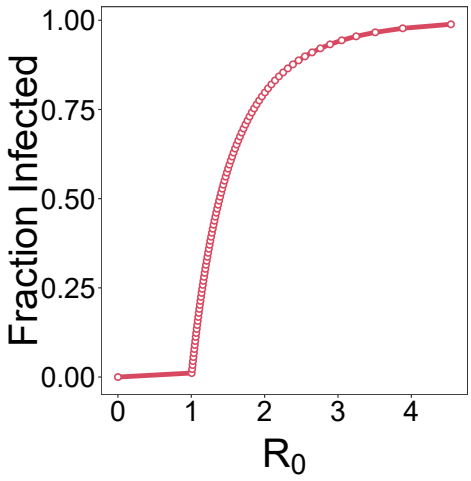

FIGURE 2.3: Relative outbreak size vs. basic reproduction number. Note that even for supercritical R_0 the outbreak size is in general smaller than the total population.

The analysis of the late phase of an epidemic also yields information about potentially infected and recovered populations. Let us consider the second equation of Eq. (2.3).

$$\frac{dI}{dt} = \alpha SI - \gamma I \tag{2.10}$$

In the late phase of an SIR-type epidemic, the fraction of infected is actually small. Given sufficiently large values of R_0, the fraction of susceptible is also small in this phase (see Fig. 2.3). Thus, we neglect the quadratic term in Eq. (2.10). This gives $\frac{dI}{dt} = -\gamma I$, which yields

$$I(t) = I(0)e^{-\gamma t}. \tag{2.11}$$

Therefore, the infection decays exponentially for large t and the inverse recovery rate $1/\gamma$ defines the characteristic time of the epidemic.

An SIS model is also conceptually similar to an SIR model with the difference where the infected individuals return to the susceptible state after a certain period. SIS and SIR model share similarities as they're both single-event model. The main difference is that SIS models show an endemic state for $t \to \infty$, i.e. both S and I take finite values in the long term so that fraction of infected remains in the system permanently.

2.2.3 SEIR

For certain crucial infections, there is a significant incubation period during which the susceptible individuals are infected but not yet infectious themselves. Over that time period, the individual is in compartment E (for exposed). There is a difference between infected and infectious, in general. Categorically, infected individuals are invaded by a pathogen and act as

hosts for its multiplication. On the contrary, only the *infectious* individuals can infect others and infected individuals are not necessarily infectious (Rolle and Mayr, 2006). The infection mechanism is now extended to include the exposed compartment as susceptible-exposed-infected-recovered (SEIR) and the model equation can be formulated as:

$$\begin{aligned} \frac{dS}{dt} &= -\alpha SI \\ \frac{dE}{dt} &= \alpha SI - \gamma E \\ \frac{dI}{dt} &= \gamma E - \mu I \\ \frac{dR}{dt} &= \mu I \end{aligned} \tag{2.12}$$

where S, E, I and R are the numbers of susceptible, exposed, infected and recovered individuals respectively. The model Eq. (2.12) is called SEIR-model and α is the infection rate and γ is the incubation rate, μ is the recovery rate. A typical solution of Eq. (2.12) is shown in the Fig. 2.4.

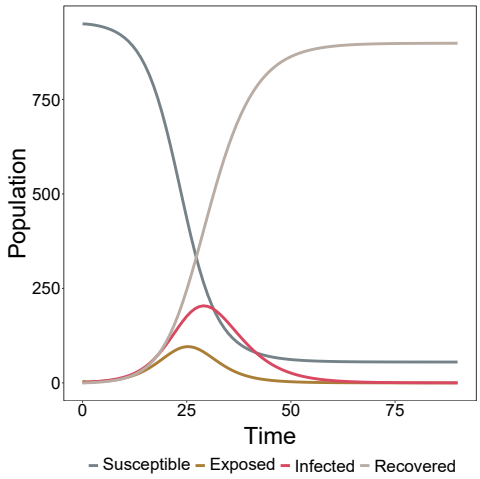

FIGURE 2.4: Solution of the susceptible-infected-recovered (SIR) model Eq. (2.12). Parameters: $\alpha = 0.1$, $\gamma = 0.5$, $\mu = 0.2$, $N = 1000$, $S(0) = 950$, $E(0) = 40$, $I(0) = 5$, $R(0) = 5$.

Here, the basic reproduction number can be explained as the product of four elements and can be expressed as:

R_0 = (Number of contacts per unit time)(Disease transmission per contact) (Duration of infection) (Surviving exposed stage). Additionally, it can also be interpreted through the product of model parameters as infection rate of one person in a population of S_0 susceptible (where S_0 is the initial susceptible population) multiplied with mean time in I.

2.2.4 Next Generation Matrix

The basic reproduction number R_0 is arguably the most important metric in the field of epidemiology. It is a quantity that helps to provide insight for emerging infectious diseases in outbreak situations. Its value provides the necessary information when designing control interventions for established

infections. From a theoretical perspective R_0 plays a vital role in the analysis of stability of the infectious disease models. In the frame work of mathematical epidemiology, one can divide the population into a finite number of discrete categories and can construct a matrix that includes the numbers of newly infected individuals in the various categories in consecutive generations. This matrix, usually denoted by $\mathcal{K}$, is termed as the next-generation matrix (NGM). It was introduced in (Diekmann, Heesterbeek, and Metz, 1990) who defined R_0 as the dominant eigenvalue of $\mathcal{K}$.

The disease dynamics are produced by a system of nonlinear ordinary differential equations (ODEs) that describes the changes with time for all sub-populations. To compute R_0, one can use the states that apply to infected individuals i.e. to begin with those equations ascribing the production of new infections and the changes in the states amongst the infected individuals. This can be defined as the infected subsystem. The first step is to linearise the infected nonlinear subsystem about the disease-free equilibrium (DFE). Epidemiologically speaking, this process reflects that the potential for initial spread of an infectious agent when it is introduced into a fully susceptible population and this is what characterises R_0. One can decompose this Jacobian matrix ($\mathcal{K} = \mathcal{F} + \mathcal{V}$) into two parts: $\mathcal{F}$, where $\mathcal{F}$ is the transmission matrix (describing the production of new infections) and $\mathcal{V}$ is the transition matrix (describing changes in state). The next step is to compute the dominant eigenvalue or, the spectral radius ρ of the matrix $-\mathcal{F}\mathcal{V}^{-1}$. However, this decomposition described in (Diekmann, Heesterbeek, and Roberts, 2010) and later in (Driessche and Watmough, 2000; Driessche and Watmough, 2002) do not typically lead to the NGM as introduced in (Diekmann, Heesterbeek, and Metz, 1990). The reason can be attributed to the fact that the decomposition relates to the expected off-spring of individuals of any epidemiological state and not just only epidemiological newborns. As an example, an exposed state and a consecutive infectious state are both considered to be infected states but the switching from the exposed state to infectiousness does not involve a new infection occurring. This may lead to confusion. To distinguish, we call $\mathcal{K}_{\mathcal{L}} = -\mathcal{F}\mathcal{V}^{-1}$ as the NGM with large domain. One must bear with the fact that $\rho(\mathcal{K}_{\mathcal{L}}) = \rho(\mathcal{K})$. Usually, the dimension of $\mathcal{K}$ is lower than that of $\mathcal{K}_{\mathcal{L}}$, and it makes the computations to find R_0 is easier. In some cases, a further dimension reduction is possible. It happens when $\det(\mathcal{K}) = 0$ and is termed as lower-dimensional matrix the NGM with small domain, and denote it by $\mathcal{K}_{\mathcal{S}}$. In this case also $\rho(\mathcal{K}_{\mathcal{S}}) = \rho(\mathcal{K})$.

In a nutshell, we can write down the formula to find $\mathcal{K}_{\mathcal{L}}$, $\mathcal{K}$ and $\mathcal{K}_{\mathcal{S}}$ as following:

$$\mathcal{K}_{\mathcal{L}} = -\mathcal{F}\mathcal{V}^{-1} \tag{2.13}$$

$$\mathcal{K} = \Psi^t \mathcal{K}_{\mathcal{L}} \Psi \tag{2.14}$$

Where where Ψ is an arbitrary matrix composed of unit column vectors (e_i) such that the ith row of the transmission matrix is not zero.

For the small domain, the transmission matrix ($\mathcal{F}$) is scaled into two separate vectors (Ω, Λ). A row vector (Ω), and a column vector (Λ) are defined to satisfy $\mathcal{F}_{ij} = \Omega_i \Lambda_j$ and

$$\mathcal{K}_{\mathcal{S}} = -\Omega \mathcal{V}^{-1} \Lambda \tag{2.15}$$

2.2.5 Climate Variability and Seasonality

In contrast to the elementary models described in Sections 2.2.1, 2.2.2, 2.2.3, quite often the model parameters are explicitly or implicitly depend on different climatic variables. Seasonal patterns in disease dynamics exhibit pronounced variability across different geographical regions, showing single or multiple peaks at different times of the year. Multiple mechanistic models of disease transmission have included rainfall as a driver by focusing on multiple possible transmission pathways and the inclusion of other weather factors (Lemaitre et al., 2019; Baracchini et al., 2017; Siraj et al., 2017; Rinaldo et al., 2012; Chowell et al., 2019). Various studies give evidence of a link between vector-borne disease outbreaks and climate driven weather anomalies (Morand et al., 2013). In case of modelling, the simple SIR model (Eq. (2.12)) always predicts the damped oscillations towards pathogens extinctions if the magnitude of R_0 is too small and this is at odds with the recurrent outbreaks observed in many real pathogens (Babad et al., 1995; Conlan and Grenfell, 2007). Seasonal force of epidemics due to the climate driven factors are the main factor to keep the disease cycle alive and kicking as well as the seasonal contact rates to facilitate the epidemics cycle. In the simplest settings we can observe the consequences of this by considering a sinusoidal forcing on α according to $\alpha(t) = \alpha_0(1 + \alpha_1 \cos(2\pi t))$ in the model Eq. (2.3) with the vital dynamics i.e. including the birth and death. Then we have the following system of ODEs:

$$\begin{aligned} \frac{dS}{dt} &= \mu N - \alpha(t)SI - \mu S \\ \frac{dI}{dt} &= \alpha(t)SI - \gamma I - \mu I \\ \frac{dR}{dt} &= \gamma I - \mu R \end{aligned} \tag{2.16}$$

with μ being the birth and death rates (which we assume to be equal), and N is the total population. It is to be noted that the model Eq. (2.16) is not a SIR rather it is a generalisation of SIR model Eq. (2.3).

We should keep in mind that the individuals are born in the S-state, and can die in any state. The birth and death rates are set equal to maintain the constant population size.

A typical solution of Eq. (2.16) is shown in the Fig. 2.5.

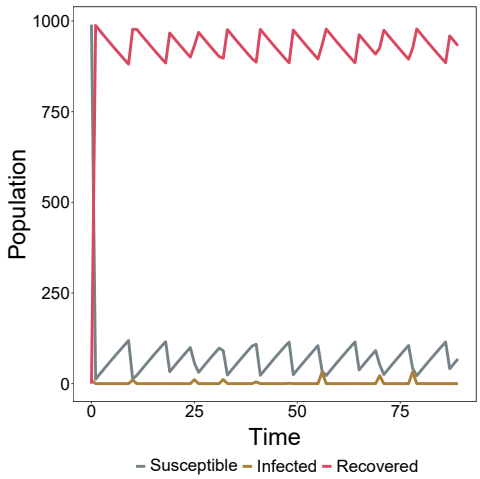

FIGURE 2.5: Solution of the susceptible-infected-recovered (SIR) model Eq. (2.16). Parameters: $\mu = 1/70$, $\alpha_0 = 400$, $\alpha_1 = 0.6$, $\gamma = 365/14$, $N = 1000$, $S(0) = 990$, $I(0) = 10$, $R(0) = 0$.

2.2.6 Differential-Difference Models

The models presented in Sections 2.2.1, 2.2.2, 2.2.3 illustrate only the very basic characteristics of epidemic dynamics. However, it is also one of the main aim in the field of epidemiology to have an understanding of the modes of the transmission dynamics. The transmission dynamics can lean on the detailed structures and causes complex mechanism. Often this dynamics is not continuous and suffers from several discontinuities like irregular vector activities, host behaviour, the movements or, the migration of vector-host species.

Differential-difference model has recently gathered plethora of applications because of its ability to describe many real life problems from fluid mechanics to ecology. In fact, the differential-difference model is particularly preferable to depict discontinuous phenomenon and is the preferred model to describe the interplay of the continuous and discontinuous processes (Cooke, 1963; Bellmann, 1963). In this section we shall outline some of the main features and application before proceeding to the next section on the spatial models.

Seasonal appearance and then the disappearance of pathogens is actually a complex phenomenon. This mechanism can facilitate the pathogens either to persist or to extinct in the long term. In different eco-epidemiological scenario, the wet winter and spring growing seasons alternate with the hot, dry summers, during which the host species grows and it can help to increase the activities of the vector. In this condition the usage of differential-difference modelling approach is more suitable to describe the punctuated seasonality of this system and multi host-pathogens or vector system. In the transmission season, ODE models are the effective model governing the multi-population interactions and in the dormant season the population growth and the multi-population interactions are described by the difference equations (Moore et al., 2011a; Borer et al., 2009; Borer et al., 2007).

Continuous ODE model systems can give a reasonable description of the transmission in a continuous scenario but during the punctuated seasonal

transmission, mathematical models constructed with the help of the Differential Difference model system are closer to reality compared to the ODE model only. We will notice the employment of such modelling technique in the Section 2. In spite of providing specific knowledge about the potential outbreaks, locally based ODE models are not feasible enough to include the flow and transportation of the infectious agents or pathogens and to model the spatial transmission of epidemics. In the next section, we briefly report important results in the complex metapopulation network research and focus on the interplay between the metapopulation network and epidemics in Section 2.3.

2.3 Spatially extended models

Abundant number of biological and biophysical systems show characteristics at multiple spatial, temporal or population scales (Herring, 1991). Coarser methods such as PDE, IE are typically fast to simulate and easy to code. These methods can include a spatial structure. Whilst in that scale, many individual-level details that required low concentration or small spatial scale. However, to simulate at such individual level throughout a large domain is computationally is very challenging.

This spatial dimension acts as a crucial agent in many eco-epidemiological phenomena as we understand that things are distributed through space in a heterogeneous manner and thus creating differentiation, segregation and discontinuities. If we select the geometric approach then we can potentially use the functionalities of a geographic information system (GIS) in order to create the connections amongst the different layers of information pertaining to the sundry aspects of the eco-epidemiological phenomena to study and to establish the evidences of possible spatial regularities in this work. Each of the spatial models has its own specific advantages and integrates in its own way the spatial features of the eco-epidemiological phenomena being studied. While the statistical approach concentrates on the covariation mechanisms of the eco-epidemiological phenomena, and therefore, space can be included in the analysis as the statistical mean. Dynamical models can incorporate spatial features like landscape data, water bodies, etc that act in similar ways to intervene as a frame for the studied objects and also through interacting features of the models. Hence connecting the dynamics of different interacting entities. When the cellular automata are employed to represent geographic space, the main driving force of the change is spatial as any potential change can be measured based on the neighbourhood configuration. Each of these modelling frameworks can be used with the goal of describing, exploring or explaining. The lines that separate these approaches are not always simple to distinguish and depend actually on the researchers.

2.3.1 Metapopulation models

The models and the results discussed are so far based on a single habitat patch i.e. modelled on a single dwelling region and the disease dynamics are contained in a single zone. In several systems, however, the internal contact features are unknown, but the contacts amongst the different subpopulations can be made available or readily available for the further analysis. A subpopulation can assume to be a city in a mobility network, an agricultural

holding in a livestock trade network or a habitat in ecology, for example. A metapopulation is a set of subpopulations which can be connected by migration process (Grenfell and Harwood, 1997; Hanski, 1998). Recent literatures have revealed the profuse usage of metapopulation approaches to model large scale disease outbreaks (Bajardi et al., 2011; Colizza et al., 2006; Colizza and Vespignani, 2008; Lentz, Selhorst, and Sokolov, 2012), such as influenza (Balcan et al., 2009) and SARS (Hufnagel, Brockmann, and Geisel, 2004).

The computation of outbreak thresholds in the context of metapopulations was addressed in (Arino, 2017; Arino, Ducrot, and Zongo, 2012; "Diseases in Metapopulations"; Colizza et al., 2006; Colizza and Vespignani, 2008). The impact of the movement matrices on disease spread in metapopulations was addressed in (Lentz, Selhorst, and Sokolov, 2012) Although metapopulation approaches provide a useful tool for the modelling of epidemics, they systematically overestimate the outbreak size when compared to individual resolved approaches (Keeling et al., 2010b).

In the backdrop of epidemics every subpopulation has a different infection status, i.e. a distribution of S, I and R (Please see the Fig. 2.6).

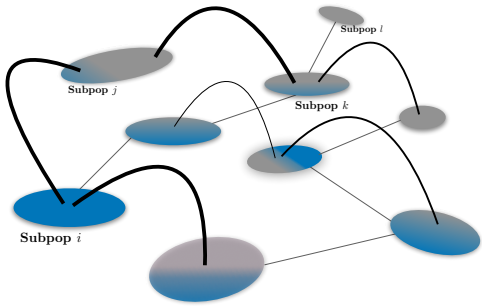

FIGURE 2.6: Several metapopulations i, j, k and l of different size and infection status. The infection status is represented by the local colour distribution. The edges (i, j), (k, l) indicate migration from i to j and k to l respectively.

In the context of local infection model, we incorporate a migration term so that the general from of an SIR-infection-model can be formulated for a subpopulation i as

$$\frac{dI_i}{dt} = F(S_i, I_i, R_i) + M(S_i, I_i, R_i, S_j, I_j, R_j, \tau) \tag{2.17}$$

The first term F in Eq. (2.17) is a *local reaction* term, while the *migration* M to other subpopulations could depend on the local distribution and the infection status of other subpopulations connected to i. Additionally, the migration between subpopulations could occur on a time-scale τ different from the time-scale of the local infection. The impact of these time-scales on disease spread was analysed in (Lentz, Selhorst, and Sokolov, 2012). We investigate the interplay between metapopulation-network properties and disease outbreaks in Section 4.

CHAPTER 3

West Nile Virus Spread in Germany - Local Spread Model

This chapter contains the materials from the paper: "Locally temperature - driven mathematical model of West Nile Virus spread in Germany" (Bhowmick et al., 2020).

3.1 Background Story

In this chapter we formulate an ODE based dynamic model to describe the spreading process of WNV in the presence of migratory birds in Germany. WNV is an arthropod-borne virus (arbovirus) transmitted by the bites of infected mosquitoes. It can also infect horses and humans. In some cases it can be fatal too. Birds are actually the natural reservoir, and humans and other mammals are dead-end hosts who do not have any active role in circulating the disease. In 2018, WNV detected for the first time in Germany and there has been a reported case of seroconversion of an exposed veterinarian. So it readily shows the importance of evaluation of the circumstances, under which WNV may establish in Germany or in some zones of Germany. Thus it paves the way for the modelling endeavour.

3.2 Introduction

The main vector responsible for spreading WNV among birds and from birds to humans and mammals are mosquitoes of the *Culex pipiens* complex (Zeller and Schuffenecker, 2004). Many European countries have an abundance of *Culex pipiens* and *Culex pipiens s.l./C. torentium* mosquitoes, which are effective WNV vectors and these vectors are also present in Germany and the susceptibility is well documented in (Ziegler et al., 2019). During the last couple of years, there have been severe outbreaks in the Balkan area (Bakonyi et al., 2013; Escribano-Romero et al., 2015).

Temporal changes in vector development, vector activity and the WNV transmission potential (Mulatti et al., 2014; Hartley et al., 2012; Spanoudis et al., 2018; Lalubin et al., 2013) are all influenced by temperature. In the current climatic situation, it appears that WNV is expanding its geographical range in Europe, while escalating an increase in the numbers of epidemics or sporadic cases in birds, humans and equines (Semenza and Suk,

2018; Veronesi et al., 2018). Global warming may speed up the transmission of WNV infections in the coming years (Barrett, 2018).

The active role played by the migrating birds in introducing new viruses to Europe has often been shown (Calistri et al., 2010). Migratory birds can possibly carry viruses northward to their breeding sites in Europe when they get the infection during the spring migration. In (Michel et al., 2018), the authors have reported WNV neutralising antibodies against WNV in migratory birds in Germany.

The numbers of reported cases of WNV in animals and humans are shown in Fig. 3.1. It seems that there is a constant rise in the reported incidence of both animal and human cases in the EU, as well as there is a possible dissemination of cases to the new locations.

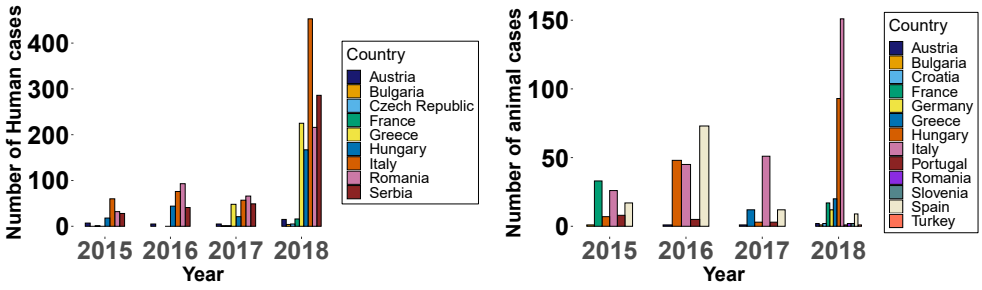

(A) (B)

FIGURE 3.1: (A) Human cases and (B) animal cases.

In the present chapter, we model the dynamics of WNV transmission using an ODE based compartment model, where each population is represented as groups of susceptible, exposed, infected and recovered accordingly to their health status. Such modelling paradigm is a popular choice amongst the mathematical modellers and this type of model have been used already to model different vector borne diseases (Wonham, De-Camino-Beck, and Lewis, 2004; Castillo-Chavez et al., 2002) while incorporating also seasonality and weather driven factors (Lou and Zhao, 2010; Wang and Zhao, 2017; Abiodun, Witbooi, and Okosun, 2017; Okuneye, Abdelrazec, and Gumel, 2018; Rubel et al., 2008; Laperriere, Brugger, and Rubel, 2011) to make it more feasible. It is known that migratory birds are a reservoir of WNV and can introduce the virus to Europe (Peterson, Vieglais, and Andreasen, 2003; Figuerola et al., 2008; Bakonyi et al., 2006) during the migration period. Therefore, we model the dynamics of the infection process as well as the population dynamics of vectors and hosts, the latter including migratory birds after following the footsteps of (Bergsman, Hyman, and Manore, 2016).

3.3 Mathematical model

We use an SEI (susceptible - exposed - infected) type model for the mosquito species as vectors for WNV. For the birds species, we use an SEIR (susceptible - exposed - infected - recovered) model. We include logistic growth in the interacting population. For the population dynamics, we use the following

equation

$$\begin{aligned} \frac{dP}{dt} &= (b-m)\left(1-\frac{P}{K}\right)P, \\ \implies \frac{dP}{dt} &= \left(b-(b-m)\frac{P}{K}\right)P - mP, \end{aligned} \tag{3.1}$$

where P stands for the population (bird or mosquito), and b, m and K stand for birth rate, death rate and carrying capacity, respectively.

Life cycle of a mosquito comprises of both aqueous and terrestrial stages but the transmission process (biting) happens only in the terrestrial stage. So, we consider only this stage of the mosquito life cycle. Additionally, the life cycle of a mosquito is primarily temperature driven. Therefore, the main driving parameters of the model are all explicitly temperature dependent. The transmission mechanism of WNV is a continuing cycle between mosquitoes and birds. A vector (mosquito) bites an infected host (bird) and gets infected by WNV after having a blood meal and the virus amplifies within the host and is transmitted to another birds. Other vertebrates are dead-end hosts and they do not have active role in spreading WNV. The birds can develop clinical disease, e.g. encephalitis, but the infection may also remain inapparent (Gamino and Höfle, 2013; Michel et al., 2018). That is why we divide the infected bird population into *clinical* and *subclinical* birds. We assume that the subclinical birds will remain susceptible to the disease even after they recover from WNV, while birds that survive a clinically manifested WNV infection are considered protected from re-infection. In addition, we include migratory birds in the model. They act in a similar manner like the local birds, but periodically introduce the disease from other endemic areas.

A summary of the infection cycle is given in Fig. 3.2.

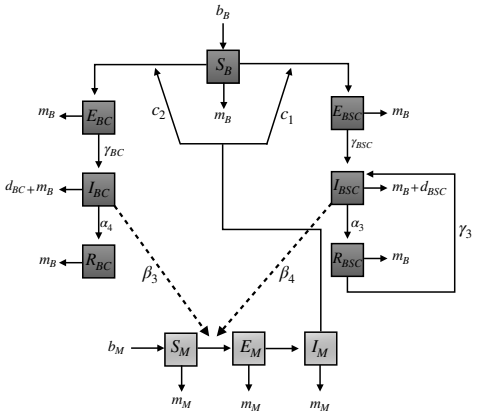

FIGURE 3.2: Infection cycle in mosquitoes (vector) and birds (host) populations. The bird population is divided into clinical (BC) and subclinical (BSC) birds. All compartments include birth b and mortality m rates.

3.3.1 Compartment Model

For the *mosquitoes* that serve as vectors for WNV, we use the following system of ordinary differential equations (ODEs):

$$\begin{aligned}
\frac{dS_M}{dt} &= (b_M N_M - m_M S_M)\left(1 - \frac{S_M}{K_M}\right) - \frac{c_2 S_M I_{BC}}{K_B} \\
&\quad - \frac{c_1 S_M I_{BSC}}{K_B} \\
\frac{dE_M}{dt} &= \frac{c_2 S_M I_{BC}}{K_B} + \frac{c_1 S_M I_{BSC}}{K_B} - \gamma_M E_M - m_M E_M \\
\frac{dI_M}{dt} &= \gamma_M E_M - m_M I_M,
\end{aligned} \tag{3.2}$$

where S_M, E_M and I_M represent the *susceptible, exposed* and *infected* mosquito population, respectively. The total mosquito population is given by $N_M = S_M + E_M + I_M$. Transmission parameters are c_1 from infected subclinical local birds to the mosquitoes and c_2 from infected clinical local birds to the mosquitoes. An overview over all parameters and their values is given in Table A.1.

Please note that crucial parameters of the system Eq. (3.2) are all temperature dependent. This applies for the birth rate, $b_M = b_M(T)$, and mortality rate, $m_M = m_M(T)$, as well as the transmission coefficients $c_1 = c_1(T)$ and $c_2 = c_2(T)$. We choose the functional relationships for $b_M(T)$ and $m_M(T)$ according to (Laperriere, Brugger, and Rubel, 2011; Rubel et al., 2008). The extrinsic-incubation period ($\gamma_M(T)$) for mosquitoes are also temperature dependent (Reisen, Fang, and Martinez, 2006; Dohm, O'Guinn, and Turell, 2002; Kilpatrick et al., 2008; Eldridge, 1968; Rubel et al., 2008), where T represents the temperature. We have not included the hibernating phase of the adult blood feeding mosquitoes to keep the model simple (Eldridge, 1968; Spielman, 2001).

Similar to the mosquito population, we model the dynamics of the *local bird* population using the following system of equations:

$$\begin{aligned}
\frac{dS_B}{dt} &= \left[b_B - (b_B - m_B)\frac{N_B}{K_B}\right] N_B - m_B S_B - \frac{(\beta_3 + \beta_4) I_M S_B}{K_B} \\
\frac{dE_{BC}}{dt} &= \frac{\beta_4 I_M S_B}{K_B} - m_B E_{BC} - \gamma_{BC} E_{BC} \\
\frac{dE_{BSC}}{dt} &= \frac{\beta_3 I_M S_B}{K_B} - m_B E_{BSC} - \gamma_{BSC} E_{BSC} \\
\frac{dI_{BC}}{dt} &= \gamma_{BC} E_{BC} - m_B I_{BC} - \alpha_4 I_{BC} - d_{BC} I_{BC} \\
\frac{dI_{BSC}}{dt} &= \gamma_{BSC} E_{BSC} - m_B I_{BSC} - \alpha_3 I_{BSC} + \gamma_3 R_{BSC} - d_{BSC} I_{BSC} \\
\frac{dR_{BC}}{dt} &= \alpha_4 I_{BC} - m_B R_{BC} \\
\frac{dR_{BSC}}{dt} &= \alpha_3 I_{BSC} - \gamma_3 R_{BSC} - m_B R_{BSC},
\end{aligned} \tag{3.3}$$

where we distinguish between clinical (BC) and subclinical (BSC) birds. For the local bird population, S_B, E_{BC}, E_{BSC}, I_{BC}, I_{BSC}, R_{BC}, R_{BSC}, N_B stand for susceptible, exposed (clinical and subclinical), infected (clinical

and subclinical), recovered (clinical and subclinical) and the total bird population, respectively. As above, the remaining parameters are explained in Table A.1.

The wild bird population is a natural reservoir for WNV (Reed et al., 2003a; Malkinson et al., 2002). It is known that migratory birds also may have an active role to the spread of WNV along their paths of migration (Rappole and Hubálek, 2003; López et al., 2008). Observational studies indicate that individuals infected with WNV may delay the departure for the migration and therefore, increase the persistence of the disease (Rappole and Hubálek, 2003). In our current work, we include the possible introduction of WNV into the local bird population by migratory birds in Germany.

The appearance of migratory birds is rather a complex seasonal phenomenon. We imitate this mechanism by modelling the presence of migratory birds in the summer months, while their population size is set to zero in winter. The hypothesis we assume is that the migratory birds are active for the season of migration and after that their active population becomes zero. Given a migration period τ of half a year and setting the day of migration to Germany $\tau_0 = 0$, migrating birds are present, if, $\tau \in [2\tau, 2\tau+1]$ with $\tau \in \mathbb{N}_0$. Consequently, we set the compartments $S_{Bm} = E_{Bm} = I_{Bm} = R_{Bm} \equiv 0$, if $\tau \notin [2\tau, 2\tau + 1]$ (the compartments are similar to the local birds compartments). Migrating birds might return to Germany from endemic areas in every season. So, we introduce a single infected migrating bird into Germany every season of migration.

Once migratory birds are present in Germany, we assume that they behave like the local bird population and they have an active role as a spreader of WNV. Therefore, we use a similar model for migratory bird population 3.4 as we do for the local bird population in Eq. (3.3). Our model includes local and migratory birds for one location and incorporates seasonality as described by (Moore et al., 2011b). The resulting model system is a Difference-ODE model system. We obtain the following equation system for the *migratory bird* population:

$$\begin{aligned}
\frac{dS_{Bm}}{dt} &= \left[b_{Bm} - (b_{Bm} - m_{Bm})\frac{N_{Bm}}{K_{Bm}}\right] N_{Bm} - m_{Bm}S_{Bm} \\
&\quad - \frac{\beta_5 I_M S_{Bm}}{K_{Bm}} \\
\frac{dE_{Bm}}{dt} &= \frac{\beta_5 I_M S_{Bm}}{K_{Bm}} - m_{Bm}E_{Bm} - \gamma_{Bm}E_{Bm} \\
\frac{dI_{Bm}}{dt} &= \gamma_{Bm}E_{Bm} - \alpha_9 I_{Bm} - m_{Bm}I_{Bm} - d_{Bm}I_{Bm} \\
\frac{dR_{Bm}}{dt} &= \alpha_9 I_{Bm} - m_{Bm}R_{Bm}.
\end{aligned} \tag{3.4}$$

Due to the inclusion of migratory birds, the equations for the mosquito population Eq. (3.3) have to be modified to include the potential role of the

migratory birds in spreading WNV. For the mosquito population we get

$$\begin{aligned}
\frac{dS_M}{dt} &= (b_M N_M - m_M S_M)\left(1 - \frac{S_M}{K_M}\right) - \frac{c_2 S_M I_{BC}}{K_B} \\
&\quad - \frac{c_1 S_M I_{BSC}}{K_B} - \frac{c_3 S_M I_{Bm}}{K_{Bm}} \\
\frac{dE_M}{dt} &= \frac{c_2 S_M I_{BC}}{K_B} + \frac{c_1 S_M I_{BSC}}{K_B} + \frac{c_3 S_M I_{Bm}}{K_{Bm}} - \gamma_M E_M - m_M E_M \\
\frac{dI_M}{dt} &= \gamma_M E_M - m_M I_M
\end{aligned} \tag{3.5}$$

Table A.1 summarises all the associated model parameters of equations Eq. (3.3), Eq. (3.4) and Eq. (3.5). The transmission coefficients c_1, c_2, c_3, β_3, β_4, β_5 are considered as the product of the biting rate and the probability of transmission between mosquito to bird and bird to mosquito according to refs. (Laperriere, Brugger, and Rubel, 2011; Rubel et al., 2008).

3.4 Basic Reproduction Number R_0

Basic reproduction number R_0 is an epidemiological metric that contains the necessary information about the parameter conditions for a disease to persist in the population. If $R_0 < 1$, the infection will become extinct and if $R_0 > 1$, the disease will be established in the population and the incidence will increase. For the purpose of calculation of R_0, we follow the next generation matrix approach as proposed by (Diekmann, Heesterbeek, and Metz, 1990). The authors have proposed to formulate the ODEs epidemic system by splitting the state variables and the entering fluxes related to the infectious agents. T_i is the flux of newly infected in compartment i and Σ_i is the flux of entering or leaving fluxes related to the compartment i. With such a partition after considering the infected individuals, one can write these equations written in the form $\frac{dx_i}{dt} = T_i(x) - \Sigma_i(x)$, in this splitting, T_i is the rate of appearance of new infections in compartment i, and Σ_i is the rate of other transitions between compartment i and other infected compartments. Now define $\mathcal{F} = \left[\frac{\partial T_i(x_0)}{\partial x_j}\right]$ and $\mathcal{V} = \left[\frac{\partial \Sigma_i(x_0)}{\partial x_j}\right]$, where x_0 is the disease-free equilibrium (DFE). $\mathcal{F}$ is a positive matrix and $\mathcal{V}$, an M-matrix, i.e an M-matrix is a Z-matrix with eigenvalues whose real parts are nonnegative. Matrix $\mathcal{K} = \mathcal{F}\mathcal{V}^{-1}$ has (i, j) entry equal to the expected number of secondary infections in compartment i produced by an infected individual introduced in compartment j. Thus $\mathcal{K}$ is the next generation matrix and according to the authors $R_0 = \rho(\mathcal{F}\mathcal{V}^{-1})$, evaluated at disease-free equilibrium (DFE) is defined to the basic reproduction number and ρ denotes the spectral radius.

We first put our model system Eq. (3.2) and Eq. (3.3) in the matrix form and then we linearise the model equations involving only the exposed and the infected states around the disease-free equilibrium (DFE). The mechanism of linearising around the DFE mimics the fact that R_0 describes the initial spread of an infection to a completely susceptible population. Then the linearised matrix can be decomposed into two matrices $\mathcal{F}$ and $\mathcal{V}$, where $\mathcal{F}$ is the transmission part and $\mathcal{V}$ stands for the transition part. The DFE point for the bird population is $(S_B, E_{BC}, E_{BSC}, I_{BC}, I_{BSC}, R_{BC}, R_{BSC}) = (S_B^*, 0, 0, 0, 0, 0, 0)$, similarly for the mosquito population it is $(S_M, E_M, I_M) =$

$(S_M^*, 0, 0)$ and for the migratory birds, it is $(S_{Bm}, E_{Bm}, I_{Bm}, R_{Bm}) = (S_{Bm}^*,$ 0, 0, 0). Simple algebra takes us to the DFE as $E_0 = (K_M,$ 0, 0, $K_B,$ 0, 0, 0, 0, 0, 0, $K_{Bm},$ 0, 0, 0) including the migratory bird population. We take account of the system Eq. (3.3) and Eq. (3.4) which include the infectious terms as the difference of T_i, the new infection terms at the compartment i and Σ_i is the transition from compartment i. For the moment, we focus only on local birds and include migratory birds later. Hence, we get the following vector system as:

$$\frac{d}{dt}\begin{bmatrix} E_M \\ I_M \\ E_{BC} \\ E_{BSC} \\ I_{BC} \\ I_{BSC} \end{bmatrix} = \begin{bmatrix} \frac{c_2 S_M I_{BC}}{K_B} + \frac{c_1 S_M I_{BSC}}{K_B} \\ 0 \\ \frac{\beta_4 I_M S_B}{K_B} \\ \frac{\beta_3 I_M S_B}{K_B} \\ 0 \\ \gamma_3 R_{BSC} \end{bmatrix} - \begin{bmatrix} \gamma_M E_M + m_M E_M \\ -\gamma_M E_M + m_M I_M \\ m_B E_{BC} + \gamma_{BC} E_{BC} \\ m_B E_{BSC} + \gamma_{BSC} E_{BSC} \\ -\gamma_{BC} E_{BC} + m_B I_{BC} + \alpha_4 I_{BC} + d_{BC} I_{BC} \\ -\gamma_{BSC} E_{BSC} + m_B I_{BSC} + \alpha_3 I_{BSC} + d_{BSC} I_{BSC} \end{bmatrix}$$

Computing the Jacobian matrices of $\mathcal{F}$ and $\mathcal{V}$ at the DFE gives the following matrices:

$$\mathcal{F}_{Loc} = \begin{bmatrix} 0 & 0 & 0 & 0 & \frac{K_M c_2}{K_B} & \frac{K_M c_1}{K_B} \\ 0 & 0 & 0 & 0 & 0 & 0 \\ 0 & \beta_4 & 0 & 0 & 0 & 0 \\ 0 & \beta_3 & 0 & 0 & 0 & 0 \\ 0 & 0 & 0 & 0 & 0 & 0 \\ 0 & 0 & 0 & 0 & 0 & 0 \end{bmatrix}$$

$$\mathcal{V}_{Loc} = \begin{bmatrix} \gamma_M + m_M & 0 & 0 & 0 & 0 & 0 \\ -\gamma_M & m_M & 0 & 0 & 0 & 0 \\ 0 & 0 & \gamma_{BC} + m_B & 0 & 0 & 0 \\ 0 & 0 & 0 & \gamma_{BSC} + m_B & 0 & 0 \\ 0 & 0 & -\gamma_{BC} & 0 & \alpha_4 + m_B + d_{BC} & 0 \\ 0 & 0 & 0 & -\gamma_{BSC} & 0 & \alpha_3 + m_B + d_{BSC} \end{bmatrix}$$

The index *Loc* indicates that we are taking account of local bird population only. We multiply $\mathcal{V}_{Loc}$, after finding the inverse of $\mathcal{V}_{Loc}$, and $\mathcal{V}_{Loc}^{-1}$ and then calculate the largest eigenvalue of the resulting matrix. The basic reproduction number is then given by $R_{0,Loc} = \rho(\mathcal{F}_{Loc}\mathcal{V}_{Loc}^{-1})$, where ρ is the largest eigenvalue of the matrix $\mathcal{F}_{Loc}\mathcal{V}_{Loc}^{-1}$.

This gives

$$R_{0,Loc} = \sqrt{\frac{1}{m_M}\frac{\gamma_M}{\gamma_M + m_M}\frac{K_M}{K_B}\left[\frac{\gamma_{BC}}{\gamma_{BC} + m_B}\frac{1}{\alpha_4 + m_B + d_{BC}}c_2\beta_4 + \frac{\gamma_{BSC}}{\gamma_{BSC} + m_B}\frac{1}{\alpha_3 + m_B + d_{BSC}}c_1\beta_3\right]} \tag{3.6}$$

Eq. (3.6) can be expressed as follows:

$$R_{0,Loc} = \sqrt{\ell_M \sigma_M \phi \left[\sigma_{BC}\xi_{BC}\tau_{M\longleftrightarrow BC} + \sigma_{BSC}\xi_{BSC}\tau_{M\longleftrightarrow BSC}\right]}, \tag{3.7}$$

where $\ell_M = \frac{1}{m_M}$, $\sigma_M = \frac{\gamma_M}{\gamma_M + m_M}$, $\phi = \frac{K_M}{K_B}$, $\sigma_{BC} = \frac{\gamma_{BC}}{\gamma_{BC} + m_B}$, $\xi_{BC} = \frac{1}{\alpha_4 + m_B + d_{BC}}$, $\tau_{M\longleftrightarrow BC} = c_2\beta_4$, $\sigma_{BSC} = \frac{\gamma_{BSC}}{\gamma_{BSC} + m_B}$, $\xi_{BSC} = \frac{1}{\alpha_3 + m_B + d_{BSC}}$, $\tau_{M\longleftrightarrow BSC} = c_1\beta_3$.

Eq. (3.7) represents sum of the product of number of clinical and subclinical bird infections caused by a single infected mosquito and the number

of mosquito infections caused by local birds including clinical and subclinical birds (Driessche, 2017).

The biological meaning of the terms in Eq. (3.7) can be interpreted as following. ℓ_M is the life-span of a mosquito, σ_M is the proportion of mosquitoes that survive the incubation period, ϕ is the number of initially susceptible mosquitoes per local bird population at the disease-free equilibrium, σ_{BC} is the proportion of clinical birds that survive incubation period, ξ_{BC} is the clinical bird's infectious lifespan, $\tau_{M\longleftrightarrow BC}$ is the product of transmission probabilities between clinical birds to mosquitoes and mosquitoes to clinical birds. The meaning of the parameters related to the subclinical birds are similar.

Analysing Eq. (3.7) further, we are able to determine the level of control required to prevent transmission. Here, the ratio of mosquitoes to bird at E_0, ϕ is an important threshold. Equating $R_{0,Loc}$ to its critical value 1, we get the following the critical value of ϕ_c:

$$\phi_c = \frac{1}{\ell_M \sigma_M \left[\sigma_{BC}\xi_{BC}\tau_{M\longleftrightarrow BC} + \sigma_{BSC}\xi_{BSC}\tau_{M\longleftrightarrow BSC}\right]} \tag{3.8}$$

Above this threshold, an outbreak can occur. Therefore, reducing the relative mosquito to local bird density should be a way to prevent a potential outbreak of WNV infections in the study area.

The calculation of R_0 while incorporating the seasonal appearance of migratory birds are included in the Appendix Eq. (A.1), Eq. (A.2), Eq. (A.3)

$$R_{0,Mig} = \sqrt{\ell_M \sigma_M \left[\begin{array}{r}\phi(\sigma_{BC}\xi_{BC}\tau_{M\longleftrightarrow BC} + \sigma_{BSC}\xi_{BSC}\tau_{M\longleftrightarrow BSC})+ \\ \phi_{Bm}(\sigma_{Bm}\xi_{Bm}\tau_{M\longleftrightarrow Bm})\end{array}\right]} \tag{3.9}$$

The relationship between $R_{0,Loc}$ and $R_{0,Mig}$ is as follows:

$$R^2_{0,Mig} = R^2_{0,Loc} + \phi_{Bm}(\sigma_{Bm}\xi_{Bm}\tau_{M\longleftrightarrow Bm}) \tag{3.10}$$

All the expressions in Eq. 3.10 are positive and it is evident that $R^2_{0,Mig} > R^2_{0,Loc}$. We notice that $\tau_{M\longleftrightarrow Bm}$ is temperature-dependent and represents the product $c_3(T)\beta_5(T)$. Therefore, the increased value of R_0 is governed by the mosquito biting rate, by the ratio of mosquito to migratory bird density and the probabilities of disease transmission from mosquitoes to migratory birds and vice versa.

Eq. (3.9) can also be described as a combination of three different basic reproduction numbers where $R_0^{(BC)}$, $R_0^{(BSC)}$ and $R_0^{(Mig)}$ are the involvements of clinical, subclinical and migratory birds separately. These are given by the transmission between mosquito-clinical and clinical-mosquito, mosquito-subclinical and subclinical-mosquito and mosquito-migratory birds and migratory birds-mosquito, respectively.

3.4.1 Temperature Data

Many model parameters including transmission rates, mortality and birth rates of mosquitoes are all temperature-dependent. We have utilised the temperature data from 1/1/2007 to 1/1/2017 from the DWD server (Deutscher-Wetterdienst, 2017) to adapt the model to the climatic situation in Germany.

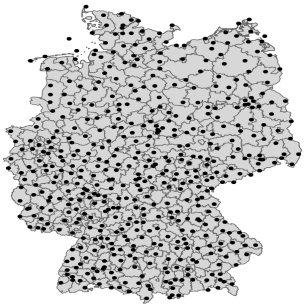

FIGURE 3.3: Weather stations

The considered weather stations are depicted in Fig. 3.3. The time resolution of the downloaded data is 1 day. The temperature T is considered as a function of time, i.e. $T = T(t)$, where t represents the time. Hence, the temperature-dependent model parameters are also functions of time.

3.5 Simulations and Results

3.5.1 Infection Curves

We solve the model system (Eq. (3.3), Eq. (3.4), Eq. (3.5)) numerically utilising an implicit Euler scheme with a time step of day in R (R Core Team, 2018) to comply with the intervals for which the weather data are downloaded. Our model simulates mosquito and host infection states for the period of $2007 - 2017$. Since the model parameters depend only on the temperature, no additional input is required for running the simulation. The initial conditions are $1,000$ mosquitoes, 500 local birds and 50 migratory birds on each site during the simulation are selected according to (Rubel et al., 2008; Laperriere, Brugger, and Rubel, 2011). All mosquitoes and birds are susceptible except for one infected migratory bird. Seasonally, a new single infected migratory bird is introduced into the population to model the import of WNV from endemic areas. Note that due to the population growth dynamics (Eq. (3.3), Eq. (3.4), Eq. (3.5)), both birds and mosquito population grow over time.

3.5.2 Single season simulation

Culex mosquitoes are the primary vectors of WNV in summer for the transmission to birds, but they are also the overwintering reservoir too. According to the authors in (Rudolf et al., 2017; Wallace, 2008; Reisen et al., 2006), it is obvious that WNV persists in mosquitoes throughout the winter episode in Europe. Therefore, we keep the number of overwintering mosquitoes as 1% of the initial condition according to (Rubel et al., 2008; Laperriere, Brugger, and Rubel, 2011)to accommodate this phenomena. Given the fact that the procured data starts in winter time, the initial susceptible mosquito population is set to be $N_{M,min}$, where $N_{M,min}$ denotes the minimum number of hibernating adult mosquitoes. This concept is used to avoid the condition that due to the weather driven system, the mosquito population may become extinct during the simulation (Laperriere, Brugger, and Rubel, 2011; Rubel et al., 2008). We take a subset consisting of 12 weather stations from the downloaded data (Fig. 3.3) from the northern, southern and central zones

in Germany. A map with their locations is shown in the Fig. A.1. They show significant differences in temperatures and this is the reason to subset the weather data. When we run the simulation for these locations for one year, we observe that there is a significant difference in the total numbers of infected local birds and mosquitoes between the northern and southern zones. The plots in Fig. 3.4 show the infected local bird population for the subset data in Germany for one season. Due to the low temperature in the north, the infection spread is comparative lower as well as the growth of the vector population. In the south, due to its comparatively high temperature, there is an increase of the growth of the mosquitoes and henceforth on the infection process.

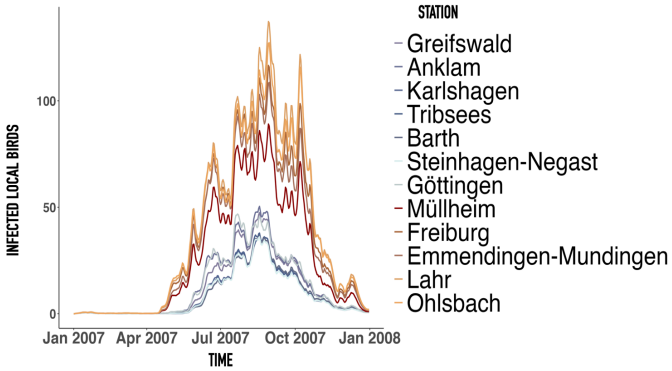

FIGURE 3.4: Infection curves of the local bird population for different locations in Germany. Outbreaks are typically larger in southern regions.

3.5.3 Multi-season simulation

With the purpose of demonstration of different infection dynamics happening in Germany, we choose two locations: Lahr ($48°20'N\ 7°52'E$) and Greifswald ($54°5'N\ 13°23'E$) and they are referred in Fig. 3.5 To assess the potential role of migratory birds introducing WNV on the local spread of the disease, we keep the same initial conditions in the simulations. The simulated time

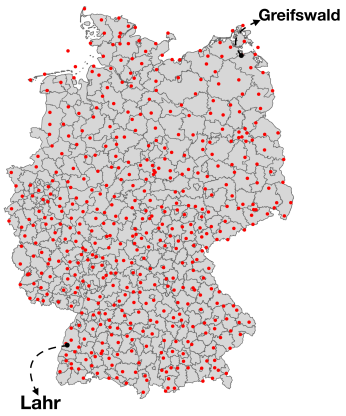

FIGURE 3.5: Lahr in the Southwest and Greifswald in the Northeast are pointed in the map of Germany.

series shows that the infected mosquito population is governed by temperature, whereas the infection dynamics is different in the bird population for

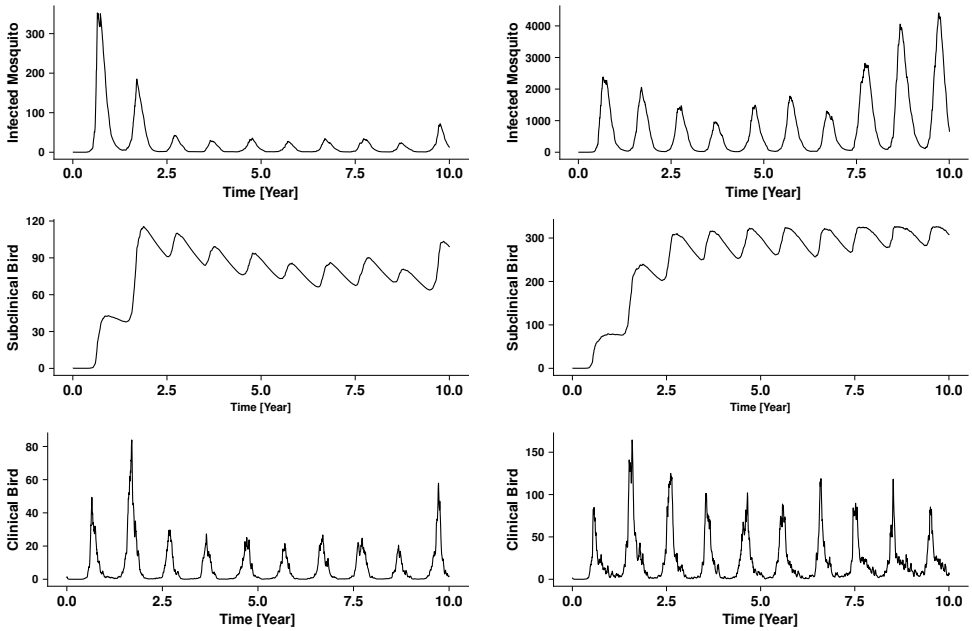

(A) Greifswald (North) (B) Lahr (South)

FIGURE 3.6: Upper panel: Infected mosquito population. Middle panel: Infected subclinical bird population. Lower panel: Infected clinical bird population. Locations are (a) Greifswald and (b) Lahr. Note the difference in scales.

these two different locations. The time series of the clinical and the subclinical birds differ substantially for the two locations Greifswald and Lahr. The strong correlation between the growth of infected adult mosquitoes and temperature, i.e. higher temperature yields eventually a higher amplitude in the infection curve for the host and the vector population can be observed from Fig. 3.6. We notice that the growth of the infected adult mosquito population is solely driven by the environmental factor, but for the local birds, we observe differences for the two subclasses of clinical and subclinical birds. In the process of infection dynamics, a fraction of the subclinically infected birds, once they have recovered, is again susceptible to the disease and get infected again. Therefore, they boost the infected subclinical population and keeps the disease cycle going on.

We can observe the similar qualitative characteristics in the infection curves for both locations considered in the model despite having the differences in scales. Seasonal peaks in the host and vector species attribute to the fact that larger numbers of infectious mosquitoes will cause larger numbers of infected local birds.

3.5.4 Impact of bird migration

In this section we explore the impact of the presence of migratory birds on the infection cycle in the local bird population. Fig. 3.7 depicts the influence of migratory birds on the disease dynamics. It is interesting to notice that during the time frame of the simulation, the infection peak in the migratory

birds is followed by the peak in the local bird population. Similar pattern can be observed in both locations, Lahr and Greifswald.

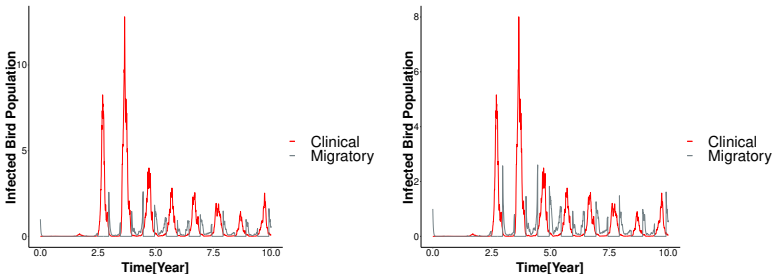

(A) (B)

FIGURE 3.7: Simulated time series of the clinical and migratory bird population. Locations are Greifswald (a) and Lahr (b).

Presence of an infected migratory bird can trigger the infection process in the local mosquito population. Mosquitoes after taking the blood meal from the infected migratory birds, transmit the infection to other birds, thus establishing the disease cycle. The periodic arrival and the presence of migratory birds boosts the dynamics of the infection cycle.

Basic reproduction number R_0 is a function of temperature (T) and time (t). To illustrate this fact, we choose Greifswald to simulate the seasonal course of R_0. We show R_0 (according to Eq. (3.10)) for the relevant temperature range in Fig. 3.8. During the winter season, the activities of mosquitoes are low and due to this reason, the disease transmission process is discontinued and this is coupled with the absence of migratory birds.

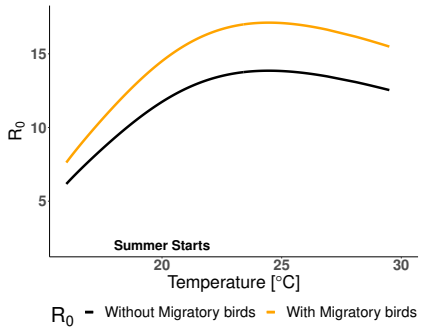

FIGURE 3.8: Simulated R_0 vs temperature in Greifswald. The presence of migratory birds increases R_0 by 25% on average.

As predicted by Eq. (3.10), we observe that $R_{0,Mig}$ for migrating birds to be increased by a factor of $\sqrt{\phi_{Bm}(\sigma_{Bm}\xi_{Bm}\tau_{M\longleftrightarrow Bm})}$ compared to $R_{0,Loc}$. It is clear from Fig. 3.8 that the presence of migratory birds in Greifswald escalates the magnitude of R_0 by approximately 25%, depending on the exact temperature. In both the places, Lahr and Greifswald the increased values of R_0, are in accord with our conjecture that migratory birds act as an active catalyst for the spread of WNV. The temporal course of the basic reproduction number for both locations is shown in Fig. 3.9.

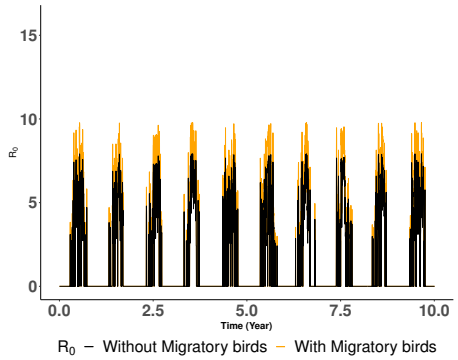

FIGURE 3.9: Simulated time evolution of R_0 in Greifswald.

Fig. 3.9 shows the time evolution of R_0 and it is clear from the figure that the presence of migratory birds in Greifswald escalates the magnitude of R_0. Therefore, the meaning of Eq. (3.9) after solving numerically for each model time step and averaging it ($\overline{R_0}$) over the years can be described as the average number of secondary infections caused by the introduction of a single infected individual into an entirely susceptible population at the time of bird migration (summer or spring) in a year in the presence of the migratory birds (Rubel et al., 2008). It should be noted that during the time of migration i.e. when the migratory birds are present in Germany, increase in the magnitude of R_0 is accentuated and in the winter the magnitude decreases.

3.5.5 Sensitivity Analysis

Here, we explore the sensitivity of the infection outcome with respect to the different model parameters. We perform the simulations to observe the impact of different parameters on the disease dynamics and we represent them graphically. We mainly focus on three mosquito parameters: mosquito mortality rate (m_M), mosquito birth rate (b_M) and overwintering of mosquitoes, mosquito to local bird ratio (ϕ), respectively. For this purpose, we change the above said parameters values by -50% and -25% from the reference value. Let's explore the influence of mosquito mortality (m_M) on the potential spread.

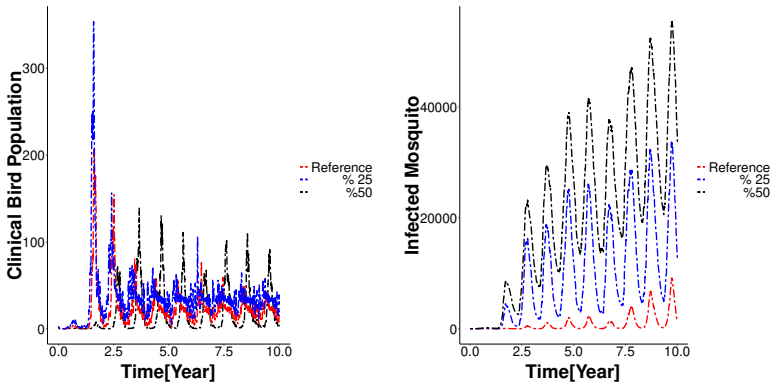

(A) Clinical birds.

(B) Infected mosquitoes.

FIGURE 3.10: Mortality rate of mosquitoes (m_M) is a sensitive parameter. Simulated time series of clinical bird (a) and infected mosquito population (b).

We notice that the lower the mosquito mortality, higher is the amplitude of infection on the local birds while accounting the -50% and -25% reduction and the reference case. Fig. 3.10 shows the impact of the reduction in the mosquito mortality yields the positive influence on the infected population.

The ratio $\phi = S_M^*/S_B^*$ between blood feeding mosquito and local bird population is an important parameter to look through (Colborn et al., 2013). Following (Wonham, De-Camino-Beck, and Lewis, 2004), ϕ can also play the role as an indicator of WNV in case of a real outbreak. Three different values of ϕ are chosen and the values are $\phi_1 = 10$, $\phi_2 = 20$, $\phi_3 = 30$ respectively for the three simulations for the demonstration purpose. The result is depicted in Fig. 3.11. The impact of ϕ on clinical and subclinical population WNF-infected local bird populations are clearly visible. With a higher availability of blood meals and bites per mosquito, the infection spreads quicker than the lower value of ϕ.

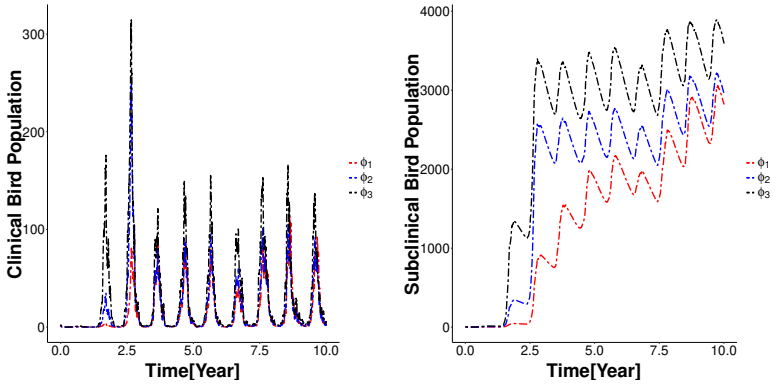

(A) Clinical

(B) Subclinical

FIGURE 3.11: Time series is sensitive to the parameter ϕ. Simulated time series of WNV-infected clinical (a) and subclinical (b) local bird population.

We explore the influence of mosquito birth rate b_M, mosquito mortality m_M and mosquito to local bird ratio ϕ on the basic reproduction number R_0. In Fig. 3.12 we show R_0 over time for Greifswald for different values of the mentioned parameters.

Red dots in Fig. 3.12a refer to the reference case (as in the main text), blue dots refer to a reduction of the mosquito birth rate b_M by 25 %, and black dots refer to a reduction of 50 %. It is noticeable from Fig. 3.12a that the reduction of b_M impedes the growth of the mosquitos and it disrupts the disease transmission consequently. Reduction of b_M is reflected in a decrease of R_0.

Red dots in Fig. 3.12b refer to the reference case (as in the main text), blue dots refer to a reduction of the mosquito mortality m_M by 25 %, and black dots refer to a reduction of 50 %. It is noticeable from Fig. 3.12b that the reduction of m_M causes an increase in the transmission of the infection amongst the local bird population and escalates the the value of basic reproduction number R_0.

Red dots in Fig. 3.12c refer to the value ϕ_1, blue dots refer to ϕ_2 and black dots refer to ϕ_3, where the values of ϕ_i $(i = 1, 2, 3)$ are the same as mentioned before. It is noticeable from Fig. 3.12c that the increase of ϕ yields in the increase in R_0. We see from Fig. 3.12 that decreasing the mosquito mortality increases R_0. Similarly, we observe that increasing ϕ also increases R_0. This follows also from Eq. (3.9).

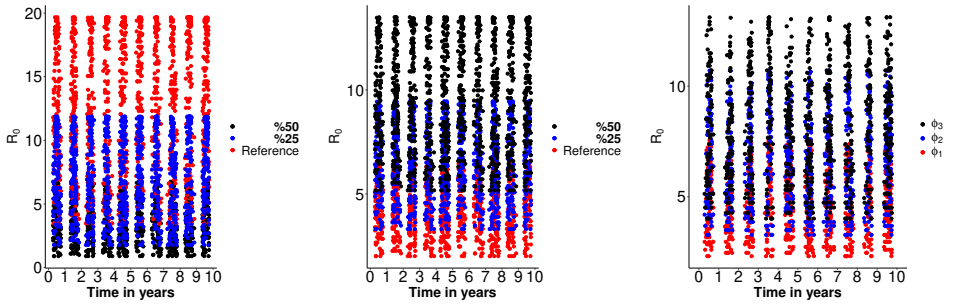

(A) (B) (C)

FIGURE 3.12: Time evolution of R_0 and the impact of (A) mosquito birth rate (b_M) , (B) mosquito mortality (m_M), and (C) mosquito to bird ratio (ϕ) on R_0. The location is Greifswald.

3.5.6 Impact of climate change

To understand the effect of climate change on the spread of WNV in Germany, we first employ the simple extrapolation of temperatures over 20 years, after fitting the temperature data to a simple trigonometric function of the form $a + b\cos(\theta - \phi)$ in the Fig. 3.13a and the predicted temperature data with the inclusion of linear trend under RCP8.5 condition is shown in Fig. 3.13b. For the trend we use a slope of $4.6°C$ in 80 years, i.e. $0.0575°C$ per year.

We can notice the convergence of the local infected bird population to a completely susceptible population in the long term dynamics in Gerifswald. It can be attributed to the fact that the transmission has stopped rapidly

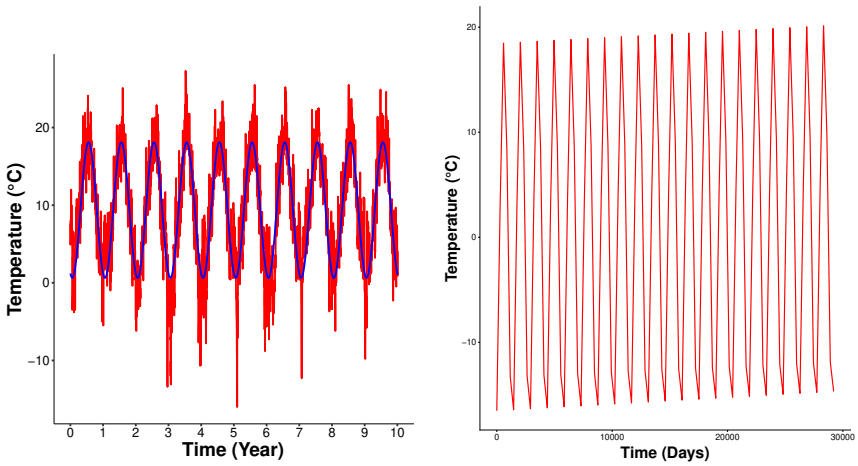

(A) (B)

FIGURE 3.13: Daily weather data of Greifswald during 2007 to 2017 and the predicted temperature data with the inclusion of linear trend under the RCP 8.5 condition

and a permanent WNV transmission cycle is not established in the local bird population where as in Lahr the situation is entirely different. Our simulations predict that the converging population will adopt a cyclic behaviour, thus indicating that there will be a continuation of transmission for a long period. And this is the same for the mosquito and local bird populations.

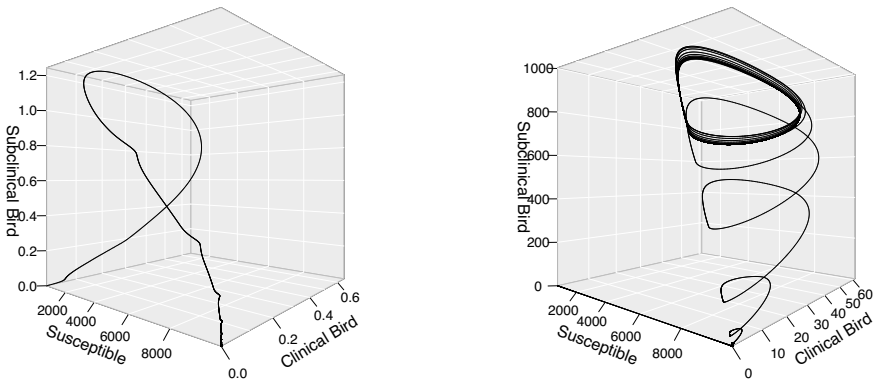

(A) Phase space plot of local bird population in Greifswald

(B) Phase space plot of local bird population in Lahr

FIGURE 3.14: Phase space plots of local bird populations for two locations in Germany. (a) Greifswald, north and (b) Lahr, south. Time period is 2007-2027 using simple temperature extrapolation.

It is to be noted that the given the backdrop of increase in the global temperature (Hansen et al., 2006), activities of mosquitoes and the risk of WNV transmission will gradually increase (Semenza and Suk, 2018). Therefore, we include the growth of temperature as a linear trend in the fitted temperature

in our model, under the assumption that the annual average land temperature is projected to increase by $4.8°C$ per 100 years under Representative Concentration Pathway (RCP)8.5 (Team, Pachauri, and Meyer(eds.), 2014;).

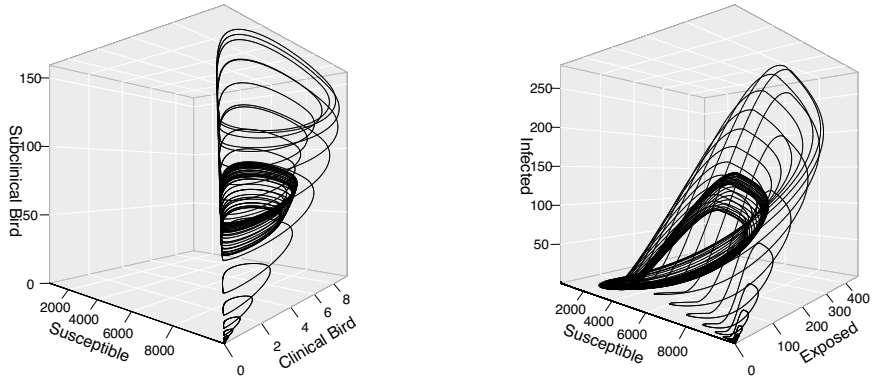

(A) Phase space plot of local bird population in Greifswald

(B) Phase space plot of mosquito population in Greifswald

FIGURE 3.15: Phase space plots of local bird populations for two locations in Germany. (a) Greifswald, north and (b) Lahr, south. Time period is 2017-2100 using temperature extrapolation with a linear trend according to climate change.

The results of this simulation are shown Fig. 3.15. The phase plots are strikingly similar to the phase space plots of Lahr in Figure 3.14. This suggests that the WNV infection cycle may also establish in Northeast Germany in the nearer future under the RCP8.5 conditions.

3.5.7 Potential Spatial Distribution Map

For the purpose of assessing the potential risk associated with a continuous spatial transmission of WNV, we plot the sizes of potential outbreaks on a map of Germany in Figure 3.16. Our simulations suggest that the southern and the central zones of Germany might suffer a higher proportion of established WNV infections, while in the northern part, the risk of established, continuous transmission is comparatively lower. We observe that the potential spatial distribution map (Fig. 3.16) includes the regions where WNV outbreaks occurred in birds and horses in Germany in 2018 (Schröder and Klöß, 2004) with a large number of infected birds as predicted by our model.

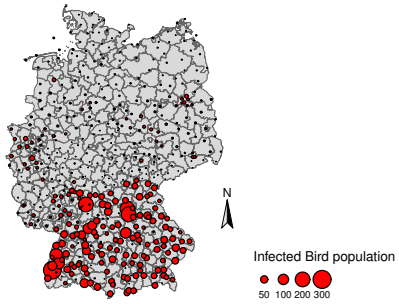

FIGURE 3.16: Spatial distribution of outbreak sizes at the end of the outbreak season for birds.

3.6 Conclusion of this section

The presented work here left us with some critical observations. It is readily understandable that the threat of WNV spread in the new areas in the northern Europe are looming large and is a matter of concern. Our findings from the simulations give us certain insights of the potential spread of WNV in Germany given the backdrop of large number of reported cases in Germany and its neighbouring countries. Our main observations are the following: First, the impulsive system of Eq. (3.2), Eq. (3.3), Eq. (3.4) system shows the potential role of migratory birds in WNV dissemination in Germany. The expressions of basic reproduction number in Eq. (3.9) helps us to quantify the same. Additionally, the seasonal flux of infected migratory birds to Germany from other endemic areas keeps the disease cycle active and persisting.

Second, the sensitivity analysis gives us the clues about the model parameters that govern the potential spread of the infection in Germany. Mosquito to local birds ratio (ϕ), mosquito mortality (m_M) and the mosquito birth rate (b_M) are found to be most influential parameters. This implies that the targeted reductions in the suitable habitable mosquitoes and applying the necessary herbicide should be efficient to curb the bite of WNV.

Third, there is a clear difference of the infection profiles in the northern areas of Germany and the southern areas of the same. Given the higher temperature in the southern zones, there is higher potential that WNV will spread quicker than the northern areas having comparatively lower temperature. Our simulations infer a large difference of the infection sizes at the end of the season between the north and the south of Germany.

Fourth, we use the simple trigonometric interpolations for the purpose of predicting the possible future outcomes. The simulations that we perform after converting the model system to a non-autonomous model system, show us that in the south WNV will be able to establish its foothold after one season but in the north the population will become completely susceptible after introducing an infected agent. It should be noted that the linear trend of temperature growth is assumed to be the same for north as well as for south.

Finally, the observations above raise two questions for the context of WNV spread in Germany. 1. What are the changes we can witness in the spread of WNV in Germany when we incorporate the climate change situation into our model? 2. How the potential density of the infected birds will appear on the spatial scale over Germany? In order to answer

those questions, we first interpolate the temperature data including the linear trend as predicted by IPCC and find that under RCP4.5 conditions, the disease transmission stops in the northern regions of Germany but in RCP8.5 conditions, WNV will potentially establish its foothold even in the northern regions in the future. To answer the second, we decide to project the densities of the infected birds on the spatial scale while the bubble sizes correspond to the possible infection sizes around Germany.

Our main findings are that the presence of migratory birds returning from the endemic areas to Germany can accentuate the cases of WNV, and steady growth in the global temperature will work as an additional fuel to the spread and establishment of WNV in Germany.

CHAPTER 4

Spatial Spread Model: Coupling Network and Metapopulation Model

This chapter includes the materials from the communicated paper named "Can a patchy model describe the potential spread of West Nile virus in Germany?" (Bhowmick et al., 2021) The paper is under the review in the Ecological Modelling.

The previous chapter has demonstrated that the temperature driven ODE based model provides the necessary framework to comprehend the mechanism behind the spread. Given the time series of the temperature data, the ODE based model is able to capture plausible infection dynamics while incorporating the environmental stochasticity. The potential of such an ODE based local dynamical model lies in the plethora of methods that has been developed in the last decades (Wonham, De-Camino-Beck, and Lewis, 2004; Castillo-Chavez et al., 2002; Rubel et al., 2008; Laperriere, Brugger, and Rubel, 2011; Bergsman, Hyman, and Manore, 2016). As depicted in Sections 3.3 and 3.5.7, the locally temperature driven model can predict a spatial distribution that involves the actual cases of WNV in Germany.

Populations are assumed to live in different habitat fragments, called patches and accordingly, disease or population dynamics are happening in different patches can be different. Immigration from other patches can lead to a distinct dynamics over all when compared to a single patch. In a sense, the population spreads the risk of disease dissemination by spatial connection. Nevertheless, the locally ODE based models readily can not include immigration of infected agents from one habitat patch to another one. According to (Boulinier et al., 2016; White, Forester, and Craft, 2018), host and the vector movement of the interacting populations are of equally concern. This chapter addresses some of the theoretical problems owing to spread of epidemics in the patchy environment.

4.1 Introduction

Different factors such as vector and host movements, pathogen transmission heterogeneity, environmental factors etc. (VanderWaal and Ezenwa, 2016; White, Forester, and Craft, 2018) influence the spatiotemporal process of West Nile Virus (WNV) dissemination. Previously reported studies have revealed that the increase in the temperature and the host-vector mobility helps the spread of mosquito-borne diseases (Boulinier et al., 2016; Shapiro,

Whitehead, and Thomas, 2017). The summer of 2018 had facilitated the favourable meteorological conditions for the potential geographical spread of WNV in Germany and perhaps WNV had been introduced by the wild birds as they can act as amplifying hosts (Ziegler et al., 2019). Migratory birds may play a significant role as a transporter to new regions along their major flyways across the globe (Rappole, Derrickson, and Hubálek, 2000; Reed et al., 2003b).

There has been an increase of WNV cases in Germany after the first reported case of WNV in the following seasons (Ziegler et al., 2020). The activity of WNV was reported in the Eastern part Germany to the Northern zone of Germany. The combination of phylogenetic analysis and the geographical reach of WNV in Germany from north to the south reveals that WNV may have been introduced to Germany from Czech Republic already before 2018 (Ziegler et al., 2019). These show that there is a further risk of potential spatial transmission of WNV in Germany.

In (Hadfield et al., 2019; Janousek, Marra, and Kilpatrick, 2014; Fitzgibbon et al., 2019), the authors quantify the importance of movement of livestock and the dispersal of vector in the disease transmission. In our current work we are interested in the spatial spread of WNV under the effect of host and vector mobilities. Most WNV spread models are mathematical deterministic compartmental ODE based models (Durand, Benoit et al., 2010; Wang, Wu, and Zhao, 2019; Bowman et al., 2005). However, these ODE based models do not necessarily include the mobility patterns of the hosts or vector or both, temperature or landscape data types. For the comprehension purpose, we introduce different contact networks which are formulated with the help of distance based networks. We explore this heterogeneous model with the purpose to explain how WNV will be transmitted across spatial scales that can be rendered into local surveillance and action. Motivated by this, we endeavour to systematically examine the potential spatial spread of WNV in Germany.

4.2 Spatial Model

In this section we extend our previously developed temperature driven local model (Bhowmick et al., 2020) into a metapopulation model with associated networks. The usage of a metapopulation model is necessary given that the migratory birds have an important role in potentially introducing WNV and spreading it in its migratory routes (Swetnam et al., 2018; Duggal et al., 2019). We describe the model equations in this section after including the migrations of the interacting populations. For the mosquito population (please see Eq. (3.2) for the local model without the movements amongst the patches), the metapopulation model equation system is following after we include the movements between the patches.

$$
\begin{aligned}
\frac{dS_{M_i}}{dt} &= [b_{M_i}N_{M_i} - m_{M_i}S_{M_i}]\,[1 - S_{M_i}/K_{M_i}] - \frac{S_{M_i}}{K_{B_i}}\,(c_{2_i}I_{BC_i} + c_{1_i}I_{BSC_i}) \\
&+ \sum_j m_{ij}S_{M_j} - \sum_j m_{ji}S_{M_i} \\
\frac{dE_{M_i}}{dt} &= \frac{S_{M_i}}{K_{B_i}}\,(c_{2_i}I_{BC_i} + c_{1_i}I_{BSC_i}) - \gamma_M E_{M_i} - m_{M_i}E_{M_i} \\
&+ \sum_j m_{ij}E_{M_j} - \sum_j m_{ji}E_{M_i} \\
\frac{dI_{M_i}}{dt} &= \gamma_M E_{M_i} - m_{M_i}I_{M_i} + \sum_j m_{ij}I_{M_j} - \sum_j m_{ji}I_{M_i}
\end{aligned} \tag{4.1}
$$

This was the metapopulation model for the mosquitoes including the movement between two arbitrary patches j and i and m_{ij} represents the rate of migration and it is assumed here that $m_{ii} = 0$. Let us assume that M is the movement matrix of mosquitoes and the elements of M are defined as $(M)_{ij} = m_{ij}$ for $i \neq j$ and $M_{ii} = -\sum_{j=1}^{n} m_{ji}$.

The metapopulation model system for the local-bird population after including the migration amongst the patches is following

$$
\begin{aligned}
\frac{dS_{B_i}}{dt} &= \left[b_{B_i} - (b_{B_i} - m_{B_i})\frac{N_{B_i}}{K_{B_i}}\right] - m_{B_i}S_{B_i} - \frac{(\beta_{3_i} + \beta_{4_i})I_{M_i}S_{B_i}}{K_{B_i}} \\
&+ \sum_j p_{ij}S_{B_j} - \sum_j p_{ji}S_{B_i} \\
\frac{dE_{BC_i}}{dt} &= \frac{\beta_{4_i}I_{M_i}S_{B_i}}{K_{B_i}} - m_{B_i}E_{BC_i} - \gamma_{BC_i}E_{BC_i} + \sum_j p_{ij}E_{BC_j} \\
&- \sum_j p_{ji}E_{BC_i} \\
\frac{dE_{BSC_i}}{dt} &= \frac{\beta_{3_i}I_{M_i}S_{B_i}}{K_{B_i}} - m_{B_i}E_{BSC_i} - \gamma_{BSC_i}E_{BSC_i} + \sum_j p_{ij}E_{BSC_j} \\
&- \sum_j p_{ji}E_{BSC_i} \\
\frac{dI_{BC_i}}{dt} &= \gamma_{BC_i}E_{BC_i} - m_{B_i}I_{BC_i} - \alpha_{4_i}I_{BC_i} - d_{BC_i}I_{BC_i} + \sum_j p_{ij}I_{BC_j} - \sum_j p_{ji}I_{BC_i} \\
\frac{dI_{BSC_i}}{dt} &= \gamma_{BSC_i}E_{BSC_i} - m_{B_i}I_{BSC_i} - \alpha_{3_i}I_{BSC_i} + \gamma_{3_i}R_{BSC_i} - d_{BSC_i}I_{BSC_i} \\
&+ \sum_j p_{ij}I_{BSC_j} - \sum_j p_{ji}I_{BSC_i} \\
\frac{dR_{BC_i}}{dt} &= \alpha_{4_i}I_{BC_i} - m_{B_i}R_{BC_i} + \sum_j p_{ij}R_{BC_j} - \sum_j p_{ji}R_{BC_i} \\
\frac{dR_{BSC_i}}{dt} &= \alpha_{3_i}I_{BSC_i} - m_{B_i}R_{BSC_i} - \gamma_3 R_{BSC_i} + \sum_j p_{ij}R_{BC_j} - \sum_j p_{ji}R_{BC_i}
\end{aligned} \tag{4.2}
$$

Here, p_{ij} represent the rate of migration between two arbitrary patches j and i of the local birds and and $p_{ii} = 0$. Let us assume that P is the

movement matrix of local birds and the elements of P are defined as $(P)_{ij} = p_{ij}$ for $i \neq j$ and $P_{ii} = -\sum_{j=1}^{n} p_{ji}$. The readers may have a look at the Eq. (3.3) for the local model without the movements amongst the patches and to notice the local infection model system.

with the initial conditions
($S_{B_i}(0)$, $S_{M_i}(0) > 0$ and $E_{BC_i}(0)$, $E_{BSC_i}(0)$, $I_{BC_i}(0)$, $I_{BSC_i}(0)$, $R_{BC_i}(0)$, $R_{BSC_i}(0)$, $E_{M_i}(0)$, $I_{M_i}(0) \geq 0$).

Let

$$\begin{aligned} \lambda_i = \frac{\beta_{3_i} I_{M_i}}{K_{B_i}}, \eta_i = \frac{\beta_{4_i} I_{M_i}}{K_{B_i}}, \delta_i = \frac{c_{2_i} I_{BC_i}}{K_{B_i}} \mu_i = \frac{c_{1_i} I_{BSC_i}}{K_{B_i}} \\ \Lambda_i = \left[b_{M_i} N_{M_i} - m_{M_i} S_{M_i}\right] \left[1 - S_{M_i}/K_{M_i}\right] \\ \Pi_i = \left[b_{B_i} - (b_{B_i} - m_{B_i}) \frac{N_{B_i}}{K_{B_i}}\right] \end{aligned} \tag{4.3}$$

Adding up Eq. (4.1) and Eq. (4.2) gives us equations for the total mosquito and birds populations, respectively, in patch $i = 1, ..., n$: while using the notations introduced above, we get

$$\begin{aligned} \frac{dN_{B_i}}{dt} &= \Pi_i - m_{B_i} N_{B_i} - d_{BC_i} I_{BC_i} - d_{BSC_i} I_{BSC_i} \\ &+ \sum_{Z} \left(\sum_{j} p_{ij} Z_j - \sum_{j} p_{ji} Z_i \right) \end{aligned} \tag{4.4}$$

$$\frac{dN_{M_i}}{dt} = \Lambda_i - m_{M_i} N_{Mi} + \sum_{Y} \left(\sum_{j} m_{ij} Y_j - \sum_{j} m_{ji} Y_i \right) \tag{4.5}$$

Here, $Y_i = \left\{S_{M_i}, E_{M_i}, I_{M_i}\right\}$ and $Z_i = \left\{S_{B_i}, E_{BC_i}, E_{BSC_i}, I_{BC_i}, I_{BSC_i}, R_{BC_i}, R_{BSC_i}\right\}$. Let the total bird and mosquito population be denoted as N_B and N_M, respectively. Then after adding the population over all the patches, we get the following

$$\begin{aligned} \frac{dN_B}{dt} &= \sum_{i} \left(\Pi_i - m_{B_i} N_{B_i} - d_{BC_i} I_{BC_i} - d_{BSC_i} I_{BSC_i}\right) \\ &+ \sum_{i} \left[\sum_{Z} \left(\sum_{j} p_{ij} Z_j - \sum_{j} p_{ji} Z_i \right) \right] \end{aligned} \tag{4.6}$$

The double sum in Eq. (4.6) sums up to zero, i.e. $\sum_i \left[\sum_Z \left(\sum_j p_{ij} Z_j - \sum_j p_{ji} Z_i\right)\right] = 0$. Since $I_{BC_i} \leq N_{B_i}$ and $I_{BSC_i} \leq N_{B_i}$, it follows that

$$\sum_{i} \Pi_i - \sum_{i} (m_{B_i} + d_{BC_i} + d_{BSC_i}) N_{B_i} \leq \frac{dN_{B_i}}{dt} \leq \sum_{i} \Pi_i - \sum_{i} m_{B_i} N_{B_i} \tag{4.7}$$

and thus,

$$\sum_{i} \Pi_i - \max_{1 \leq i \leq n} \left(m_{B_i} + d_{BC_i} + d_{BSC_i}\right) N_{B_i} \leq \frac{dN_{B_i}}{dt} \leq \sum_{i} \Pi_i - \min_{1 \leq i \leq n} \left(m_{B_i}\right) N_{B_i} \tag{4.8}$$

From here, we can claim that $\forall t \geq 0$,

$$\min\left[\frac{\sum_i \Pi_i}{\max_{1\leq i\leq n}(m_{B_i}+d_{BC_i}+d_{BSC_i})}, N_B(0)\right] \leq N_B(t) \leq \max\left[\frac{\sum_i \Pi_i}{\min_{1\leq i\leq n}(m_{B_i})}, N_B(0)\right]. \tag{4.9}$$

In a detailed manner we can also perform the following calculations to show the boundedness beside what we have shown before. From Eq. 4.6, we can get

$$\frac{dN_B}{dt} = \sum_i \frac{dN_{B_i}}{dt} \leq \sum_i \Pi_i - m_{B_i} N_{B_i} \tag{4.10}$$

If we apply the standard comparison theorem (Lakshmikantham, Leela, and Martynyuk, 1989) then we can get

$$N_{B_i}(t) \leq N_{B_i}(0)e^{-\sum_i m_{B_i} t} + \frac{\sum_i \Pi_i}{\sum_i m_{B_i}}(1 - e^{-\sum_i m_{B_i} t}) \tag{4.11}$$

Therefore, the total population of local birds is bounded. similarly, we can also get the similar expression for the total mosquito and it is also bounded.

$$N_{M_i}(t) \leq N_{M_i}(0)e^{-\sum_i m_{M_i} t} + \frac{\sum_i \Lambda_i}{\sum_i m_{M_i}}(1 - e^{-\sum_i m_{M_i} t}) \tag{4.12}$$

In a similar fashion, when we construct the metapopulation model system associated with the migratory birds (please see Eq. (3.4) for the local model without the movements amongst the patches) and it is following

$$\begin{aligned}
\frac{dS_{Bm_i}}{dt} &= \left[b_{Bm_i} - (b_{Bm_i} - m_{Bm_i})\frac{N_{Bm_i}}{K_{Bm_i}}\right] - m_{Bm_i} S_{Bm_i} - \frac{\beta_{5_i} I_{M_i} S_{Bm_i}}{K_{Bm_i}} \\
&+ \sum_j t_{ij} S_{Bm_j} - \sum_j t_{ji} S_{Bm_i} \\
\frac{dE_{Bm_i}}{dt} &= \frac{\beta_{5_i} I_{M_i} S_{Bm_i}}{K_{Bm_i}} - m_{Bm_i} E_{Bm_i} - \gamma_{Bm_i} E_{Bm_i} \\
&+ \sum_j t_{ij} E_{Bm_j} - \sum_j t_{ji} E_{Bm_i} \\
\frac{dI_{Bm_i}}{dt} &= \gamma_{Bm_i} E_{Bm_i} - m_{Bm_i} I_{Bm_i} - \alpha_{9_i} I_{Bm_i} - d_{Bm_i} I_{Bm_i} \\
&+ \sum_j t_{ij} I_{BC_j} - \sum_j t_{ji} I_{BC_i} \\
\frac{dR_{Bm_i}}{dt} &= \alpha_{9_i} I_{Bm_i} - m_{Bm_i} R_{Bm_i} + \sum_j t_{ij} R_{Bm_j} - \sum_j t_{ji} R_{Bm_i}
\end{aligned} \tag{4.13}$$

Here, t_{ij} represent the rate of migration between two arbitrary patches j and i of the migratory birds and and $t_{ii} = 0$. Let us assume that T is the movement matrix of migratory birds and the elements of T are defined as $T_{ij} = t_{ij}$ for $i \neq j$ and $(T)_{ii} = -\sum_{j=1}^{n} t_{ji}$. In a Matrix form the above

Eq. (4.13) can be written as

$$\begin{aligned}
\dot{\mathbf{S}_{\mathbf{Bm}}} &= \mathbf{\Psi} - diag(\xi + m_{Bm})\mathbf{S_{Bm}} + T\mathbf{S_{Bm}} \\
\dot{\mathbf{E}_{\mathbf{Bm}}} &= diag(\xi)\mathbf{S_B} - diag(\gamma_{Bm} + m_B)\mathbf{E_{Bm}} + T\mathbf{E_{Bm}} \\
\dot{\mathbf{I}_{\mathbf{Bm}}} &= diag(\gamma_{Bm})\mathbf{E_{Bm}} - diag(\alpha_9 + m_{Bm} + d_{Bm})\mathbf{I_{Bm}} + T\mathbf{I_{Bm}} \\
\dot{\mathbf{R}_{\mathbf{Bm}}} &= diag(\alpha_9)\mathbf{I_{Bm}} - diag(m_{Bm})\mathbf{R_{Bm}} + T\mathbf{R_{Bm}}
\end{aligned} \tag{4.14}$$

Symbolically speaking, if we denote the dependent variables as $\mathbf{Z_{Bm}}$, where $\mathbf{Z_{Bm}} = (\mathbf{S_{Bm}}, \mathbf{E_{Bm}}, \mathbf{I_{Bm}}, \mathbf{R_{Bm}})$, respectively, then $\mathbf{Z_{Bm}} = (Z_{Bm_1}, ..., Z_{Bm_n})^T$ and

$$\mathbf{\Psi}_i = \left[b_{Bm_i} - (b_{Bm_i} - m_{Bm_i})\frac{N_{Bm_i}}{K_{Bm_i}} \right], \xi_i = \frac{\beta_{5_i}\mathbf{I_{M_i}}}{K_{Bm_i}} \tag{4.15}$$

For a detailed descriptions of the model parameters please see the Table A.1 and the Section 3.3.1

Similarly, we can reframe Eq. (4.1) and Eq. (4.2) into the matrix form as follow:

$$\begin{aligned}
\dot{\mathbf{S}_{\mathbf{M}}} &= \mathbf{\Lambda} - diag(\delta + \mu)\mathbf{S_M} + M\mathbf{S_M} \\
\dot{\mathbf{E}_{\mathbf{M}}} &= diag(\delta + \mu)\mathbf{S_M} - diag(\gamma_M + m_M)\mathbf{E_M} + M\mathbf{E_M} \\
\dot{\mathbf{I}_{\mathbf{M}}} &= diag(\gamma_M)\mathbf{E_M} - diag(m_M)\mathbf{I_M} + M\mathbf{I_M}
\end{aligned} \tag{4.16}$$

Similarly, if we denote the dependent variables as $\mathbf{Z_M}$, where $\mathbf{Z_M} = (\mathbf{S_M}, \mathbf{E_M}, \mathbf{I_M}, \mathbf{R_M})$, respectively, then $\mathbf{Z_M} = (Z_{M_1}, ..., Z_{M_n})^T$. The birth terms are described in Eq. (4.3). For the local birds:

$$\begin{aligned}
\dot{\mathbf{S}_{\mathbf{B}}} &= \mathbf{\Pi} - diag(\lambda + \eta + m_B)\mathbf{S_B} + P\mathbf{S_B} \\
\dot{\mathbf{E}_{\mathbf{BC}}} &= diag(\eta)\mathbf{S_B} - diag(\gamma_{BC} + m_B)\mathbf{E_{BC}} + P\mathbf{E_{BC}} \\
\dot{\mathbf{E}_{\mathbf{BSC}}} &= diag(\lambda)\mathbf{S_B} - diag(\gamma_{BSC} + m_B)\mathbf{E_{BSC}} + P\mathbf{E_{BSC}} \\
\dot{\mathbf{I}_{\mathbf{BC}}} &= diag(\gamma_{BC})\mathbf{E_{BC}} - diag(\alpha_4 + m_B + d_{BC})\mathbf{I_{BC}} + P\mathbf{I_{BC}} \\
\dot{\mathbf{I}_{\mathbf{BSC}}} &= diag(\gamma_{BSC})\mathbf{E_{BSC}} - diag(\alpha_3 + m_B + d_{BSC})\mathbf{I_{BSC}} + diag(\gamma_3)\mathbf{R_{BSC}} \\
&+ P\mathbf{I_{BSC}} \\
\dot{\mathbf{R}_{\mathbf{BC}}} &= diag(\alpha_4)\mathbf{I_{BC}} - diag(m_B)\mathbf{R_{BC}} + P\mathbf{R_{BC}} \\
\dot{\mathbf{R}_{\mathbf{BSC}}} &= diag(\alpha_3)\mathbf{I_{BSC}} - diag(m_B + \gamma_3)\mathbf{R_{BSC}} + P\mathbf{R_{BSC}},
\end{aligned} \tag{4.17}$$

4.3 Network Generation: Constructing Movement Matrices

4.3.1 Vector Mobility Model

It is rather complicated to describe the exact mobility pathways of mosquitoes and their movement along the geospatial co-ordinates. However, we can explore the estimation about the flight range of Culex mentioned in (Myhre and Akre, 1994; Verdonschot and Besse-Lototskaya, 2014; Vinogradova, 2000). After following (Verdonschot and Besse-Lototskaya, 2014), we have observed the detailed flight range of Culex Pipiens and the average maximum distance

(m) is 9695, minimum of maximum distance (m) is 350, maximum of maximum distance (m) is 22,530 and the dispersal capacity is *strong*. The authors in (Verdonschot and Besse-Lototskaya, 2014) defined *strong* as the dispersal capacity is greater than 2km. Given their dispersal capacity, it will be better to include the precise and daily movement of the mosquitos. We will show that the mosquito movement matters in case of spreading the disease from one site i to the neighbouring site j. Let the distance between two patches be (i and j) as D_{ij}, then according to (Alcalay, Tsurim, and Ovadia, 2017), the dispersal rates between two sub-populations ($M_{i,j}$) are assumed to follow negative-exponential distribution. But in our modelling effort, we follow the distribution proposed by (Moulay and Pigné, 2013) as it was relatively simpler. Here, we have used the fact that Culex pipens have *strong* dispersal capability, henceforth the D_{max} used by (Moulay and Pigné, 2013) is different than what we have considered (Verdonschot and Besse-Lototskaya, 2014) but the dispersal probability is a function of the linear decreasing distance as in (Moulay and Pigné, 2013). According to (Moulay and Pigné, 2013), D_{max} is defined to be the maximum interaction radius of mosquitoes. The dispersal network with such linear dispersal kernel is calculated as follows:

Algorithm 1 Mosquito movement network algorithm

procedure MosNet(i, j) ▷ Routine to create link between i and j
  $D_{ij} \leftarrow Euclidean\_Distance$(i, j) ▷ Euclidean distance between i and j
  $D_{max} \leftarrow Maximum\_Distance$(i,j) ▷ Maximum distance between i and j
  $p(D_{ij}) \leftarrow \frac{D_{max}-D_{ij}}{D_{max}}$
  $p_{rand} \leftarrow rand$(0,1) ▷ Generate a random number between 0 and 1
  if $p_{rand} < p(D_{ij})$ **then**
    Create an undirected link between i and j
  end if
end procedure

As an example of such generated mosquito network after using the Algorithm: 1 is shown in Fig. 4.1.

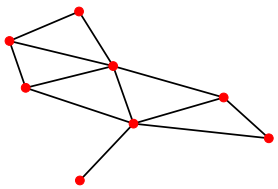

FIGURE 4.1: One realisation of the stochastic network of mosquito

Due to the uncertain and dynamic nature of mosquito movements and activities in a habitat patch, their structural and behavioural movements are not deterministic in nature. Henceforth, to employ deterministic networks for modelling and analysis of the potential spread of WNV may not be appropriate and the stochastic networks will be apt for this situation.

4.3.2 Host Mobility Model

Local Bird Mobility Model

Local birds can fly long or short distance in foraging for resources and often require to alternate between the searching for foods and finding potential mates (Beal, 2018; Butler, Templeton, and Fernández-Juricic, 2018; Cohen and Todd, 2018), consequently, benefitting from it. It is rather a complicated process to decipher their movements and flight patterns. As a result to construct a network including the exact pathways of the local birds is itself a challenging issue. So we decide to follow the seed dispersal model (Da Silveira et al., 2016; Donoso et al., 2016-12-01; Levey, Tewksbury, and Bolker, 2008; Banños-Villalba et al., 2017). We have used the seed dispersal as a proxy for the movement network of the birds. The dispersal probability is of Weibull distribution type (Carlo and Morales, 2008; Nathan et al., 2008; Nogales et al., 2012; Calviño-Cancela et al., 2006; Herrmann et al., 2016; M., Bicca-Marques, and Chapman, 2018).

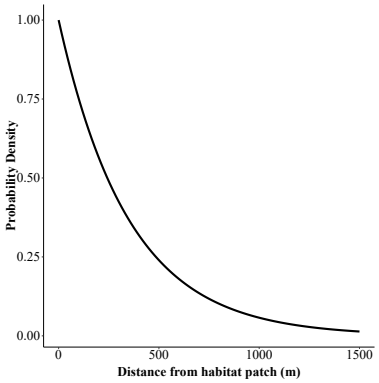

FIGURE 4.2: Dispersal probability of the bird

To construct the movement matrix (P) of the local birds (both the clinical and subclinical), we have made use of similar routine just the way we have constructed the mosquito movement network (M) in Algorithm: 1. It is to be noted that the probability that a subclinical bird will fly from one habitat patch to another habitat patch is higher compared to a clinical bird and we have utilised it while performing the simulations.

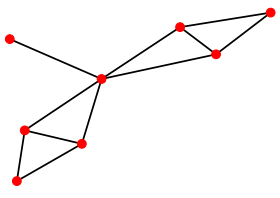

FIGURE 4.3: One realisation of the stochastic network of local bird

An example of such generated local bird network is shown in Fig. 4.3.

Migratory Bird Mobility Model

Power-law behaviour is ubiquitous in various topics. Its presence can be noticed in the frequency of use of words (Zipf, 1950) in any human language to wars (Roberts and Turcotte, 1998; Kuby et al., 2009). Additionally, we can observe the examples of networks with power-law degree distributions as links in the world-wide-web (Barabási and Albert, 1999b), or, scientific citations (Solla Price, 1965). According to the authors in (Newman, 2005; Moon et al., 2019), power-law can exhibit frequent short-range disease transmissions with incidental long-range disease transmission routes and this kind of nature can be found in the patterns of migratory birds flight paths. Even to model the spatial dynamics of different infectious diseases, power-law transmission is employed in several occasions (Meyer and Held, 2014). For a rigorous mathematical description on the power-law generated networks, one can follow (Voitalov et al., 2019; Newman, 2003; Albert and Barabási, 2002). With such knowledge in our hands, we have established the movement matrix (N) of the long dispersal bird using a similar routine as we have done for the mosquito movement network and the local bird movement network in Algorithm: 1. It should be mentioned that to construct the dispersal networks of the migratory birds also, the distance function that we have used is Haversine distance.

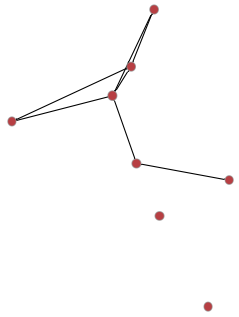

FIGURE 4.4: One realisation of the stochastic network of migratory bird

An example of such generated migratory bird network is shown in Fig. 4.4.

4.4 Mathematical Results

4.4.1 Disease-Free Equilibrium

To find the disease-free equilibrium (DFE) E_0, we consider the following matrix system

$$\begin{aligned} \Lambda - diag(\delta + \mu)S_M + MS_M &= 0 \\ \Pi - diag(\lambda + \eta + m_B)S_B + PS_B &= 0 \end{aligned} \tag{4.18}$$

or, in compact form as

$$HS = \Omega \tag{4.19}$$

where

$$H = \begin{bmatrix} diag(\delta+\mu) - M & 0 \\ 0 & diag(\lambda+\eta+m_B) - P \end{bmatrix}, S = \begin{bmatrix} S_M \\ S_B \end{bmatrix} \Omega = \begin{bmatrix} \Lambda \\ \Pi \end{bmatrix}$$

, the detailed mathematical expressions of Λ, δ, μ etc. are described in Eq. (4.3), Eq. (4.15). Since all off-diagonal entries of H are nonpositive and the sum of the entries in each column of H is positive, H is a nonsingular M-matrix, $H^{-1} \geq 0$ (Berman and Plemmons, 1979). Therefore, the linear system Eq. (4.19) has a unique positive solution $S^0 = (S^0_{M_1}, S^0_{M_2}, ..., S^0_{M_n}, S^0_{B_1}, S^0_{B_2}, ..., S^0_{B_n}) = H^{-1}\Omega > 0 \, \forall i$.

4.4.2 Basic Reproduction Number R_0 of the patchy model

To compute the basic reproduction number, we will use the *Next generation method* used by (Driessche and Watmough, 2002). Using the notation used in (Driessche and Watmough, 2002), we can decompose the model system Eq. (4.1) and Eq. (4.2) as $\boldsymbol{\mathcal{F}(\mathcal{I})} - \boldsymbol{\mathcal{V}(\mathcal{I})}$. $\boldsymbol{\mathcal{F}(\mathcal{I})}$, $\boldsymbol{\mathcal{V}(\mathcal{I})}$ represent as the flow of new infections and the remaining transfers within and out of the infected classes, respectively and the bold symbols symbolise that the elements are all vectors. For convenience and not to be repetitive about the matrix calculations of basic reproduction number, we only demonstrate the calculations related to the subclinical bird population as $\gamma_{3_i} = 0$ will give the R_0, connected with the clinical bird population.

$$\boldsymbol{\mathcal{F}_{\mathcal{BSC}}(\mathcal{I})} = \begin{bmatrix} \frac{c_{1_1} I_{BSC_1} S_{M_1}}{K_{B_1}}, & 0, & \frac{\beta_{3_1} I_{M_1} S_{B1}}{K_{B_1}}, & \gamma_{3_1} R_{BSC_1}, & \dots, \\ \frac{c_{1_n} I_{BSC_n} S_{M_n}}{K_{B_n}}, & 0, & \frac{\beta_{3_n} I_{M_n} S_{Bn}}{K_{B_n}}, & \gamma_{3_n} R_{BSC_n} & \end{bmatrix}^T$$

Using the notations used before, we have

$$\boldsymbol{\mathcal{F}_{\mathcal{BSC}}(\mathcal{I})} = \begin{bmatrix} \mu_1 S_{M_1}, & 0, & \lambda_1 S_{B1}, & \gamma_{3_1} R_{BSC_1}, & \dots, \\ \mu_n S_{M_n}, & 0, & \lambda_n S_{Bn}, & \gamma_{3_n} R_{BSC_n} & \end{bmatrix}^T$$

$$\boldsymbol{\mathcal{V}_{\mathcal{BSC}}(\mathcal{I})} = -\begin{bmatrix} -\gamma_M E_{M_1} - m_{M_1} E_{M_1} + \sum m_{1j} E_{M_j} - \sum m_{j1} E_{M_1} \\ \gamma_M E_{M_1} - m_{M_1} I_{M_1} + \sum m_{1j} I_{M_j} - \sum m_{j1} I_{M_1} \\ -\gamma_{BSC_1} E_{BSC_1} - m_{B_1} E_{BSC_1} + \sum p_{1j} E_{BSC_j} - \sum p_{j1} E_{BSC_1} \\ \gamma_{BSC_1} E_{BSC_1} - m_{B_1} I_{BSC_1} - \alpha_{3_1} I_{BSC_1} - d_{BSC_1} I_{BSC_1} + \sum p_{1j} I_{BSC_j} - \sum p_{j1} I_{BSC_1} \\ \vdots \\ -\gamma_M E_{M_n} - m_{M_n} E_{M_n} + \sum m_{nj} E_{M_j} - \sum m_{jn} E_{M_n} \\ \gamma_M E_{M_n} - m_{M_n} I_{M_n} + \sum m_{nj} I_{M_j} - \sum m_{jn} I_{M_n} \\ -\gamma_{BSC_n} E_{BSC_n} - m_{B_n} E_{BSC_n} + \sum p_{nj} E_{BSC_j} - \sum p_{jn} E_{BSC_n} \\ \gamma_{BSC_n} E_{BSC_n} - m_{B_n} I_{BSC_n} - \alpha_{3_n} I_{BSC_n} - d_{BSC_n} I_{BSC_n} + \sum p_{nj} I_{BSC_j} - \sum p_{jn} I_{BSC_n} \end{bmatrix}$$

Letting $\boldsymbol{F_{BSC}} = [\frac{\partial \boldsymbol{\mathcal{F}_{\mathcal{BSC}}}}{\partial \mathbf{W}} \mid_{(S^0, \mathbf{0})}]$ and $\boldsymbol{V_{BSC}} = [\frac{\partial \boldsymbol{\mathcal{V}_{\mathcal{BSC}}}}{\partial \mathbf{W}} \mid_{(S^0, \mathbf{0})}]$ as the Jacobian matrices evaluated at the disease free equilibrium $(S^0, \mathbf{0})$. Here, $\mathbf{W}$ represents the infectious and infected compartments i.e. $W = \mathbf{E_M}, \mathbf{I_M}, \mathbf{E_{BSC}}, \mathbf{I_{BSC}}$. Following (Driessche and Watmough, 2002), the matrix $\mathcal{NGM}_{\mathcal{BSC}} = \boldsymbol{F_{BSC}} \boldsymbol{V^{-1}_{BSC}}$ is the next generation matrix for the subclinical birds and it is well defined.

The elements of the Jacobians have the following forms

$$\frac{\partial \mu_i}{\partial E_{M_i}} = \frac{\partial \mu_i}{\partial I_{M_i}} = \frac{\partial \mu_i}{\partial E_{BSC_i}} = \frac{\partial \lambda_i}{\partial E_{M_i}} = \frac{\partial \lambda_i}{\partial E_{BSC_i}} = \frac{\partial \lambda_i}{\partial I_{BSC_i}} = 0$$
$$\frac{\partial \mu_i}{\partial E_{M_j}} = \frac{\partial \mu_i}{\partial I_{M_j}} = \frac{\partial \mu_i}{\partial E_{BSC_j}} = \frac{\partial \lambda_i}{\partial E_{M_j}} = \frac{\partial \lambda_i}{\partial E_{BSC_j}} = \frac{\partial \lambda_i}{\partial I_{BSC_j}} = 0, \quad i \neq j$$

$$\frac{\partial R_{BSC_i}}{\partial E_{M_i}} = \frac{\partial R_{BSC_i}}{\partial E_{I_i}} = \frac{\partial R_{BSC_i}}{\partial E_{BSC_i}} = \frac{\partial R_{BSC_i}}{\partial I_{BSC_i}} = 0$$
$$\frac{\partial R_{BSC_i}}{\partial E_{M_j}} = \frac{\partial R_{BSC_i}}{\partial E_{I_j}} = \frac{\partial R_{BSC_i}}{\partial E_{BSC_j}} = \frac{\partial R_{BSC_i}}{\partial I_{BSC_j}} = 0, \quad i \neq j$$

The partial derivatives are evaluated at $(S^0, \mathbf{0})$. Matrices $\boldsymbol{F_{BSC}}$ and $\boldsymbol{V_{BSC}}$ are $4n \times 4n$.

If we write down the block matrices, then we have the following:

$$\boldsymbol{F_{BSC}} = \begin{bmatrix} \mathbf{0} & \mathbf{F_{11}} \\ \mathbf{F_{22}} & \mathbf{0} \end{bmatrix} \tag{4.20}$$

where, $\mathbf{F_{11}} = diag\left(\frac{\partial \lambda_1}{\partial I_{M_1}} S^0_{B_1}, ..., \frac{\partial \lambda_n}{\partial I_{M_n}} S^0_{B_n}\right)$,
$\mathbf{F_{22}} = diag\left(\frac{\partial \mu_1}{\partial I_{BSC_1}} S^0_{M_1}, ..., \frac{\partial \mu_n}{\partial I_{BSC_n}} S^0_{M_n}\right)$. $\boldsymbol{V_{BSC}} = [\boldsymbol{V_{BSC_{ij}}}]$, where

$$\boldsymbol{V_{BSC_{ij}}} = diag\begin{bmatrix} -m_{ij} & -m_{ij} & -p_{ij} & -p_{ij} \end{bmatrix}; \quad i \neq j \tag{4.21}$$

and

$$\boldsymbol{V_{BSC_{ii}}} = \begin{bmatrix} \gamma_M + m_{M_i} + \sum m_{ji} & -\gamma_M & 0 & 0 \\ 0 & m_{M_i} + \sum m_{ij} & 0 & 0 \\ 0 & 0 & \gamma_{BSC_i} + m_{B_i} + \sum p_{ji} & -\gamma_{BSC_i} \\ 0 & 0 & 0 & m_{B_i} + \alpha_{3_i} + d_{BSC_i} + \sum p_{ji} \end{bmatrix} \tag{4.22}$$

Similarly the next generation matrix ($\mathcal{NGM}_{\mathcal{BC}}$) associated with the clinical birds is $\boldsymbol{F_{BC}} \boldsymbol{V_{BC}^{-1}}$. It is to be noted that a simple juxtaposition of two block matrices $\mathcal{NGM}_{\mathcal{BC}}$ and $\mathcal{NGM}_{\mathcal{BSC}}$ will give us above mentioned $\mathcal{NGM}$ for the whole model system Eq. (4.1) and Eq. (4.2). The calculations performed for the non-spatial case in the Section 3.4 can demonstrate the simpler computations of $\mathcal{NGM}$ and the juxtapositions of two block matrices $\mathcal{NGM}_{\mathcal{BC}}$ and $\mathcal{NGM}_{\mathcal{BSC}}$. After including clinical and sub-clinical birds in different patches, unified next generation matrix ($\mathcal{NGM}$) of the system Eq. (4.1) and Eq. (4.2) is $\mathcal{NGM} = \begin{bmatrix} \mathcal{NGM}_{\mathcal{BC}} & \mathcal{NGM}_{\mathcal{BSC}} \end{bmatrix}$.

So, the basic reproduction number is

$$\mathcal{R}_0 = \rho(\mathcal{NGM}) \tag{4.23}$$

where ρ is the spectral radius of the matrix $\mathcal{NGM}$. The analytical closed form of spatial $\mathcal{R}_0$ is cumbersome to continue with but the non-spatial $\mathcal{R}_0$ is relatively simpler to find and one can clearly observe the additive characteristics of $\mathcal{R}_0$ mentioned in Eq. (3.7) and the additive feature remains the same for Eq. (4.23). Additionally, one can also observe the inclusion of the migration rates of the vector and the host populations into the Jacobians and consequently, into the $\mathcal{NGM}$. According to Driessche and Watmough,

2002, the local stability of the disease free equilibrium $E_0 = (S^0, \mathbf{0})$ is governed by $\mathcal{R}_0$. If $\mathcal{R}_0 < 1$, then E_0 is asymptotically unstable and unstable whenever $\mathcal{R}_0 > 1$.

4.5 Simulations and Results

The study area comprised of 11,054 German Gemeinden (Municipalities). We use the deterministic metapopulation Eq. (4.16), Eq. (4.17) and Eq. (4.14) to apprehend the WNV transmission in the local bird populations in each Gemeinde. We explicitly demonstrate the vector population and the mobility in the simulations. But we do not have the either the population distribution of birds or the mosquito across the different Gemeinden level.

Keeping this in mind we at first keep all the local birds initially susceptible in all the Gemeinden then we introduce I_{Inf} number of infected migratory birds in selected Gemeinden. The first case of WNV was detected in Halle, a city in Saxony-Anhalt, Germany (Ziegler et al., 2020; Michel et al., 2018). This is why for the first season simulation the infection is seeded in the city Halle.

Three different contact networks are incorporated for the simulations in between-Gemeinden movements of vectors and the hosts.

(I) The vector network, representing the mosquito flies

(II) The local birds network, represents the movements of the local birds in a habitat patch and

(III) The migratory birds network, represents sporadic movements of the migratory birds ranging long distance flight pathways.

The nodes are the centroid of Gemeinden and the links amongst them are formed after employing all the different algorithms (please see 4.3.1, 4.3.2, 4.3.2 for detailed descriptions) are devised for the network generations. In the Fig. 4.5, we plot the migratory birds pathway being constructed through the power-law distance based kernel. In order to mimic the presence of the migratory birds in Germany, the network associated migratory birds are active for six months and the rest of the year it remains inactive.

In the simulations, we observe the spread of infection of each newly infected Gemeinden. Previously, WNV free Gemeinden might be infected through different networks that we have considered. In order to facilitate the stochastic nature the network generation process, we have evaluated the results after multiple realisations i.e. under different networks of the interacting species. We have considered 10 realisations of these stochastic networks while performing the spatial spread of WNV in Germany. After that, we register the cumulative number of infected birds, both the local and the migratory birds in each season of WNV circulation per Gemeinden in Germany and average it per realisation as presented in Fig. 4.6.

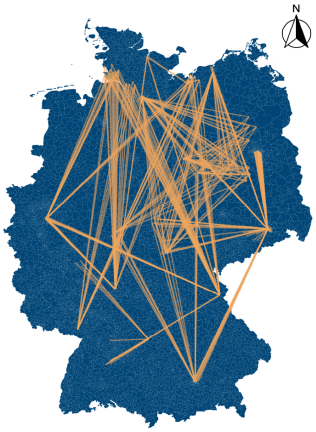

FIGURE 4.5: Dispersal networks for power-law distance based kernel of migratory birds in Germany described in the section 4.3.2.

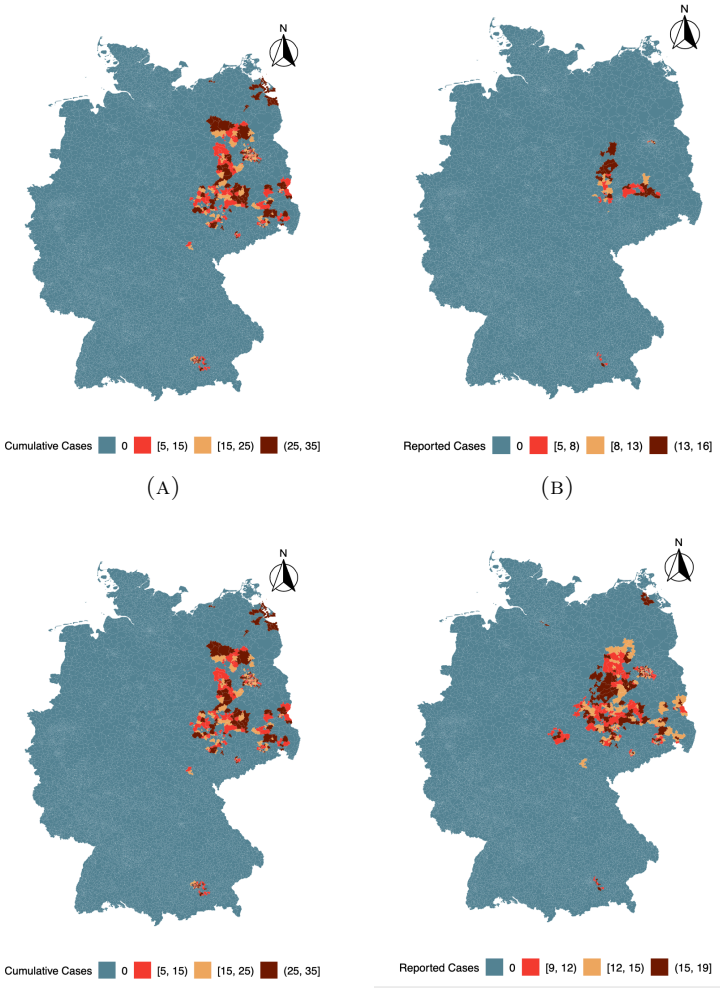

(A) (B)

(C) (D)

FIGURE 4.6: (a) Potential spatial spread of WNV in Germany after season 1 (b) Cumulative reported cases of WNV in Gemeinden, Germany in 2018, data from (*TSIS*) (c) Potential spatial spread of WNV in Germany after season 2 (d) Cumulative reported cases of WNV in Gemeinden, Germany in 2019, data from (*TSIS*).

Simulated infection dissemination data can help us to project the spatial spread of WNV on the map of Germany. Complementarily to Fig. 4.5, we include in Fig. 4.6 further simulation results on the temporal and spatial changes of WNV. We compute the cumulative number of infected birds within each region while assuming that the disease moves from the seeding zone to the other places through the combinations of the different spatial dispersal networks after running the simulations i.e. when we include multiple realisations of stochastic network generation process. In the Fig. 4.6a and Fig. 4.6b, we can visualise the spatial distribution of potential WNV cases while incorporating the probable spatial transmission of WNV in Germany and the cumulative reported cases of WNV in the year 2018 according to the counting per Gemeinden polygon (*TSIS*).

Here, the Gemeinden polygons are defined as the geometric boundaries or the shapes of each municipalities in Germany. We simulate the same for the next season. It appears that by the end of the WNV season 1, apparently the spatial spread of WNV infection is mostly restricted within the eastern zone of Germany with some spontaneous cases in the north and in the southern zones.

Fig. 4.6c depicts the simulated possible spatial spread of WNV in Germany and in Fig. 4.6d, cumulative reported cases of WNV in the year 2019 according to the counting per Gemeinden polygons are noted. It is interesting to notice that WNV is circulating in the previously detected Gemeinden along with newly infected zones in the contiguous regions of Germany. We can infer that the bite of WNV is far reaching in Germany with the cases of WNV on the move through the spatial dispersal of migratory birds. The spatial transmission of WNV range with the theoretical predictions and this depicts the dependence of spatial spread of WNV into the newer zones and the flyways of migratory birds, even though the newly infected zones are relatively far geographically. It is to be noted that in mechanism of infection dynamics, a fraction of the local bird population which are subclinically infected can recover and susceptible to the WNV and can be re-infected while flying from one habitat patch to another one. Therefore, this process increases the infected subclinical population and keeps the disease cycle alive in the local scale and the higher migration rates of the subclinical birds facilitates the potential dissemination of WNV in Germany. Finally, we would like to mention two things.

(I) Subclinical transmission should accelerate the disease dynamics although the qualitative behaviour of the potential geographical distribution of WNV cases may not be affected. Please see the Sections 3.5.3 and 3.5.7 for the local model as the similar features can be observed in the patchy model too.

(II) We can remark that our deterministic metapopulation-network modelling approach permit us to measure the significant role of migratory birds dispersal in the spatial spread of WNV in Germany.

4.5.1 Structural Similarity Index (SSIM)

With the intention to compare and qualify the spatial predictions of the simulations with the real reported case scenario, we utilise the *structural similarity index*. The Structural SIMilarity (SSIM) index (Zhou Wang et

al., 2004) is a method through which one can measure the similarities between two images, but it can also be applicable in comparing the structural properties of any other 2-dimensional data, i.e. the spatial distribution of WNV cases in our case. The computing formula for the SSIM is following:

$$SSIM(x, y) = \frac{(2\mu_x\mu_y + c_1)(2\sigma_x + c_2)}{(\mu_x^2\mu_y^2 + c_1)(\sigma_x^2 + \sigma_y^2 + c_2)} \tag{4.24}$$

where x and y are appropriate-sized windows of the images to compare, μ_x and μ_y are the average of x and y, σ_x^2 and σ_y^2 are the variances of x and y while σ_{xy} is the covariance of x and y. Here, x and y are two nonnegative image signals. In our work, we have assumed the values of x and y are to be 8. The parameters $c1 = (k_1L)^2$,$c_2 = (k_2L)^2$ are two variables to stabilise the division with a weak denominator, where L is the dynamic range of the discrete pixel values. The two additional parameters are $k_1 = 0.01$ and $k_2 = 0.03$ by assumption. To obtain a similarity metric between two outputs, the SSIM values are averaged over all possible subsections of the images, defined by sliding windows of size 8×8 pixels in our work. The range of the value of the SSIM index is between 0 and 1. Two images are nearly identical when their SSIM is close to 1. For each epidemiological week in the period we compute the SSIM between the reported WNV cases and the simulated scenarios.

To understand the difference between the simulated and the observed data, we have used structural similarity (SSIM) index (Massaro, Kondor, and Ratti, 2019) in each epidemiological season, with the proper choices for mosquito to bird ratio (ϕ) and compare their distribution in Fig. 4.7. We compute SSIM score for each epidemiological season during the WNV

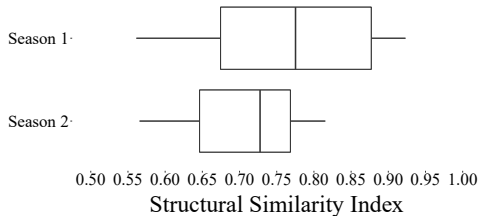

FIGURE 4.7: Spatial analysis of model outcome and the reported cases of WNV in Germany during the $2018 - 2019$ outbreaks. The variations come after running different realisations.

outbreaks in Germany after 10 different realisations of the potential spatial spread of WNV in Germany. In these realisations, due to the stochastic nature of our network generating algorithms, different network structures or geographies are being utilised of the interacting species. We endeavour to compute the SSIM score for each epidemiological season of WNV outbreaks in Germany after aggregating the cumulative number of infected local birds per Gemeinden polygon. The distribution of SSIM scores or index are shown as boxplots for each epidemiological season. These boxplots can help us to understand the strength of our model while accounting the minimum, 1^{st} quartile, median and 3^{rd} quartile and the maximum of computed SSIM values. It is noticeable the range of SSIM scores in the second season is comparatively smaller to that off in the previous season. We have used the

following algorithm (Algorithm 2) to produce the boxplots associated with the outcomes from the simulations and the reported cases per Gemeinden in Germany.

Algorithm 2 To Calculate SSIM Array

1: **procedure** SSIM_ARRAY(Im_A, Im_B) ▷ Compute SSIM Scores
2: Im_A ▷ Cumulative reported cases of WNV per Gemeinde
3: Im_B_i ▷ Cumulative simulated cases of WNV per Gemeinde per 10 realisations
4: $SSIM_i \leftarrow$ STRUCTURAL _SIMILARITY(Im_A, Im_B_i) ▷ Python function (Walt et al., 2014)
5: Return $SSIM_i$
6: **end procedure**

We can notice that in the initial phase of WNV spread in Germany, the model performs well while approximating the observed spatial dissemination. In the following season though the performance of the model is slightly worse compared to the results from the previous season. This actually highlights the challenges and the complexities of such spreading process. Nevertheless, the performance of the model is satisfactory in the backdrop of limited information that we have at this stage of our current study.

4.6 Conclusion of this section

We analysed the potential spatial spread of WNV in Germany through the combinations of the movement matrices of interacting species. Our main observations are following: First, the importance of the movement of the vector in the spatial transmission of WNV and its role in escalating the value of $\mathcal{R}_0$ (Please see the mathematical forms of Eq. (4.20), Eq. (4.21), Eq. (4.22) as they include the migration rates of the vector population and it is absent when we discussed the same for the local model in the Section 3.4 and the migration rates of the vector population will be included in Eq. (4.23)). This implies that a lot of information will be lost while modelling such a global spatial spread of vector-borne disease if we ignore the vector movement entirely in the local scale.

Second, the significant role played by the migratory birds is demonstrated through devising the networks generated through the similar algorithm 1 as described in section 4.3.2. Transmission of WNV in Germany can likely be estimated through the trajectories of the migratory birds in Germany and consequently sustaining it through the favourable temperature and the movements of local birds from one habitat patch to the other ones.

Third, the algorithm 2, employed to test the strength of our modelling assumptions and the methodologies to compare with the real outbreaks of WNV in Germany, is able to catch the likely spread of WNV fairly well (see Fig. 4.7). SSIM score (Eq. (4.24)) is a handy tool to analyse the comparative studies of the reported cases of WNV seasonally.

Finally, the observations above raise two questions for the context of epidemics on networks:

1. How do the generated links of the migratory birds affect the WNV outbreak in Germany?

2. What is the role of the vector in transmission of WNV?

In order to answer these questions, we generated the flight networks that allow for a spatial projections to comprehend the nature of WNV spread in Germany and solved an infection model coupled with the vector mobility, tailor made for such a case. Our main findings are that the links created by the host populations are of utter importance and the local links created by the vector populations are essential to sustain the bite of WNV locally and hence it has an ever reaching potential.

CHAPTER 5

Mathematical Model of CCHFV Spread And Its Control

This chapter includes the materials from the paper : " Ticks on the run: A mathematical model of Crimean-Congo Haemorrhagic Fever (CCHF)-key factors for transmission" (Bhowmick et al., 2022).

In the previous chapters we have demonstrated that the locally weather driven ODE system can provide a deep insight into the processes behind WNV spreading. Additionally, we incorporate the movement patterns of both the vectors and the hosts (birds) to asses the potential spread of WNV in Germany. Given the developed ODE model of WNV spread in Germany in section 3.3, we can quantify the dissemination of epidemics locally and spatially. Having the necessary toolbox of mathematical methods that has been developed in the previous chapters, we model another potential disease Crimean Congo Haemorrhagic Fever, a tick-borne disease that has followed the same footprint of WNV, engulfing Germany. Fig. 5.1 depicts the increasing trend of reported cases of CCHF in EU.

However, since CCHFV is a tick-borne disease, the mathematical formulation of the model should be changed accordingly and the mathematical treatment of the same shall be somewhat different than what we have analysed in the previous chapter (Matser et al., 2009). For tick-borne diseases, the interpretation of R_0 is less intuitive as there are different infected types involved in transmission mechanism, that is, multiple hosts types and vectors (Hartemink et al., 2008). This chapter describes and analyses some of the theoretical challenges due to the complexities of such tick-borne disease models.

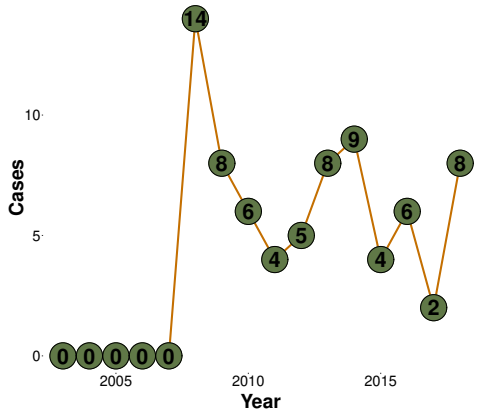

FIGURE 5.1: Reported human cases of CCHFV in EU.

5.1 Introduction

To begin with, we would like to highlight the difference between the model developed in section 3.3 and our current effort. Particularly we show the intricacies and the inherited challenges with the modelling endeavour that can gauge the relative importance of different routes for the establishment of a tick-borne disease. Fig. 5.2 shows the presence of multiple hosts along with the different paths of CCHFV transmission and it represents the transmission cycle of CCHFV. The thickness of the arrow represents the transmission probabilities during the lifecycle of *Hyalomma* ticks. Usually in purely a vector-host transmission model the average number of hosts infected by a vector and conversely, the number of vectors infected by a host, is actually averaged.

In this kind of model, when we take the product of the host to vector and vector to host basic reproduction yields number of infected hosts but in our model system having the presence of more number of hosts and vector species along with the additional transmission paths which makes the usage of the direct method futile but the mathematical formulations and the techniques are being developed in the previous chapter principally the very same.

In this chapter, we derive an analytic expression for R_0 for tick-borne CCHFV based on Next Generation Matrix (NGM) approach. We then parameterise the NGM for CCHF. The sensitivity and elasticity analysis of R_0 can provide the great details about the transmission parameters which can be used for control while taking account of multiple host and interacting population.

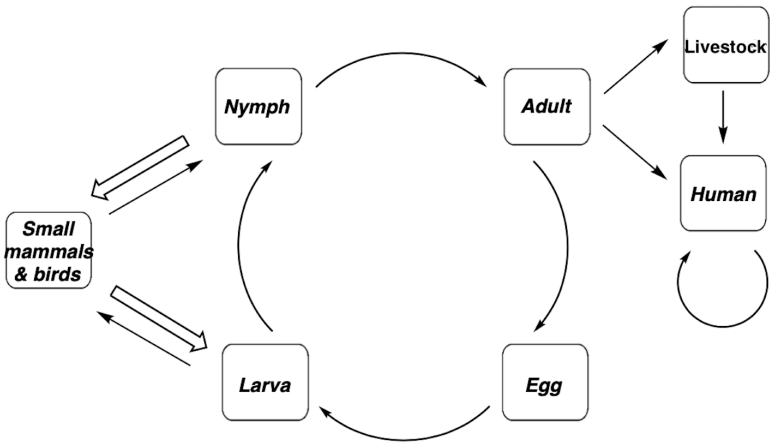

FIGURE 5.2: Life cycle of *Hyalomma*

5.1.1 Biological framework

Crimean-Congo Haemorrhagic Fever is a tick-borne zoonotic disease maintained in nature in an enzootic vertebrate-tick-vertebrate cycle caused by the CCHFV (Logan et al., 1989; Gonzalez et al., 1992; Spengler and Estrada-Peña, 2018). CCHFV persists in the ticks for their whole lifespan (Gargili et al., 2017). It is transmitted within the tick population by transstadial, venereal (transstadial transmission is defined to be the sequential passage of parasites acquired during one life stage, through the molt to the next stage and venereal transmission can be characterised as the infections that are passed from one person to another through sexual contact)and by co-feeding (Logan et al., 1989; Gonzalez et al., 1992). Ticks belonging to the genus *Hyalomma* are the main vector and reservoir for the above said virus (Gargili et al., 2017). CCHFV is prevalent in wide geographical areas including Asia, Africa, South-Eastern Europe and the Middle East (Zhang et al., 2018; Chinikar et al., 2010; Messina et al., 2015). Several outbreaks of CCHF have been observed in Europe, primarily in the Balkan and mediterranean countries in the last decades. Given the high mortality rate of CCHF amongst human, it carries a high threat towards the public health (Sas et al., 2018). Due to the global warming and the increase in habitat suitability of the ticks carrying (*Hyalomma*) CCHFV, a possible establishment of *Hyalomma* is foreseeable for the coming years (House, Turell, and Mebis, 1992; Hansford et al., 2019; Okely et al., 2019).

CCHFV is transmitted to human either by tick bites, by contact with infected animal blood, body fluids. People involved in the livestock industry and veterinarians are more vulnerable to CCHFV. Human-to-human transmission occurs while having close contact with the blood, secretions, organs or other bodily fluids of infected patients. Nosocomial infection (it is described as a hospital-acquired infection) can also happen during the treatment of the CCHFV infected patients. CCHF is considered as an important vector borne disease as it creates a severe illness and a high case fatality in humans (Chinikar et al., 2010).

A significant amount of effort has been taken to model tick borne diseases but most of the mathematical work is primarily limited to some specific tick-borne disease like Lyme disease (Lou and Wu, 2017) and some of them are

general frameworks (Gaff and Gross, 2007). Only a handful of mathematical attempts have been taken to model the spread of CCHFV (Switkes et al., 2016; Cooper, 2007). There are several epidemiological works explaining various aspect of CCHFV and its corresponding biology and the Ribonucleic acid (RNA)structure (Chinikar et al., 2010; Hawman and Feldmann, 2018; Emmerich et al., 2018; Gargili et al., 2017) of CCHFV. In (Abbas et al., 2017), the authors have used a distributed lag nonlinear model (DLNM) to explore the relationship between the cases of CCHF and the temperature. The authors in (Mostafavi et al., 2013) have used a Poisson regression analysis to explore the predicting factors of CCHF in Zabol and Zahedan, Iran. The authors in (Hoch et al., 2016) have calculated the basic reproduction number (R_0) to analyse the potential scenarios for determining the control of CCHFV spread. Sensitivity analysis performed in (Hoch, Breton, and Vatansever, 2018) for various parameter values revealed the importance of transstadial transmission while including the different environmental factors. It also contains the different stage structures of *Hyalomma* and their feeding behaviour but it does not include the dissemination of CCHFV in humans. From the perspective of deterministic modelling, a limited number of modelling endeavours have been carried out (Switkes et al., 2016). The authors in (Switkes et al., 2016) have developed a deterministic system of nonlinear differential equations including different transmission routes (SI-SEIR type) and analysed the threshold parameters. This modelling effort lacks the potent role of humans as humans are an integral part of the transmission cycle and they play a major role in detecting the disease due to the high case/fatality ratio in humans as well as the authors did not include the complete possible control measures to curb the infection spread in different geographical areas. Moreover, in case of transient epidemics [1], the behaviour of average system predicted by R_0 can be different. Keeping that in mind we calculate a recently described, epidemiological metric $\mathscr{E}_0$ (Hosack, Rossignol, and Driessche, 2008) that quantifies the reactivity, or epidemicity, of the system. This can be helpful to understand the disease dynamics in countries like Germany. Based on previously described models, we refine our model by including human infections in our current work.

5.2 Mathematical Model

To model the dynamics of CCHFV infection what includes adult ticks, livestock, and human we have followed certain assumptions and these are following: (1) Homogenous mixing is assumed among all the interacting population at all stages and the CCHFV infection does not alter their movements, (2) livestock has more contacts with adult ticks than with other life-stages of ticks, (3) biting rates of ticks are assumed to be at constant rates in all infection stages (susceptible, exposed and infected), (3) CCHFV infection in *Hyalomma* ticks does not affect the birth or death rates of ticks, (4) livestock will not die of CCHFV infection (Gargili et al., 2017), but for humans we included disease induced deaths (Sas et al., 2018). To simplify the model and the complexity of the model, only the adult stage of ticks is included in the model.

[1] i.e., outbreaks that can fade out in due course of time

We have employed a compartmental model consisting of three interacting populations: human, adult ticks and livestock (Fig. 5.3).

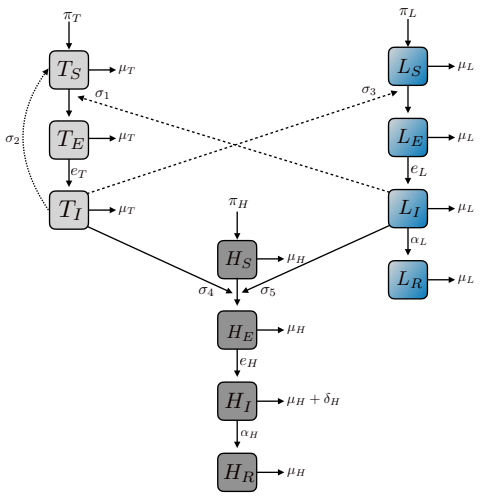

FIGURE 5.3: Infection process among adult ticks, livestock and human.

Our model has four different health status: the S classes are susceptible individuals, the E classes are exposed – i.e. infected but non-infectious – individuals, the class I are infectious ones, and R consists of recovered and immune individuals. Only the individuals in the I class can potentially infect the susceptible ones. In ticks, persistence of the virus is of life long (Papa et al., 2017) . Thus, it does not include an R class. From the point of view of population growth birth rates in the model system are constants, and in the absence of CCHF, the susceptible populations converge to the disease-free equilibrium point exponentially. In the adult tick population, we have taken into consideration SEI dynamics since the tick remains infected for life (Gargili et al., 2017), and for the livestock and human populations we have considered SEIR type dynamics.

Overall, the scheme explained above yields the following system of differential equations (a summary of the parameters and variables is given in Tables B.1 and B.2):

For the adult tick population we have:

$$\begin{aligned} \frac{dT_S}{dt} &= \pi_T - \frac{\sigma_1 T_S L_I}{L} - \frac{\sigma_2 T_S T_I}{T} - \mu_T T_S \\ \frac{dT_E}{dt} &= \frac{\sigma_1 T_S L_I}{L} + \frac{\sigma_2 T_S T_I}{T} - \mu_T T_E - e_T T_E \\ \frac{dT_I}{dt} &= e_T T_E - \mu_T T_I \end{aligned} \tag{5.1}$$

Before I present the livestock model equations Eq. (5.2), the description of the parameters defined in Eq. (5.1), are following: reproduction rate is π_T, mortality rate is μ_T, livestock-to-tick infection transmission rate is σ_1, non-systemic transmission rate is σ_2 (through co-feeding), $1/e_T$ is incubation period in tick, L is the total number of livestock.

The livestock population is described by the following system of equations:

$$\begin{aligned}
\frac{dL_S}{dt} &= \pi_L - \frac{\sigma_3 L_S T_I}{L} - \mu_L L_S \\
\frac{dL_E}{dt} &= \frac{\sigma_3 L_S T_I}{L} - e_L L_E - \mu_L L_E \\
\frac{dL_I}{dt} &= e_L L_E - \alpha_L L_I - \mu_L L_I \\
\frac{dL_R}{dt} &= \alpha_L L_I - \mu_L L_R
\end{aligned} \tag{5.2}$$

The model parameters associated with Eq. (5.2) can be described as following: π_L and μ_L are the reproduction number and the mortality rates, respectively. σ_3 is the transmission rate from tick to livestock, $1/\alpha_L$ is the recovery period of livestock, $1/e_L$ is incubation period in livestock.

The human population is described by the following system of equations:

$$\begin{aligned}
\frac{dH_S}{dt} &= \pi_H - \frac{\sigma_4 H_S T_I}{H} - \frac{\sigma_5 H_S L_I}{H} - \mu_H H_S \\
\frac{dH_E}{dt} &= \frac{\sigma_4 H_S T_I}{H} + \frac{\sigma_5 H_S L_I}{H} - e_H H_E - \mu_H H_E \\
\frac{dH_I}{dt} &= e_H H_E - \alpha_H H_I - \mu_H H_I - \delta_H H_I \\
\frac{dH_R}{dt} &= \alpha_H H_I - \mu_H H_R
\end{aligned} \tag{5.3}$$

Now, I describe the model parameters defined in 5.3. π_H and μ_H are the reproduction number and the mortality rates, respectively. $1/\alpha_H$ is the recovery period of human, $1/e_H$ is incubation period in human, σ_5 is the transmission rate from livestock to human, σ_4 is the transmission rate from tick to human, δ_H is the CCHF-induced death rate.

5.2.1 Basic Reproduction Number R_0

We would like to know under which condition the virus can spread in an initially susceptible population, when a single infected individual is introduced. The epidemiological metric R_0 can help us to find this. We first find the disease free equilibrium E_0, which is a fixed point of the system Eq. (5.1), Eq. (5.2), Eq. (5.3). It is given by

$$E_0 = (T_S^*, 0, 0, L_S^*, 0, 0, 0, H_S^*, 0, 0, 0) = \left(\frac{\pi_T}{\mu_T}, 0, 0, \frac{\pi_L}{\mu_L}, 0, 0, 0, 0, \frac{\pi_H}{\mu_H}, 0, 0, 0, 0\right).$$

If the disease free equilibrium E_0 is stable, the disease dies out before it can infect individuals, and it can spread over the population if E_0 is unstable. The stability condition for E_0 can be as $R_0 > 1$ (Keeling and Rohani, 2011). To compute the basic reproduction number, we use the *Next Generation Matrix* method (NGM) as described in 2.2.4. We find the matrices related to the new infection (transmission matrix) $\mathcal{F}$ and the remaining transfers

(transition matrix) $\mathcal{V}$ as

$$\mathcal{F} = \begin{pmatrix} 0 & \frac{T_S^*\sigma_2}{T} & 0 & \frac{T_S^*\sigma_1}{L} & 0 & 0 \\ 0 & 0 & 0 & 0 & 0 & 0 \\ 0 & \frac{L_S^*\sigma_3}{L} & 0 & 0 & 0 & 0 \\ 0 & 0 & 0 & 0 & 0 & 0 \\ 0 & \frac{H_S^*\sigma_4}{H} & 0 & \frac{H_S^*\sigma_5}{H} & 0 & 0 \\ 0 & 0 & 0 & 0 & 0 & 0 \end{pmatrix}$$

and

$$\mathcal{V} = \begin{pmatrix} e_T + \mu_T & 0 & 0 & 0 & 0 & 0 \\ -e_T & \mu_T & 0 & 0 & 0 & 0 \\ 0 & 0 & e_L + \mu_L & 0 & 0 & 0 \\ 0 & 0 & -e_L & \alpha_L + \mu_L & 0 & 0 \\ 0 & 0 & 0 & 0 & e_H + \mu_H & 0 \\ 0 & 0 & 0 & 0 & -e_H & \alpha_H + \delta_H + \mu_H \end{pmatrix}.$$

For the next generation matrix $\mathcal{K}_\mathcal{L} = -\mathcal{F}\mathcal{V}^{-1}$, we get

$$\mathcal{K}_\mathcal{L} = \begin{pmatrix} \frac{T_S^* e_T \sigma_2}{T(e_T+\mu_T)\mu_T} & \frac{T_S^*\sigma_2}{T\mu_T} & \frac{T_S^* e_L \sigma_1}{L(\alpha_L+\mu_L)(e_L+\mu_L)} & \frac{T_S^*\sigma_1}{L(\alpha_L+\mu_L)} & 0 & 0 \\ 0 & 0 & 0 & 0 & 0 & 0 \\ \frac{L_S^* e_T \sigma_3}{L(e_T+\mu_T)\mu_T} & \frac{L_S^*\sigma_3}{L\mu_T} & 0 & 0 & 0 & 0 \\ 0 & 0 & 0 & 0 & 0 & 0 \\ \frac{H_S^* e_T \sigma_4}{L(e_T+\mu_T)\mu_T} & \frac{H_S^*\sigma_4}{L\mu_T} & \frac{H_S^* e_L \sigma_5}{H(\alpha_L+\mu_L)(e_L+\mu_L)} & \frac{H_S^*\sigma_5}{H(\alpha_L+\mu_L)} & 0 & 0 \\ 0 & 0 & 0 & 0 & 0 & 0 \end{pmatrix}, \quad (5.4)$$

and according to (Diekmann, Heesterbeek, and Roberts, 2010), the next generation matrix ($\mathcal{K}_\mathcal{L}$) can further be reduced. as one can observe that $\det(\mathcal{K}) = 0$ and thus facilitates further reduction of $\mathcal{K}_\mathcal{L}$ in lower-dimensional NGM matrix with small domain as mentioned in the section 2.2.4. Therefore, after using the Eq. (2.15), we can get the following:

$$\mathcal{K} = \begin{pmatrix} \frac{T_S^* e_T \sigma_2}{T(e_T+\mu_T)\mu_T} & \frac{T_S^* e_L \sigma_1}{L(\alpha_L+\mu_L)(e_L+\mu_L)} & 0 \\ \frac{L_S^* e_T \sigma_3}{L(e_T+\mu_T)\mu_T} & 0 & 0 \\ \frac{H_S^* e_T \sigma_4}{L(e_T+\mu_T)\mu_T} & \frac{H_S^* e_L \sigma_5}{H(\alpha_L+\mu_L)(e_L+\mu_L)} & 0 \end{pmatrix}. \quad (5.5)$$

The matrix $\mathcal{K}$ Eq. (5.5) can be biologically interpreted as

$$\mathcal{K} = \begin{pmatrix} Tick \hookrightarrow Tick & Livestock \hookrightarrow Tick & 0 \\ Tick \hookrightarrow Livestock & 0 & 0 \\ Tick \hookrightarrow Human & Livestock \hookrightarrow Human & 0 \end{pmatrix}, \quad (5.6)$$

where $X \hookrightarrow Y$ means population X is infecting population Y.

It is to be noted that the epidemiological metric R_0 is defined to be the spectral radius of the NGM Eq. (5.5) and the spectral radius of a square matrix is the largest absolute value of its eigenvalues. It holds the key to understand the possible spread of CCHFV in the naive population. We can decompose the total basic reproduction number R_0 into different contributions. These are infection from tick to tick via co-feeding (R_T) and infection

from tick to livestock R_{LA}. For the entire model system we get

$$R_0 = \frac{R_T}{2} + \sqrt{\left(\frac{R_T}{2}\right)^2 + R_{LA}}\,, \tag{5.7}$$

where

$$R_T = \left[\frac{\pi_T}{T}\frac{e_T}{(e_T+\mu_T)}\frac{\sigma_2}{\mu_T}\frac{1}{\mu_T}\right] \tag{5.8}$$

is the contribution of tick-to-tick transmission due to co-feeding and

$$R_{LA} = \left[\frac{\pi_T}{L}\frac{e_L}{(e_L+\mu_L)}\frac{\sigma_1}{\mu_T}\frac{1}{(\alpha_L+\mu_L)} + \frac{\pi_L}{L}\frac{e_T}{(e_T+\mu_T)}\frac{\sigma_3}{\mu_L}\frac{1}{\mu_T}\right] \tag{5.9}$$

is the contribution of tick-to-livestock transmission. If we exclude the transmission through co-feeding then the basic reproduction number is simply $R_0^{\mathrm{w}} = \sqrt{R_{LA}}$, where the index w stands for without co-feeding. The epidemic threshold is the critical point, where $R_0 = 1$. It follows from equation Eq. (5.7) that at the critical point the contributions of both transmission ways simply add up, i.e. $R_T^C + R_{LA}^C = 1$. It is also interesting to note that in the critical threshold value, possibly the weightage of two different transmission modes may have the equal roles.

The terms in Eq. (5.8) can be described as the following: $\frac{e_T}{e_T+\mu_T}$ is the probability that an adult tick will survive the incubation period and become infectious through co-feeding, $\frac{1}{\mu_T}$ is the lifespan of an adult tick, $\frac{\sigma_2}{\mu_T}$ is the probability of CCHFV transmission from an adult tick to another adult tick after co-feeding in its lifetime, $\frac{\pi_T}{T}$ is the ratio between the birth rate of adult tick and the total number of adult ticks. In the same way the terms in Eq. (5.9) can be followed: $\frac{e_L}{e_L+\mu_L}$ is the the proportion of livestock that will survive the incubation period and become infectious later on, $\frac{1}{\alpha_L+\mu_L}$ is livestock's infectious lifespan, $\frac{\sigma_1}{\mu_T}$ is the probability of CCHFV transmission from the livestock to an adult tick in its lifetime, $\frac{\sigma_3}{\mu_L}$ is the probability of CCHFV transmission from an adult tick to livestock in its lifetime, $\frac{\pi_T}{L}$ is the ratio between the birth rate of adult tick and the total number of livestock and $\frac{\pi_L}{L}$ is the ratio between the birth rate of livestock and the total number of livestock. The factor $\frac{1}{2}$ actually means that CCHFV can transfer only from the adult ticks and livestock to humans but not in the other way.

Finally, employing the parameter values provided in B.2, we find the following figures for the basic reproduction number Eq. (5.7)

$$R_0 = 3.4, \tag{5.10}$$

where the contributions are for the co-feeding $R_T = 1.2$, and for the tick to livestock infection $R_{LA} = 7.5$, respectively. The chosen parameters are the minima of the respective parameter ranges. When we perform the same calculations with the maximum values of the parameters, we get $R_T = 2.4$, $R_{LA} = 10.75$, and $R_0 = 4.9$, respectively.

5.2.2 Inclusion of human-to-human transmission

CCHFV is a viral zoonosis with the potential cases of human-to-human transmission (Ergönül, 2006) with case fatality rates from 5% to 80% (Sas

et al., 2018). Human-to-human transmission can also occur through the contact with body fluids of patients comprising CCHFV during the first 7–10 days of illness (Bente et al., 2013). There are reported cases of nosocomial spread of the disease (Naderi et al., 2013; Yadav et al., 2016; Pshenichnaya and Nenadskaya, 2015; Conger et al., 2015; Gürbüz et al., 2009) and through possible sexual transmission (Pshenichnaya et al., 2016; Ergonul and Battal, 2014). CCHFV can represent a potential threat for humans who has unprotected contact with other body fluids (Bodur et al., 2010). To include the nosocomial spread of CCHFV and human-to-human transmission of CCHF, we have included another transmission route as human-human transmission (Garrison, Smith, and Golden, 2019) as depicted in Fig. 5.4.

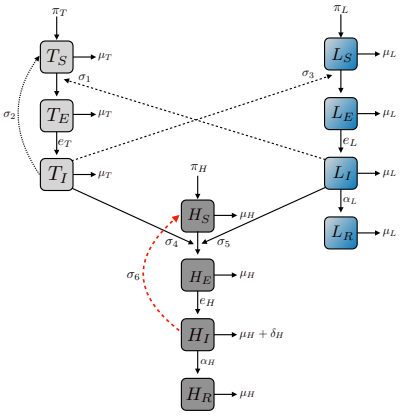

FIGURE 5.4: Infection process among the adult ticks, livestock and human including human to human transmission.

So, our model Eq. (5.1), Eq. (5.2), Eq. (5.3) system changes into the following:

$$\begin{aligned}
\frac{dH_S}{dt} &= \pi_H - \frac{\sigma_4 H_S T_I}{H} - \frac{\sigma_5 H_S L_I}{H} - \frac{\sigma_6 H_S H_I}{H} - \mu_H H_S \qquad (5.11)\\
\frac{dH_E}{dt} &= \frac{\sigma_4 H_S T_I}{H} + \frac{\sigma_5 H_S L_I}{H} + \frac{\sigma_6 H_S H_I}{H} - e_H H_E - \mu_H H_E\\
\frac{dH_I}{dt} &= e_H H_E - \alpha_H H_I - \mu_H H_I - \delta_H H_I\\
\frac{dH_R}{dt} &= \alpha_H H_I - \mu_H H_R
\end{aligned}$$

The next generation matrix ($\mathcal{K}_{\mathcal{L}}$), associated with the above mentioned system is the following:

$$\mathcal{K}_{\mathcal{L}} = \begin{pmatrix}
\frac{T_S^* e_T \sigma_2}{T(e_T+\mu_T)\mu_T} & \frac{T_S^* \sigma_2}{T\mu_T} & \frac{T_S^* e_L \sigma_1}{L(\alpha_L+\mu_L)(e_L+\mu_L)} & \frac{T_S^* \sigma_1}{L(\alpha_L+\mu_L)} & 0 & 0\\
0 & 0 & 0 & 0 & 0 & 0\\
\frac{L_S^* e_T \sigma_3}{L(e_T+\mu_T)\mu_T} & \frac{L_S^* \sigma_3}{L\mu_T} & 0 & 0 & 0 & 0\\
0 & 0 & 0 & 0 & 0 & 0\\
\frac{H_S^* e_T \sigma_4}{L(e_T+\mu_T)\mu_T} & \frac{H_S^* \sigma_4}{L\mu_T} & \frac{H_S^* e_L \sigma_5}{H(\alpha_L+\mu_L)(e_L+\mu_L)} & \frac{H_S^* \sigma_5}{H(\alpha_L+\mu_L)} & \frac{H_S^* e_H \sigma_6}{H(\alpha_H+\delta_H+\mu_H)(e_H+\mu_H)} & \frac{H_S^* \sigma_6}{H(\alpha_H+\delta_H+\mu_H)}\\
0 & 0 & 0 & 0 & 0 & 0
\end{pmatrix}$$

According to (Diekmann, Heesterbeek, and Roberts, 2010), the next generation matrix ($\mathcal{K}_{\mathcal{L}}$) can further be reduced to

$$\mathcal{K} = \begin{pmatrix} \frac{T_S^* e_T \sigma_2}{T(e_T+\mu_T)\mu_T} & \frac{T_S^* e_L \sigma_1}{L(\alpha_L+\mu_L)(e_L+\mu_L)} & 0 \\ \frac{L_S^* e_T \sigma_3}{L(e_T+\mu_T)\mu_T} & 0 & 0 \\ \frac{H_S^* e_T \sigma_4}{L(e_T+\mu_T)\mu_T} & \frac{H_S^* e_L \sigma_5}{H(\alpha_L+\mu_L)(e_L+\mu_L)} & \frac{H_S^* e_H \sigma_6}{H(\alpha_H+\delta_H+\mu_H)(e_H+\mu_H)} \end{pmatrix} \tag{5.12}$$

with spectral radius

$$R_0 = \max\left[R_H, R_{LA}\right] \tag{5.13}$$

where

$$R_H = \left[\frac{\pi_H}{H}\frac{\sigma_6}{\mu_H}\frac{e_H}{(e_H+\mu_H)}\frac{1}{(\alpha_H+\delta_H+\mu_H)}\right] \tag{5.14}$$

The matrix $\mathcal{K}$ Eq. (5.12) can be biologically interpreted as

$$\mathcal{K} = \begin{pmatrix} Tick \hookrightarrow Tick & Livestock \hookrightarrow Tick & 0 \\ Tick \hookrightarrow Livestock & 0 & 0 \\ Tick \hookrightarrow Human & Livestock \hookrightarrow Human & Human \hookrightarrow Human \end{pmatrix} \tag{5.15}$$

5.2.3 Tick-Human Model without livestock

According to the authors in (Bente et al., 2013; Vorou, 2009; Switkes et al., 2016), many of the reported cases of CCHFV are actually due to the biting of the adult ticks. Following (Yilmaz et al., 2009), a survey conducted in Turkey shows that among all the reported cases, 68.9% cases had a history of tick-bite or the contact with ticks and 0.16% cases of nosocomial infections The authors in (Mourya et al., 2019) mentions that due to the occupational exposure, infected tick bites and crushing the infected ticks with bare hands can potentially transfer the CCHFV. The findings in (Atkinson et al., 2013) notifies that the high number of patients only tested for CCHF due to potential exposure via tick bite along with asymptomatic cases of CCHF in Tajikistan. Therefore, after ignoring the disease transmission between the livestock and the tick and including only the interaction between the human host and the adult tick while incorporating the nosocomial transmission and co-feeding, we obtain the following ODE system:

$$\begin{aligned} \frac{dT_S}{dt} &= \pi_T - \tfrac{\sigma_2 T_S T_I}{T} - \mu_T T_S \\ \frac{dT_E}{dt} &= \tfrac{\sigma_2 T_S T_I}{T} - \mu_T T_E - e_T T_E \\ \frac{dT_I}{dt} &= e_T T_E - \mu_T T_I \end{aligned} \tag{5.16}$$

$$\begin{aligned}
\frac{dH_S}{dt} &= \pi_H - \frac{\sigma_4 H_S T_I}{H} - \frac{\sigma_6 H_S H_I}{H} - \mu_H H_S \\
\frac{dH_E}{dt} &= \frac{\sigma_4 H_S T_I}{H} + \frac{\sigma_6 H_S H_I}{H} - e_H H_E - \mu_H H_E \\
\frac{dH_I}{dt} &= e_H H_E - \alpha_H H_I - \mu_H H_I - \delta_H H_I \\
\frac{dH_R}{dt} &= \alpha_H H_I - \mu_H H_R
\end{aligned} \tag{5.17}$$

Next generation matrix ($\mathcal{K}_{\mathcal{TH}}$) associated with Eq. (5.16), Eq. (5.17) is given by

$$\mathcal{K}_{\mathcal{TH}} = \begin{pmatrix}
\frac{T_S^* e_T \sigma_2}{T(e_T+\mu_T)\mu_T} & \frac{T_S^* \sigma_2}{T\mu_T} & 0 & 0 \\
0 & 0 & 0 & 0 \\
\frac{H_S^* e_T \sigma_4}{H(e_T+\mu_T)\mu_T} & \frac{H_S^* \sigma_4}{H\mu_T} & \frac{H_S^* e_H \sigma_6}{H(\alpha_H+\delta_H+\mu_H)(e_H+\mu_H)} & \frac{H_S^* \sigma_6}{H(\alpha_H+\delta_H+\mu_H)} \\
0 & 0 & 0 & 0
\end{pmatrix}$$

$$R_{TH} = \max\left[R_H, R_T\right] \tag{5.18}$$

5.3 Simulations and Results

5.3.1 Infection curves

We first try to plot the infection curves of the model system Eq. (5.1), Eq. (5.2), Eq. (5.11) and 5.2.3 using the parameters given in Table B.2. Fig. 5.5a depicts the infection dynamics incorporating human-to-human spread and Figure 5.5b demonstrates the model system in 5.2.3 in the absence of livestock. In order to find the infection profiles of adult ticks (T_I), livestock (L_I) and human (H_I) in our model Eq. (5.1), Eq. (5.2), Eq. (5.11)) and 5.2.3), we assume that 5% of the infected population for adult ticks, livestock and 0.5% for human as the initial condition.

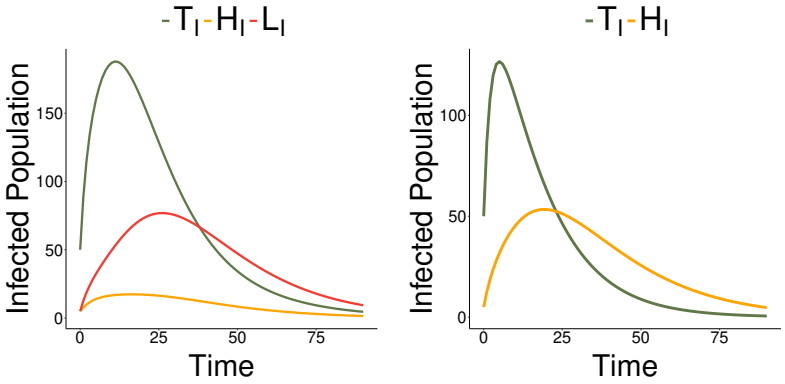

(A) (B)

FIGURE 5.5: (a) Infection curves of multi-vector model what includes the nosocomial spread of CCHFV. The infected population (T_I, L_I, H_I) converge to an endemic steady state. (b) Number of new infections caused by CCHFV in the adults ticks and human as the model system in 5.2.3 converges to an endemic state.

Infection curves of each infected compartments in the Fig. 5.5 reveals that the model system Eq. (5.1), Eq. (5.2), Eq. (5.11) and Eq. (5.16), Eq. (5.17) converge to an endemic steady state. After a tedious calculation, the endemic state is found to be $(T_S^*, T_E^*, T_I^*, L_S^*, L_E^*, L_I^*, L_R^*, H_S^*, H_E^*, H_I^*, H_R^*) = (\frac{\pi_T}{\mu_T} - \frac{(e_T+\mu_T)T_I^*}{e_T}, \frac{\mu_T T_I^*}{e_T}, T_I^*, A - BL_I^*, \frac{(\alpha_L+\mu_L)L_I^*}{e_L}, L_I^*, \frac{\alpha_L L_I^*}{\mu_L}, P - QH_I^*, \frac{(\alpha_H+\mu_H+\delta_H)H_I^*}{e_H}, \frac{(\sigma_4 T_I^*+\sigma_5 L_I^*)P}{EH+R(\sigma_4 T_I^*+\sigma_5 L_I^*)}, \frac{\alpha_H H_I^*}{\mu_H})$, where, $A = \frac{\pi_L}{\mu_L}$, $B = \frac{(e_L+\mu_L)(\alpha_L+\mu_L)}{\mu_L e_L}$, $P = \frac{\pi_H}{\mu_H}$, $Q = \frac{(e_H+\mu_H)(\alpha_H+\mu_H+\delta_H)}{e_H\mu_H}$, $T_I^* = \left(\frac{\sigma_2\pi_T}{T\mu_T} - \frac{(\mu_T+e_T)\mu_T}{e_T}\right)\left(\frac{e_T}{e_T+\mu_T}\right)$, $L_I^* = \frac{\sigma_3 W T_I^*}{C+\sigma_3 B T_I^*}$, $C = \frac{(\alpha_L+\mu_L)(e_L+\mu_L)L}{e_L}$, $H_I^* = \frac{(\sigma_4 T_I^*+\sigma_5 L_I^*)P}{EH+Q(\sigma_4 T_I^*+\sigma_5 L_I^*)}$, $E = \frac{(e_H+\mu_H)(\alpha_H+\mu_H+\delta_H)}{e_H}$.

The simulations results show us that the number of infected adult ticks, livestock and human decreases with the time after a season but it eventually goes into an endemic state with a small number of infected individuals in the multi-vector system. It is noticeable that with the inclusion of transmission route from the livestock to human, the difference of the number of infected human cases is $\approx 35\%$. We duly note that due to the lack of data regarding CCHFV, the considered model parameters in the Table B.2 are for the purpose of demonstration only. The values of R_H and R_{LA} are greater than unity, therefore, the cases of CCHF will likely persist in the population.

After following (Nguyen, Mahaffy, and Vaidya, 2019), we replace the host-specific transmission rate $(\sigma_4 \to \zeta\sigma_4, \sigma_6 \to \zeta\sigma_6)$ and calculate the value of R_H where $\zeta \in [0, 1]$.

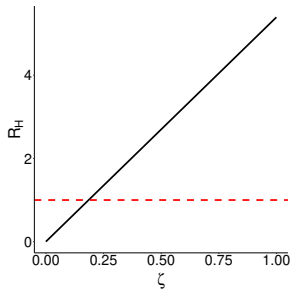

FIGURE 5.6: Relationship between basic reproduction number (R_H) and the scaling factor (ζ).

Fig. 5.6 shows graphically the impact of ζ on R_H. It is interesting to notice that when the value of $\zeta \approx 0.17$, the value of R_H is less than 1. Fig. 5.6 gives us with the suggestion that reducing the contact rate below 17% may be helpful to decrease the threat of CCHF in the population during the CCHFV infection between human and infected ticks.

5.3.2 Parameters and its impact on the persistence

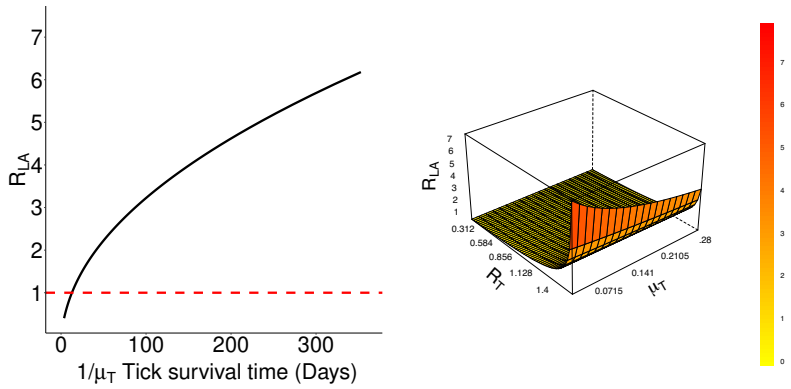

(A) (B)

FIGURE 5.7: (a) Impact of adult tick survival time on R_{LA}. R_{LA} drops below 1 provided the infected tick survival time is sufficiently small and (b) Effect of adult tick mortality (μ_T) on R_{LA} and R_T

Using the values in Table B.2, Fig. 5.7a shows the impact of decreasing the survival time of adult ticks. If R_{LA} can be reduced below 1 then survival time of adult ticks is decreased too.

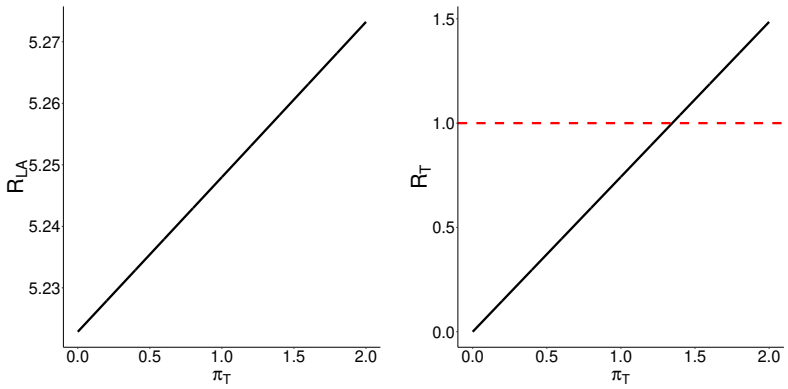

(A) (B)

FIGURE 5.8: (a) Impact of adult tick birth rate (π_T) on basic reproduction number (R_{LA}) and b) Impact of adult tick birth rate (π_T) on basic reproduction number (R_T)

Fig. 5.8 depicts that with the increasing birth date of the adult ticks (π_T) produces an increase in R_{LA} and R_T.

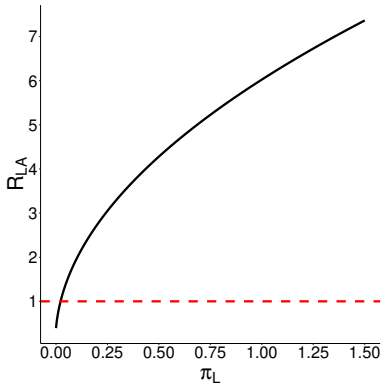

FIGURE 5.9: Impact of livestock birth rate (π_L) on basic reproduction number (R_{LA})

Fig. 5.9 depicts that the increase in the livestock growth rate increases the value of R_{LA}. Domestic livestock are the main hosts of CCHF and they may serve as hosts for virus amplification. Another reason can be attributed to the fact that an increase in the number of susceptible population escalates the magnitude of basic reproduction number.

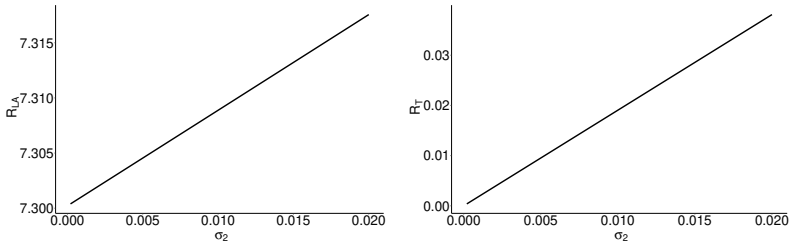

(A) (B)

FIGURE 5.10: (a) Impact of tick to tick transmission rate through co-feeding (σ_2) on basic reproduction number (R_{LA}) and (b) Effect of tick to tick transmission rate through co-feeding (σ_2) on (R_T)

In Fig. 5.10, we explore the effect of disease transmission through co-feeding (σ_2) on the persistence of CCHFV in the livestock and in the adult tick population. It is evident from the Fig. 5.10b that the increase in σ_2 has the linear effect in the magnitude of R_T. This can possibly explain the persistence of CCHFV in the adult tick population through co-feeding.

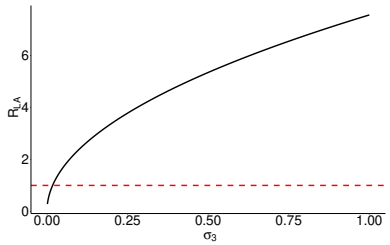

FIGURE 5.11: Impact of σ_3 (transmission rate of CCHFV from the adult tick to livestock) on R_{LA}.

Fig. 5.11 depicts the lower transmission rate from adult tick to livestock can bring the reduction in the value of R_{LA}. Therefore, the decrease in the transmission rate between adult ticks and livestock is also an important way to reduce the burden of CCHF.

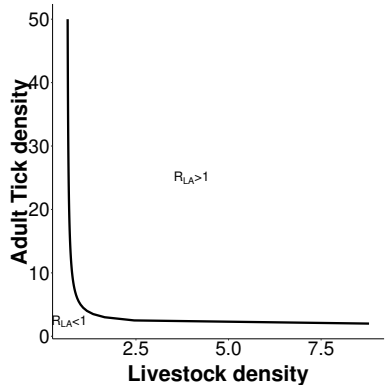

FIGURE 5.12: Relationship between adult tick density and livestock density on the predicted area of CCHF persistence.

The curve described by $R_{LA} = 1$ can give us the clue (Fig. 5.12) that the required combinations of expected livestock densities that will lead to

the persistence of CCHF. The $R_{LA} = 1$ curve shows the possible expected threshold values of the densities of the interacting populations for CCHFV to persist. Above it, CCHFV will persist and below it will not, according to the simulation.

5.4 Control strategies

Our mathematical epidemiological model can be employed to analyse different control measures that can be used by policy makers to decrease the epidemic size and the duration of such outbreaks. As it is a multi-host model, it can create intricacies to explore all possible control strategies which are difficult to undertake. This gives us with the option of aiming at the particular host types only, such as vector control, social distancing, vaccinating the livestocks etc. In this situation the usage of *Target reproduction number* $\mathcal{T}_{\mathcal{S}}$[2] is more useful compared to conventional R_0 (Heesterbeek and Roberts, 2007). For the convenience we follow the same notations like in (Shuai, Heesterbeek, and Driessche, 2013), the target reproduction number $\mathcal{T}_{\mathcal{S}}$ with respect to the target set $\mathcal{S}$ is defined as

$$\mathcal{T}_{\mathcal{S}} = \boldsymbol{\rho}\left(\mathcal{K}_{\mathcal{S}}\left(\mathcal{I} - \mathcal{K} + \mathcal{K}_{\mathcal{S}}\right)^{-1}\right) \tag{5.19}$$

where, $\mathcal{K}_{\mathcal{S}}$ is the target matrix and defined as in (Shuai, Heesterbeek, and Driessche, 2013) i.e. $[\mathcal{K}_{\mathcal{S}}]_{ij} = K_{ij}$ if $(i,j) \in \mathcal{S}$ and 0, otherwise. $\mathcal{I}$ is the identity matrix and $\boldsymbol{\rho}$ is the spectral radius of the matrix. This metric is handful to investigate the various control measures when targeting the subset of different types of host. Let us denote $\mathcal{K}$ Eq. (5.12) as following for the convenience.

$$\mathcal{K} = \begin{pmatrix} K_{11} & K_{12} & 0 \\ K_{21} & 0 & 0 \\ K_{31} & K_{32} & K_{33} \end{pmatrix} \tag{5.20}$$

There are several options through which we can effort to curb the bite of CCHFV. Different disease control strategies are illustrated below:

Livestock Sanitation: The usage of acaricide is a common technique to lower the tick burden on the livestock. Then the target set is $\mathcal{S} = \{(1,2),(2,1),(3,2)\}$. After following (Shuai, Heesterbeek, and Driessche, 2013) target reproduction number $\mathcal{T}_{\mathcal{S}}$ with respect to $\mathcal{S}$ (i.e., the type reproduction number targeting the host type 1) is using Eq. (5.19), we have;

$$\boldsymbol{\rho}\left[\begin{pmatrix} 0 & K_{12} & 0 \\ \frac{K_{21}}{1-K_{11}} & 0 & 0 \\ 0 & K_{32} & 0 \end{pmatrix}\right] = \sqrt{\frac{K_{12}K_{21}}{1-K_{11}}}$$

provided $K_{11} < 1$. So, in this case the $\mathcal{T}_{\mathcal{S}}$ (target reproduction number) is $\sqrt{\frac{K_{12}K_{21}}{1-K_{11}}}$. If we can control the magnitude of $\mathcal{T}_{\mathcal{S}}$, then we will be able to

[2] *Target reproduction number* $\mathcal{T}_{\mathcal{S}}$ is defined to quantify the measurements to control the infectious diseases with multiple host types. In our modelling framework *Target reproduction number* $\mathcal{T}_{\mathcal{S}}$ is more useful compared to conventional R_0 Heesterbeek and Roberts, 2007.

control the cases of CCHFV transmission under the constraints as defined by the target set $\mathcal{S}$.

Human Sanitation & Isolation: It is always advisable to make use of proper clothing etc while in the grazing field or to take precautionary measures when slaughtering, as well as during taking care of CCHFV affected patients. Here the target set is $\mathcal{S} = \{(3,1),(3,2),(3,3)\}$. Target reproduction number $\mathcal{T}_{\mathcal{S}}$ with respect to $\mathcal{S}$ (i.e., the type reproduction number targeting the host type 2) is

$$\boldsymbol{\rho}\left[\begin{pmatrix} 0 & 0 & 0 \\ 0 & 0 & 0 \\ a & b & K_{33} \end{pmatrix}\right] = K_{33}$$

$$a = -K_{31}\left(\frac{1}{K_{11}-1} - \frac{K_{12}K_{21}}{(K_{11}-1)^2\left(\frac{K_{12}K_{21}}{K_{11}-1}+1\right)}\right) - \frac{K_{21}K_{32}}{(K_{11}-1)\left(\frac{K_{12}K_{21}}{K_{11}-1}+1\right)},$$

$$b = -\frac{K_{12}K_{31}}{(K_{11}-1)\left(\frac{K_{12}K_{21}}{K_{11}-1}+1\right)} + \frac{K_{32}}{\frac{K_{12}K_{21}}{K_{11}-1}+1}$$

Here, $\mathcal{T}_{\mathcal{S}}$ is K_{33}. So, if we can focus only on the magnitude of K_{33}, then under the constraints of $\mathcal{S}$, we can reduce the cases of CCHFV.

Combined Control: When we combine both the control options then our target set is $\mathcal{S} = \{(1,2),(2,1),(3,1),(3,2),(3,3)\}$. Target reproduction number $\mathcal{T}_{\mathcal{S}}$ with respect to $\mathcal{S}$ is

$$\boldsymbol{\rho}\left[\begin{pmatrix} 0 & K_{12} & 0 \\ \frac{K_{21}}{1-K_{11}} & 0 & 0 \\ \frac{K_{31}}{1-K_{11}} & K_{32} & K_{33} \end{pmatrix}\right] = \max\left\{K_{33}, \sqrt{\frac{K_{12}K_{21}}{1-K_{11}}}\right\}$$

Here, $\mathcal{T}_{\mathcal{S}}$ is the maximum of K_{33} and $\sqrt{\frac{K_{12}K_{21}}{1-K_{11}}}$ and it is also quite obvious from the previous results too.

Isolation: It is difficult to prevent or control the CCHFV infection cycle in livestock and ticks, as the tick–animal–tick cycle is un-noticed, and CCHFV infection in livestock is not evident with the clinical signs. Additionally, the abundance of tick vectors is widespread and great in number, which makes it necessary for efficient tick control strategy. This could may be possible only in structured livestock farms. This makes to control tick population with the use of acaricide realistic only in well-managed livestock farms and this is uncommon in the regions (Atif et al., 2017; Baghi and Aghazadeh, 2016). In those regions where it may not be possible to make use of proper sanitation due to some economic issues, then in that condition only isolation is the option. In this situation the target set is $\mathcal{S} = \{(3,3)\}$.

$$\boldsymbol{\rho}\left[\begin{pmatrix} 0 & 0 & 0 \\ 0 & 0 & 0 \\ K_{33}\left(\frac{K_{21}\left(\frac{K_{12}K_{31}}{K_{11}-1}-K_{32}\right)}{(K_{11}-1)\left(\frac{K_{12}K_{21}}{k_{11}-1}+1\right)} - \frac{k_{31}}{k_{11}-1}\right) & -\frac{\left(\frac{K_{12}K_{31}}{K_{11}-1}-K_{32}\right)K_{33}}{\frac{K_{12}K_{21}}{K_{11}-1}+1} & K_{33} \end{pmatrix}\right] = K_{33}$$

Here, $\mathcal{T}_{\mathcal{S}}$ is K_{33} and this is very interesting to note for a country like Afghanistan where the resources are scarce.

5.5 Sensitivity analysis

Here, we carry out sensitivity analysis of the model parameters to decipher the influence of different parameters on the model output. It can be described as how uncertainty in the output of a mathematical model can cor-relate to the different sources of uncertainty in the model input parameters (Iooss and Saltelli, 2017). In this method we systemically vary the model input parameters to determine their effect on the model output.

5.5.1 Model sensitivity analysis

Having the aim to understand the effect of the input parameters on the model outcome, we perform the sensitivity analysis after computing the Partial Rank Correlation Coefficients (PRCC) with 1000 simulations per run for each of the model input parameter values sampled by the Latin Hypercube Sampling (LHS) scheme. The underlying assumption of this model that there is a monotonic relationship between the model input parameters and the model outputs.

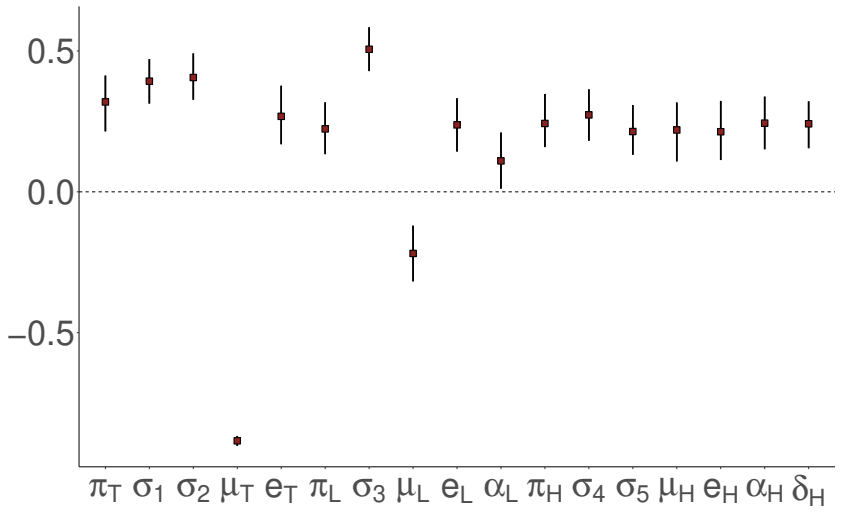

FIGURE 5.13: PRCC Analysis

To perform the PRCC sensitivity test, we take account of cumulative human cases of CCHF occurring during a simulation experiment as the model output of interest without the human-to-human spread. The advantage of this considered model output is that it captures effects of model parameters on both the persistence of CCHF and the overall impact of CCHF outbreaks over time in human. PRCC sign depicts the qualitative relationship between the model input parameters and model output of interests. A positive PRCC values means that while the corresponding model input parameters increases, the model output will also increase and on the other hand a negative PRCC value suggests a negative correlation between the model input and output (Zi, 2011) and values near zero indicates little effect on the model output.

5.5.2 NGM sensitivity analysis

It is possible to measure the impact of parameters on R_0 directly while using Eq. (5.15). Sensitivities and elasticities are measures of how infinitesimal changes in the individual entries of a stage structured population matrix will affect the population and the quantification of projection results on the parameters. After observing that R_0 Eq. (5.13) can be taken as a function of $\mathcal{K}[X, Y]$ Eq. (5.15), we denote

$$\mathcal{S}_{X,Y} = \frac{\partial R_0}{\partial \mathcal{K}[X, Y]} \tag{5.21}$$

as the sensitivity of R_0 and

$$\mathcal{T}_{X,Y} = \mathcal{K}[X, Y] \frac{\partial [\ln R_0]}{\partial \mathcal{K}[X, Y]} \tag{5.22}$$

as the elasticity of R_0. We can conclude that elasticities are *proportional sensitivities* (Lesnoff, Ezanno, and Caswell, 2003) measuring the proportional change in R_0 while given an infinitesimal one-at-a-time proportional change in $\mathcal{K}[X, Y]$. After following (Polo, Labruna, and Ferreira, 2018), we perform the sensitivity and elasticity analysis of Eq. (5.15) in R R Core Team, 2018 employing the package *popbio* Stubben and Milligan, 2007 which is an R version of the Matlab code for the analysis of matrix population models illustrated in (Caswell, 1989).

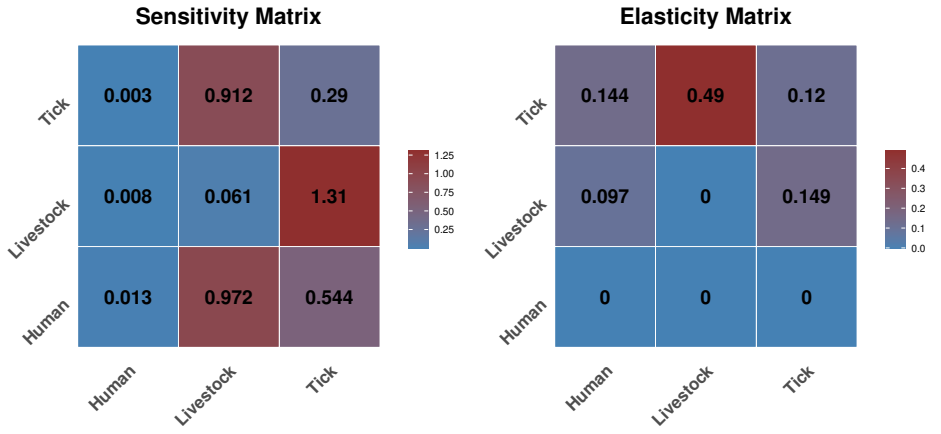

FIGURE 5.14: (A) Sensitivity and (B) elasticity matrices for Eq. (5.15)

.

From the Fig. 5.14, we can notice that the value of R_0 Eq. (5.13) is sensitive to the alteration in K_{12}, K_{21}, K_{32} and K_{31} of the elements from the matrix $\mathcal{K}$ (5.15). These entities correspond to the number of attached infected adult ticks by an infected livestock and the number of infected livestocks by an infected adult tick, followed by the number of infected humans bitten by an infected adult tick and the number of infected humans produced by a single infected livestock. It is also interesting to notice that the number of infected adult ticks produced by a single infected tick through co-feeding (K_{11}) is also a sensitive parameter according our sensitivity analysis. Elasticities are actually *proportional sensitivities* which gauge the proportional change in R_0 Eq. (5.13), given an infinitesimal one-at-a-time proportional change in the elements of the matrix $\mathcal{K}$ (5.15) with the presumption that $\mathcal{K}$ is growing or decreasing at a constant rate (Caswell, 1989). Fig. 5.14 depicts the elasticity of R_0 with respect to the matrix elements $\mathcal{K}[X, Y]$. The elasticities of the matrix elements K_{11}, K_{12}, K_{13} and K_{24} adds up–to approximately 90.3%. Explanations of elasticities give us a metric that illustrates the relative importance of disease cycle both within and among the host-tick population. However, we insist again that elasticities are formulated on infinitesimal, one-at-a-time changes, with the information that the multiple changes are additive and the effects of changes of $\mathcal{K}[X, Y]$ are

assumed to be linear (Caswell, 1989). The interaction between the infected adult tick and the livestock are the prime factor driving the CCHF cycle.

5.6 Model Fitting

To pertinent with our mathematical work with the reported cases in the different countries, we endeavour to validate the robustness of our ODE model Eq. (5.16), Eq. (5.17), we fit it to the actual CCHFV incidence data from six different countries. To solve this data fitting process, we take the help of MATLAB® (MATLAB, 2019) differential equation solver *ode45* to approximate the solution for a trial set of parameter values with the fixed initial condition. Then the fitted value is taken as input to an optimisation algorithm what updates the estimation of the parameters with each iteration. The time series of the estimated infected human population from the model Eq. (5.16), Eq. (5.17) is denoted by the vector P and the reported cases are denoted by $\widehat{P}$. We use Matlab functions *fminsearch* and *lsqcurvefit*.

1. We find the estimates of the model parameters that minimises $E_i = \|(P - \widehat{P})\|_2^2$ for each population.
2. Now holding the local parameters same for the infected human population, we then find the model parameters that minimises $E = \sum_i \|(P - \widehat{P})\|_2^2$
3. Repeat the steps(1) and (2) until either
   (a) The changes in the objective function $E = \sum_i \|(P-\widehat{P})\|_2^2$ is below predefined tolerance Tol or,
   (b) The number of iterations exceeds a limit $Max_{Iteration}$

It is to be noted that initial guess of the parameters plays an important role in convergence of Matlab optimisation functions.

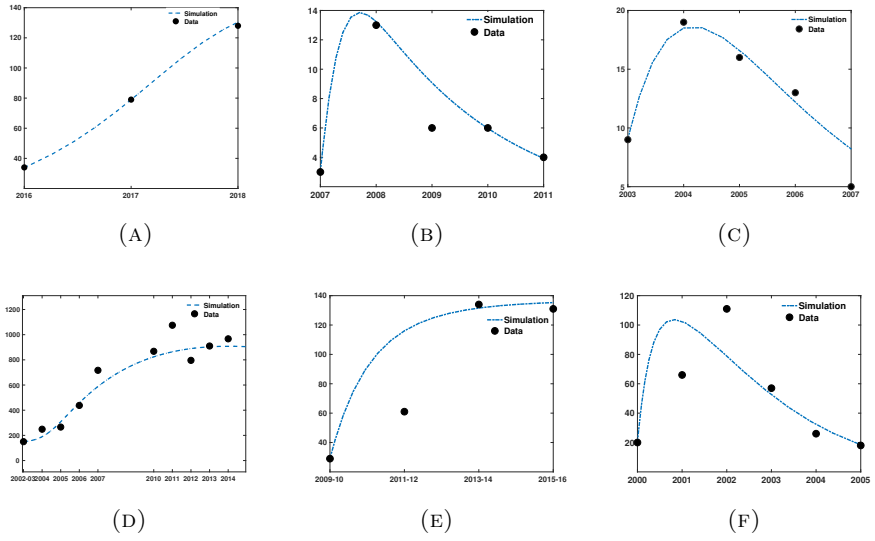

FIGURE 5.15: The comparison between the reported human CCHFV cases in Afghanistan, Bulgaria, Kosovo, Turkey, Pakistan and Iran and the simulation of $H_I(t)$ from the model.

Fitting Eq. (5.16), Eq. (5.17) to reported case is important for the modelling purpose as it does give an opportunity to procure the base transmission parameters for the purpose of perusal in the different scenarios. The simulation of human CCHFV cases in different countries is shown in Fig. 5.15.Few things can be noticed from Fig. 5.15. For example in Bulgaria and in Kosovo, increased awareness towards the perils of CCHFV perhaps has helped to decrease the cases but in case of other countries it appears that this is not the current situation. Moreover, our fitted model simulations (Fig. 5.15a, 5.15d and 5.15e) demonstrates that given the current trend of the CCHFV cases in Afghanistan, Pakistan and Turkey, the number of human CCHFV cases will increase steadily in future. Therefore, if no further effective prevention and control measures are taken, the disease will not vanish. The visual representations of the fitted transmission parameters are shown in Fig. 5.16.

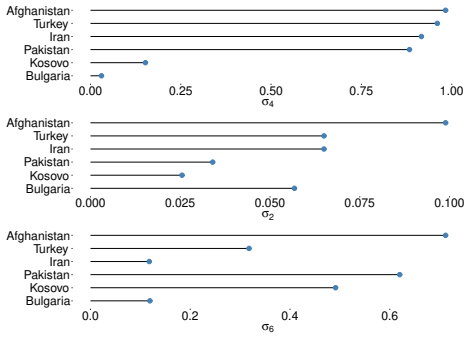

FIGURE 5.16: Fitted transmission parameters

The Fig. 5.16 is very interesting in terms of estimations of the parameters associated with the spread of CCHFV in different countries. It also depicts the heterogeneous nature of the dissemination of CCHFV. Given the high prevalence of CCHFV in Afghanistan, different routes of CCHFV transmission share equal burden whereas the nature of CCHFV is different in the Balkan countries. This should help the policy makers to focus only on the necessary measures specific to a country of concern.

5.7 Clustering of transmission parameters

Thematic query is how are the fitted transmission parameters differ from the country to country? Can we characterise them country-wise? Having that as our inspiration, we take steps to find the cosine similarity index[3] amongst the fitted transmission coefficients to inquire about the circulation of CCHFV transmission. Cosine similarity index is a metric of similarity between two non-zero vectors that measures the cosine of the angle between them. It is quite useful to determine the similarities amongst the different infection profiles of different considered countries in terms of transmission parameters.

[3]Cosine similarity index is defined between two nonzero vectors $\boldsymbol{A}$ and $\boldsymbol{B}$ as $\frac{\sum_{i=1}^{n} A_i B_i}{\sqrt{\sum_{i=1}^{n} A_i^2}\sqrt{\sum_{i=1}^{n} B_i^2}}$, where A_i and B_i are components of vector $\boldsymbol{A}$ and $\boldsymbol{B}$ respectively.

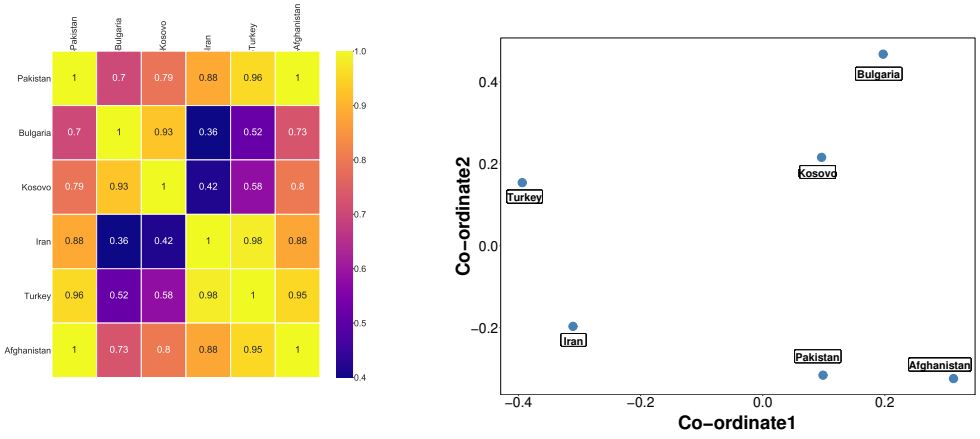

(A) (B)

FIGURE 5.17: Differences among the parameter sets of the considered countries. (A) Cosine similarity of the distance matrix (B) Spatial embedding of distance matrix.

From the Fig. 5.17a it is evident that the disease transmission parameters are not equal. We can clearly observe that Afghanistan is the most affected country and the transmission parameters (see Fig. 5.17a). amongst Afghanistan, Pakistan, Iran and Turkey are very similar compared to the Balkan countries Bulgaria and Kosovo. We are interested to infer about the CCHF infection profiles of different countries of concern. So we evaluate the multidimensional scaling to infer about the high-dimensional parameter space of the fitted transmission parameters. Fig. 5.17b depicts a 2 dimensional spatial embedding reflects the cosine distances of the parameters. It is evident that infection profiles of South Asian countries are entirely different from the Balkan and Middle Eastern countries. Possibly this information should be helpful to the policy makers, health workers to act on the appropriate eradication process of CCHFV accordingly.

5.8 Conclusion of this section

The current work in gives us the opportunity to asses some interesting observations and raise some acute questions too. During the last few years, there is a surge of CCHFV cases with an expansion beyond its global range (Wikel, 2018; Barzon, 2018). Several factors could attribute to this cause such as the variation in environment and movement of the hosts carrying *Hyalomma* ticks to newer geographical areas. It is immediately comprehensible that the potential threat of CCHFV cases in the new areas in the northern Europe are impending and is a matter of concern.

Here, we construct the CCHF transmission dynamics models (deterministic ODE models) including the interactions amongst the adult *Hyalomma* ticks, livestocks and human. Afterwards we extend our basic multi-vector model while incorporating the nosocomial spread of CCHF to investigate the potential impacts of human-human transmission on the disease dynamics.

Our findings from the numerical simulations and mathematical analysis give us some definitive insights of potential cases of CCHFV in Germany. Firstly, our model depicts the importance of inclusion of CCHFV transmission through co-feeding and its sustainability in adult tick population

through co-feeding. It escalates the value of the basic reproduction number and Eq. (5.7) quantitatively depicts the increased value. The model predicts that even the reduction of 18% of contact rate between the adult ticks and the livestock can be helpful to reduce R_0. In the absence of Livestock, Tick-Human model in Section 5.2.3, we notice the reduction in 37% of contact rates which can help in reducing the value of the basic reproduction below 1. There is an increase of approximately 35% in human CCHF cases due to contact with infected animal blood etc. Simulations depict that in case of multi-vector model system, the livestock has a significant role in disease transmission compared to only tick-human model. These additional pathways increase R_0 of CCHF, along with influence in the infection profiles of the muti-vector system and they also have a dominant role in CCHF control measures.

Secondly, the mathematical treatise on the control measures provides us with the acumen knowledge of the different control strategies and their feasibilities in different conditions. We know that the profuse usage of acaricide can detrimental impact on the environment and in some poor regions this may not be feasible. Our mathematical analysis reveals that human sanitation and isolation are also the effective ways to reduce the CCHF cases in human along with the acaricide treatment as mention in (Leblebicioglu et al., 2015).

Thirdly, we fit the reported cases of CCHF through our ODE based model Eq. (5.16), Eq. (5.17). The fitted solutions of different countries intrigue us with the following question: Are all the infection profiles of different countries the same? Does the geographical locations have an impact on the transmission parameters? To answer that we figure it out that spatially embedded multidimensional scaling can provides us the solution of this puzzle with the help of cosine similarity index amongst the transmission parameters. Spatially embedded multidimensional scaling shows us that the infection dynamics and transmission cycle are different for Balkan countries from the south Asian countries. This can possibly help the policymakers to emphasise that different countries need different control strategies.

Our current explorations are not exhaustive and it has an ample space for the possible explorations. For example to include the seasonality in the currently developed model to explore the seasonality in human incidence and the dependence on the ambient temperature (Abbas et al., 2017) or, to include the movement of animals and the migration of human during the time of Eid-ul-Azha as it is an important factor (Atif et al., 2017) to give finer resolution of the model in the spatial scale.

In spite of having its own limitations, our proposed models have its own merits. The analytical expression of R_0 and the mathematically sound explorations of control strategies make our current work so significant in the field of epidemiology. Our work highlights the potential causes and mitigations of CCHF spread.

CHAPTER 6

Conclusion

In this thesis we have constructed a necessary mathematical modelling framework to understand the potential and the eventual spread of WNV in Germany. In the backdrop of rising temperature globally and consequently in the increasing activities of the vectors (mosquitoes and ticks), we are facing the developing challenges from the zoonotic disease(eg. WNV, CCHF etc.). In the chapter 1, we readily raise the challenges pertaining to the issues related to the potential spread of WNV and CCHFV in Germany. To address such concerns, we have used some the well established mathematical tools what we have briefly mentioned and introduced in the Chapter 2. The modelling framework is comprised of a mechanistic model of Discrete-ODE hybrid type of in the Chapter 3 and the inclusion of stochastic movement matrices afterwards while the vital model parameters are temperature dependent elaborated in the Chapter 4. The influence and the importance of temperature on the transmission of WNV has been demonstrated for the local spreading model and the future projections show that the WNV can potentially establish its foothold in Germany under the sundry IPCC conditions. As a central result, we show that the concept of basic reproduction number (R_0) can be extended from an ODE based mosquito-borne model to a spatially explicit model and thence to a tick-borne disease.

Detailed information about the model parameters governing the disease dynamics is not well known in most real-world epidemic outbreaks. It turns out that with the proper sets of assumptions and the inclusions of the various weather driven factors can possibly help to break the deadlock while endeavouring such modelling effort at least qualitatively. Such modelling *mantra* can help to understand the reach and the limits of such localised modelling attempt. However, in case of spatial spread of an epidemics within a certain period across large geospatial scale, the contact matrices of the interacting species can be of utter importance in this context. Similar to that of infection parameters, the derivation of such contact matrices of the host-vector populations can also be a daunting task but with certain distance rules based dispersal formulae can potentially be the saviour. Although these contact matrices form complex networks, it emerges that a lot of times, the structures of links or the routes connecting the different nodes of habitat patch can potentially define the mechanism of spreading process in a global scale.

In the Chapter 2, we first analysed the local spread of WNV in Germany while taking account of the effect of the temperature in the model parameters. We immediately show the active role of the migratory birds

as a periodic transporter of WNV and hence sustaining the disease cycle in WNV in Section 3.3.1 in Germany. In Section 3.4, we observe the presence of the migratory birds actually accentuate the value of R_0 in a multifold magnitude and the seasonal appearance of them actually keeping the disease dynamics alive as we can notice it in Section 3.5.4. Sensitivity analysis as discussed in Section 3.5.5, reveals the significant parameters that will play the significant role in propagating WNV in the local bird population. Under the various IPCC conditions we have shown that WNV will be established even in the northern Germany. With the purpose of spatial projections of the bites of WNV over Germany, we purposefully demonstrated the potential density of the locally infected birds population.

While modelling the spatial spread of epidemics, one should take account of the net flux of the interacting populations from one habitat patch to another one and this is an important aspect to include the modelling hypothesis. We take such an endeavour in this thesis in the Section 4.2. Distance based dispersal kernels are being used to find the contact matrices as discussed in the Section 4.3 and most importantly the inception and hence the trail of the WNV infection spread can be found in the routes of the migratory birds as generated in the Section 4.3.2. We are able to find the geographical stretches of WNV in Germany through our metapopulation-network model as we have described in the Sections 4.2 and 4.3. The far reached expansion of WNV has been projected through geospatial simulations in the Section 4.5. As we know that the model validation is a job to confirm that outputs of a model possess enough fidelity to the outputs of the simulation generated process can give. Driven by the above said goal, we also evaluate the potential strength of our metapopulation-network model through structural similarities of the model outcome and the reported cases of WNV in Germany. The SSIM scores are satisfactory as this is just the inception of such a modelling effort.

Finally, the accumulated expertise on the mosquito-borne diseases has been put to the test when the CCHFV, a tick-borne disease has been modelled with the limited informations of the parameters settings as described in the Section 5.2. Due to the lack of parameter values and the complexities associated with the tick life-cycle (see Section 5.1), we undertake a simple approach to explore that mathematical tools that have been gained in the previous chapters of this thesis. Instead of increasing the complexities of the deterministic ODE models, we aspire to decode the characteristics of the different transmission routes between the host species and the ticks. The analytical expressions of R_0 developed in the Section 5.2.1 gives the clue to the possible control and hence eradication based on different constraints as mentioned in the Section 5.4. With the limited informations that we have at our disposal, we have fitted the ODE based model to understand the burden of different transmission parameters of geographically separated countries as well as aligned in the Sections 5.6 and 5.7. The findings have shown that the comparative weightage of sundry transmission parameters in the Balkan area is radically different from those in the South Asian ones and henceforth the eradication process should not be the same for all these countries.

Selbständigkeitserklärung

Ich erkläre, dass ich die Dissertation selbständig und nur unter Verwendung der von mir gemäß §7 Abs. 3 der Promotionsordnung der Mathematisch-Naturwissenschaftlichen Fakultät, veröffentlicht im Amtlichen Mitteilungsblatt der Humboldt-Universität zu Berlin Nr. 42/2018 am 11.07.2018 angegebenen Hilfsmittel angefertigt habe.

Berlin, den 5. Januar 2023 Suman Bhowmick

Declarations

I declare that I have completed the thesis independently using only the aids and tools specified. I have not applied for a doctor's degree in the doctoral subject elsewhere and do not hold a corresponding doctor's degree. I have taken due note of the Faculty of Mathematics and Natural Sciences PhD Regulations, published in the Official Gazette of Humboldt-Universität zu Berlin no. 42/2018 on 11/07/2018.

Berlin, January 5, 2023 Suman Bhowmick

List of publications

1. **S. Bhowmick**, J. Gethmann, I. M. Sokolov, F. J. Conraths, H. H. K. Lentz
SEIR-Metapopulation model of potential spread of West Nile virus
Ecological Modelling 110213, 0304-3800.

2. **S. Bhowmick**, K. K. Kasi, J. Gethmann, S. Fischer, F. J. Conraths, I. M. Sokolov, H. H.K. Lentz
Ticks on the run: A mathematical model of Crimean-Congo Haemorrhagic Fever (CCHF)-key factors for transmission
Epidemiologia, MDPI , 3(1), 116-134.

3. **S. Bhowmick**, J Gethmann, F. J. Conraths, I. M. Sokolov, H. H. K. Lentz
Locally temperature-driven mathematical model of West Nile virus spread in Germany
Journal of theoretical biology 488, 110117.

APPENDIX A

Appendix A

$$T_{Mig} = \begin{bmatrix} 0 & 0 & 0 & 0 & \frac{K_M c_2}{K_B} & \frac{K_M c_1}{K_B} & 0 & \frac{K_M c_1}{K_{Bm}} \\ 0 & 0 & 0 & 0 & 0 & 0 & 0 & 0 \\ 0 & \beta_4 & 0 & 0 & 0 & 0 & 0 & 0 \\ 0 & \beta_3 & 0 & 0 & 0 & 0 & 0 & 0 \\ 0 & 0 & 0 & 0 & 0 & 0 & 0 & 0 \\ 0 & 0 & 0 & 0 & 0 & 0 & 0 & 0 \\ 0 & \beta_5 & 0 & 0 & 0 & 0 & 0 & 0 \\ 0 & 0 & 0 & 0 & 0 & 0 & 0 & 0 \end{bmatrix} \tag{A.1}$$

$$\Sigma_{Mig} = \begin{bmatrix} \gamma_M + m_M & 0 & 0 & 0 & 0 & 0 & 0 & 0 \\ -\gamma_M & m_M & 0 & 0 & 0 & 0 & 0 & 0 \\ 0 & 0 & \gamma_{BC} + m_B & 0 & 0 & 0 & 0 & 0 \\ 0 & 0 & 0 & \gamma_{BSC} + m_B & 0 & 0 & 0 & 0 \\ 0 & 0 & -\gamma_{BC} & 0 & \alpha_4 + m_B + d_{BC} & 0 & 0 & 0 \\ 0 & 0 & 0 & -\gamma_{BSC} & 0 & \alpha_3 + m_B + d_{BSC} & 0 & 0 \\ 0 & 0 & 0 & 0 & 0 & 0 & \gamma_{Bm} + m_{Bm} & 0 \\ 0 & 0 & 0 & 0 & 0 & 0 & -\gamma_{Bm} & \alpha_9 + m_{Bm} \end{bmatrix} \tag{A.2}$$

$$R_{0,Mig} = \rho(T_{Mig}\Sigma_{Mig}^{-1})$$

$$R_{0,Mig} = \sqrt{a_1 a_7 + a_2 a_8 + a_3 a_{11}} \tag{A.3}$$

where
$a_1 = \frac{\beta_4 \gamma_M}{m_M(\gamma_m + m_M)}$, $a_2 = \frac{\beta_3 \gamma_M}{m_M(\gamma_m + m_M)}$,
$a_3 = \frac{\beta_5 \gamma_M}{m_M(\gamma_m + m_M)}$, $a_7 = \frac{K_M c_2 \gamma_{BC}}{K_B(\alpha_4 + m_B + d_{BC})(\gamma_{BC} + m_B)}$,
$a_8 = \frac{K_M c_1 \gamma_{BSC}}{K_B(\alpha_3 + m_B + d_{BC})(\gamma_{BSC} + m_B)}$, $a_{11} = \frac{K_M c_3 \gamma_{Bm}}{K_{Bm}(\alpha_9 + m_{Bm})(\gamma_{Bm} + m_{Bm})}$

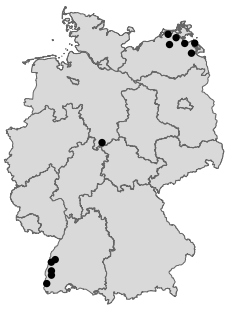

FIGURE A.1: Subsetted weather data.

Symbols	Interpretation	Source	Value
b_B	Birth Rate of local birds	(Laperriere, Brugger, and Rubel, 2011; Rubel et al., 2008)	0.00342
m_B	Mortality Rate of local birds	(Laperriere, Brugger, and Rubel, 2011; Rubel et al., 2008)	0.0012
K_B	Carrying capacity of local birds	(Laperriere, Brugger, and Rubel, 2011; Rubel et al., 2008)	10000
β_4	Transmission rate from infected mosquitoes to clinical local birds	(Laperriere, Brugger, and Rubel, 2011; Rubel et al., 2008)	f(T)
β_3	Transmission rate from infected mosquitoes to subclinical local birds	(Laperriere, Brugger, and Rubel, 2011; Rubel et al., 2008)	f(T)
γ_{BC}	Latency period of clinical local birds	(Laperriere, Brugger, and Rubel, 2011; Rubel et al., 2008)	0.667
γ_{BSC}	Latency period of subclinical local birds	(Laperriere, Brugger, and Rubel, 2011; Rubel et al., 2008)	0.567
α_4	Recovery rate of clinical local birds	(Laperriere, Brugger, and Rubel, 2011; Rubel et al., 2008)	0.182
α_3	Recovery rate of subclinical local birds	(Laperriere, Brugger, and Rubel, 2011; Rubel et al., 2008)	0.182
α_9	Recovery rate of migratory birds	(Bergsman, Hyman, and Manore, 2016)	.2222
γ_3	Rate at which recovered subclinical becomes infected	Assumed	.003
b_{Bm}	Birth Rate of migratory birds	(Bergsman, Hyman, and Manore, 2016)	.0014
m_{Bm}	Mortality Rate of migratory birds	(Bergsman, Hyman, and Manore, 2016)	.0014
K_{Bm}	Carrying capacity of migratory birds	(Bergsman, Hyman, and Manore, 2016)	100
β_5	Transmission rate from infected mosquito to the migratory birds	(Bergsman, Hyman, and Manore, 2016)	f(T)
c_3	Transmission rate from infected migratory birds to the mosquito	(Bergsman, Hyman, and Manore, 2016)	f(T)
γ_{Bm}	Latency period of migratory birds	(Bergsman, Hyman, and Manore, 2016)	.5
α_9	Recovery rate of migratory birds	(Bergsman, Hyman, and Manore, 2016)	0.1
b_M	Birth Rate of mosquitoes	(Laperriere, Brugger, and Rubel, 2011; Rubel et al., 2008)	f(T)
m_M	Mortality Rate of mosquitoes	(Laperriere, Brugger, and Rubel, 2011; Rubel et al., 2008)	f(T)
K_M	Carrying capacity of mosquitoes	(Laperriere, Brugger, and Rubel, 2011; Rubel et al., 2008)	100000
c_1	Transmission rate from infected subclinical local birds to the mosquitoes	(Laperriere, Brugger, and Rubel, 2011; Rubel et al., 2008)	f(T)
c_2	Transmission rate from infected clinical local birds to the mosquitoes	(Laperriere, Brugger, and Rubel, 2011; Rubel et al., 2008)	f(T)
γ_M	Incubation period	(Laperriere, Brugger, and Rubel, 2011; Rubel et al., 2008)	f(T)
d_{BC}	Disease induced clinical bird death	(Bergsman, Hyman, and Manore, 2016; Rubel et al., 2008)	.26
d_{BSC}	Disease induced subclinical bird death	(Bergsman, Hyman, and Manore, 2016; Rubel et al., 2008)	.26
d_{Bm}	Disease induced subclinical bird death	(Bergsman, Hyman, and Manore, 2016; Rubel et al., 2008)	.26

TABLE A.1: Model parameters

APPENDIX B

Appendix B

Variable	Description of Model Variables (3.1), (3.2), (3.3)
T_S	Susceptible adult ticks
T_E	Exposed adult ticks
T_I	Infected adult ticks
L_S	Susceptible livestocks
L_E	Exposed livestocks
L_I	Infected livestocks
L_R	Recovered livestocks
H_S	Susceptible humans
H_E	Exposed humans
H_I	Infected humans
H_R	Recovered humans
T	Total adult tick population
L	Total livestock population
H	Total human population

TABLE B.1: Variables used in the model (5.1), (5.2), (5.3).

B.1 Mathematical Properties

Theorem 1 *All the solution trajectories of the model system (3.1, 3.2, 3.3) initiating inside* Γ*, will remain within the interior of* Γ*.*

$$\Gamma = \Gamma_T \times \Gamma_L \times \Gamma_H$$

$$\Gamma_T = \left\{ (T_S, T_E, T_I) : 0 \leq T_S, T_E, T_I \leq \frac{\pi_T}{\mu_T} \right\}$$
$$\Gamma_L = \left\{ (L_S, L_E, L_I, L_R) : 0 \leq L_S, L_E, L_I, L_R \leq \frac{\pi_L}{\mu_L} \right\}$$
$$\Gamma_H = \left\{ (H_S, H_E, H_I, H_R) : 0 \leq H_S, H_E, H_I, H_R \leq \frac{\pi_H}{\mu_H} \right\}$$

Parameter	Description	Range	Unit	References
π_T	Net flow rate into susceptible adult tick population	$[2, 6]$	Ticks $\times$ day^{-1}	(Mpeshe, Haario, and Tchuenche, 2011)
π_L	Net flow rate into susceptible livestock population	$[0.5, 1.5]$	Livestock $\times$ day^{-1}	(Mpeshe, Haario, and Tchuenche, 2011)
π_H	Net flow rate into susceptible human population	$[0.5, 1.5]$	Humans $\times$ day^{-1}	(Mpeshe, Haario, and Tchuenche, 2011)
μ_T	Death rate of tick population	$[0.07, 0.21]$	day^{-1}	(Matser et al., 2009)
μ_L	Death rate of livestock population	$[1/3600, 1/360]$	day^{-1}	(Mpeshe, Haario, and Tchuenche, 2011)
μ_H	Death rate of human population	$[1/365 \times 60, 1/365 \times 40]$	day^{-1}	(Mpeshe, Haario, and Tchuenche, 2011)
$1/e_T$	Incubation period of tick	$[1, 3]$	day	(Matser et al., 2009; Shayan et al., 2015)
$1/e_L$	Incubation period of livestock	$[3, 5]$	day	(Matser et al., 2009)
$1/e_H$	Incubation period of human	$[1, 9]$	day	(Shayan et al., 2015)
σ_1	Effective contact rate: livestock to tick	$[0.11, 0.33]$	day^{-1}	(Hoch, Breton, and Vatansever, 2018; Matser et al., 2009)
σ_2	Effective contact rate: tick to tick	$[0.01, 0.04]$	day^{-1}	(Matser et al., 2009)
σ_3	Effective contact rate: tick to livestock	$[0.13, 0.71]$	day^{-1}	(Hoch, Breton, and Vatansever, 2018; Matser et al., 2009)
σ_4	Effective contact rate: tick to human	$[0.25, 0.375]$	day^{-1}	(Mpeshe, Haario, and Tchuenche, 2011)
σ_5	Effective contact rate: livestock to human	$[0.001, 0.002]$	day^{-1}	(Mpeshe, Haario, and Tchuenche, 2011)
σ_6	Effective contact rate: human to human	$[0.5, 0.75]$	day^{-1}	(Mondal, Hanif, and Biswas, 2017)
$1/\alpha_L$	Recovery period of livestock	$[14, 21]$	day	(Mpeshe, Haario, and Tchuenche, 2011)
$1/\alpha_H$	Recovery period of human population	$[15, 21]$	day	(Papa et al., 2002; Shayan et al., 2015)
δ_H	Disease induced death rate	$[0.3, 0.8]$	day^{-1}	(Schuster et al., 2016; Shayan et al., 2015)

TABLE B.2: Variables used in the model (5.1), (5.2), (5.3), (5.11).

Theorem 2 *The solution of the model system (5.1, 5.2, 5.3) is positive,* $\forall t \geq 0$.

Bibliography

.
URL: https://gisclimatechange.ucar.edu/inspector.

A. Rvachev, Leonid and Ira M. Longini (1985). "A mathematical model for the global spread of influenza." In: *Mathematical Biosciences* 75.1, pp. 3 –22.

Abbas, Tariq et al. (2017). "Seasonality in hospital admissions of Crimean-Congo hemorrhagic fever and its dependence on ambient temperature—empirical evidence from Pakistan." In: *International Journal of Biometeorology* 61.11, pp. 1893–1897.

Abdelrazec, Ahmed and Abba B. Gumel (2017). "Mathematical assessment of the role of temperature and rainfall on mosquito population dynamics." In: *Journal of Mathematical Biology* 74.6, pp. 1351–1395.

Abiodun, Gbenga J., Peter Witbooi, and Kazeem O. Okosun (2017). "Modeling and analyzing the impact of temperature and rainfall on mosquito population dynamics over Kwazulu-Natal, South Africa." In: *International Journal of Biomathematics* 10.04, p. 1750055.

Albert, Réka and Albert-László Barabási (Jan. 2002). "Statistical mechanics of complex networks." In: *Reviews of Modern Physics* 74.1, pp. 47–97.

Alcalay, Yehonatan, Ido Tsurim, and Ofer Ovadia (2017). "Modelling the effects of spatial heterogeneity and temporal variation in extinction probability on mosquito populations." In: *Ecological Applications* 27.8, pp. 2342–2358.

Alexander, M. E. and S. M. Moghadas (2005). "Bifurcation Analysis of an SIRS Epidemic Model with Generalized Incidence." In: *SIAM Journal on Applied Mathematics* 65.5, pp. 1794–1816.

Arino, Julien. "Diseases in Metapopulations." In: pp. 64–122.

— (May 2017). "Spatio-temporal spread of infectious pathogens of humans." In: *Infectious Disease Modelling* 2.2, pp. 218–228.

Arino, Julien, Arnaud Ducrot, and Pascal Zongo (2012). "A metapopulation model for malaria with transmission-blocking partial immunity in hosts." In: *Journal of Mathematical Biology* 64.3, pp. 423–448.

Atif, Muhammad et al. (2017). "The reasons why Pakistan might be at high risk of Crimean Congo haemorrhagic fever epidemic; a scoping review of the literature." In: *Virology Journal* 14.1, p. 63.

Atkinson, Barry et al. (2013). "Identification and analysis of Crimean-Congo hemorrhagic fever virus from human sera in Tajikistan." In: *International Journal of Infectious Diseases* 17.11, e1031 –e1037.

Babad, H. R. et al. (1995). "Predicting the impact of measles vaccination in England and Wales: model validation and analysis of policy options." In: *Epidemiology and Infection* 114.2, pp. 319–344.

Baghi, Hossein Bannazadeh and Mohammad Aghazadeh (2016). "Include Crimean-Congo haemorrhagic fever virus prevention in pre-travel advice." In: *Travel Medicine and Infectious Disease* 14.6, pp. 634 –635.

Bajardi, Paolo et al. (Jan. 2011). "Human Mobility Networks, Travel Restrictions, and the Global Spread of 2009 H1N1 Pandemic." In: *PLOS ONE* 6.1, pp. 1–8.

Bakonyi, Tamás et al. (Apr. 2006). "Lineage 1 and 2 strains of encephalitic West Nile virus, Central Europe." In: *Emerging Infectious Diseases* 12.4, pp. 618–623.

Bakonyi, Tamás et al. (2013). "Explosive spread of a neuroinvasive lineage 2 West Nile virus in Central Europe, 2008/2009." In: *Veterinary Microbiology* 165.1, pp. 61 –70.

Bakran-Lebl, Karin et al. (June 2016). "Impact of Network Activity on the Spread of Infectious Diseases through the German Pig Trade Network." In: *Front. Vet. Sci.,* 3.

Balcan, Duygu et al. (2009). "Multiscale mobility networks and the spatial spreading of infectious diseases." In: *Proc. Natl. Acad. Sci. U.S.A.* 106.51, pp. 21484–21489.

Banños-Villalba, Adrián et al. (2017). "Seed dispersal by macaws shapes the landscape of an Amazonian ecosystem." In: *Scientific Reports* 7.1, p. 7373.

Barabási, Albert-László and Réka Albert (1999a). "Emergence of Scaling in Random Networks." In: *Science* 286.5439, pp. 509–512.

— (1999b). "Emergence of Scaling in Random Networks." In: *Science* 286.5439, pp. 509–512.

Baracchini, Theo et al. (2017). "Seasonality in cholera dynamics: A rainfall-driven model explains the wide range of patterns in endemic areas." In: *Advances in Water Resources* 108, pp. 357 –366.

Barrett, Alan D T (Nov. 2018). "West Nile in Europe: an increasing public health problem." In: *Journal of Travel Medicine* 25.1.

Barzon, Luisa (2018). "Ongoing and emerging arbovirus threats in Europe." In: *Journal of Clinical Virology* 107, pp. 38 –47.

Bauch, Chris T. and David J. D. Earn (2004). "Vaccination and the theory of games." In: *Proceedings of the National Academy of Sciences* 101.36, pp. 13391–13394.

Beal, Martin (2018). *(Pat)Terns in space and time: Movement, activity, and habitat preference in breeding Caspian Terns (Hydroprogne caspia).*

Bellmann, Richard (1963). "New Directions of Research in the Theory of Differential Equations." In: *International Symposium on Nonlinear Differential Equations and Nonlinear Mechanics.* Ed. by Joseph P. LaSalle and Solomon Lefschetz. Academic Press, pp. 121 –134.

Bengtsson, Linus et al. (2015). "Using Mobile Phone Data to Predict the Spatial Spread of Cholera." In: *Scientific Reports* 5.1, p. 8923.

Bente, Dennis A. et al. (2013). "Crimean-Congo hemorrhagic fever: History, epidemiology, pathogenesis, clinical syndrome and genetic diversity." In: *Antiviral Research* 100.1, pp. 159 –189.

Bergsman, Louis D, James M. Hyman, and C. A. Manore (2016). "A mathematical model for the spread of west nile virus in migratory and resident birds." In: *Mathematical biosciences and engineering* 13 2, pp. 401–24.

Berman, Abraham and Robert J. Plemmons (1979). "Chapter 2 - Nonnegative Matrices." In: *Nonnegative Matrices in the Mathematical Sciences.*

Ed. by Abraham Berman and Robert J. Plemmons. Academic Press, pp. 26 –62.

Bhowmick, Suman et al. (2020). "Locally temperature - driven mathematical model of West Nile virus spread in Germany." In: *Journal of Theoretical Biology* 488, p. 110117.

Bhowmick, Suman et al. (2021). *Can a patchy model describe the potential spread of West Nile virus in Germany?* arXiv: 2101.11449 [physics.bio-ph].

Bhowmick, Suman et al. (2022). "Ticks on the Run: A Mathematical Model of Crimean-Congo Haemorrhagic Fever (CCHF);Key Factors for Transmission." In: *Epidemiologia* 3.1, pp. 116–134.

Bodur, Hurrem et al. (2010). "Detection of Crimean-Congo hemorrhagic fever virus genome in saliva and urine." In: *International Journal of Infectious Diseases* 14.3, e247–e249.

Bollobás, B., Akira Saito, and N. C. Wormald (1985). "Regular factors of regular graphs." In: *Journal of Graph Theory* 9.1, pp. 97–103.

Borer, Elizabeth T. et al. (2007). "Pathogen-induced reversal of native dominance in a grassland community." In: *Proceedings of the National Academy of Sciences* 104.13, pp. 5473–5478.

Borer, Elizabeth T. et al. (2009). "Aphid fecundity and grassland invasion: Invader life history is the key." In: *Ecological Applications* 19.5, pp. 1187–1196.

Boulinier, Thierry et al. (June 2016). "Migration, Prospecting, Dispersal? What Host Movement Matters for Infectious Agent Circulation?" In: *Integrative and Comparative Biology* 56.2, pp. 330–342.

Bowman, C. et al. (2005). "A mathematical model for assessing control strategies against West Nile virus." In: *Bulletin of Mathematical Biology* 67.5, pp. 1107–1133.

Brauer, Fred (2017). "Mathematical epidemiology: Past, present, and future." In: *Infectious Disease Modelling* 2.2, pp. 113 –127.

Butler, Shannon R., Jennifer J. Templeton, and Esteban Fernández-Juricic (2018). "How do birds look at their world? A novel avian visual fixation strategy." In: *Behavioral Ecology and Sociobiology* 72.3, p. 38.

Cailly, Priscilla et al. (2012). "A climate-driven abundance model to assess mosquito control strategies." In: *Ecological Modelling* 227, pp. 7 –17.

Calistri, Paolo et al. (Apr. 2010). "Epidemiology of West Nile in Europe and in the Mediterranean Basin." In: *The open virology journal* 4, pp. 29–37.

Calviño-Cancela, María et al. (2006). "Emus as non-standard seed dispersers and their potential for long-distance dispersal." In: *Ecography* 29.4, pp. 632–640.

Capasso, V. and L. Maddalena (1981). "Convergence to equilibrium states for a reaction-diffusion system modelling the spatial spread of a class of bacterial and viral diseases." In: *Journal of Mathematical Biology* 13.2, pp. 173–184.

Capasso, V and SL Paveri-Fontana (1979). "A mathematical model for the 1973 cholera epidemic in the European Mediterranean region." In: *Revue d'epidemiologie et de sante publique* 27.2, pp. 121–132.

Capasso, Vincenzo (Jan. 2008). *Mathematical Structure of Epidemic Systems*. Vol. 97.

Carlo, Tomás A. and Juan M. Morales (2008). "Inequalities in fruit-removal and seed dispersal: consequences of bird behaviour, neighbourhood density and landscape aggregation." In: *Journal of Ecology* 96.4, pp. 609–618.

Castillo-Chavez, Carlos et al. (2002). *Mathematical Approaches for Emerging and Reemerging Infectious Diseases: Models, Methods, and Theory.* Springer, Berlin Heidelberg New York.

Caswell, H. (1989). "Matrix Population Models : Construction." In: *Analysis, and Interpretation* 255.

Chinikar, S. et al. (2010). "Crimean-Congo hemorrhagic fever in Iran and neighboring countries." In: *Journal of Clinical Virology* 47.2, pp. 110 – 114.

Chowell, G. et al. (2019). "Assessing the potential impact of vector-borne disease transmission following heavy rainfall events: a mathematical framework." In: *Philosophical Transactions of the Royal Society B: Biological Sciences* 374.1775, p. 20180272.

Christley, Rob et al. (Dec. 2005). "Infection in Social Networks: Using Network Analysis to Identify High-Risk Individuals." In: *American journal of epidemiology* 162, pp. 1024–31.

Cohen, Samantha E. and Peter M. Todd (2018). "Relationship foraging: Does time spent searching predict relationship length?" In: *Evolutionary Behavioral Sciences* 12.3, pp. 139–151.

Colborn, James M. et al. (2013). "West Nile Virus Outbreak in Phoenix, Arizona—2010: Entomological Observations and Epidemiological Correlations." In: *Journal of the American Mosquito Control Association* 29.2, pp. 123 –132 –10.

Colizza, Vittoria and Alessandro Vespignani (2008). "Epidemic modeling in metapopulation systems with heterogeneous coupling pattern: Theory and simulations." In: *Journal of Theoretical Biology* 251.3, pp. 450 –467.

Colizza, Vittoria et al. (2006). "The role of the airline transportation network in the prediction and predictability of global epidemics." In: *Proceedings of the National Academy of Sciences* 103.7, pp. 2015–2020.

Colpitts, Tonya M. et al. (2012). "West Nile Virus: Biology, Transmission, and Human Infection." In: *Clinical Microbiology Reviews* 25.4, pp. 635–648.

Conger, Nicholas G. et al. (2015). "Health Care Response to CCHF in US Soldier and Nosocomial Transmission to Health Care Providers, Germany, 2009." In: *Emerging Infectious Diseases* 21.1, p. 23.

Conlan, Andrew J.K and Bryan T Grenfell (2007). "Seasonality and the persistence and invasion of measles." In: *Proceedings of the Royal Society B: Biological Sciences* 274.1614, pp. 1133–1141.

Cooke, Kenneth L. (1963). "Differential — Difference Equations." In: *International Symposium on Nonlinear Differential Equations and Nonlinear Mechanics*. Ed. by Joseph P. LaSalle and Solomon Lefschetz. Academic Press, pp. 155 –171.

Cooper, Ben S. (2007). "Mathematical Modeling of Crimean-Congo Hemorrhagic Fever Transmission." In: Dordrecht: Springer Netherlands. Chap. 15, pp. 187–203.

Da Silveira, Natalia Stefanini et al. (June 2016). "Effects of Land Cover on the Movement of Frugivorous Birds in a Heterogeneous Landscape." In: *PLOS ONE* 11.6, pp. 1–19.

DeutscherWetterdienst (2017). *DeutscherWetterdienst*. URL: https://www.dwd.de (visited on 11/30/2016).

Diekmann, O., J. A. P. Heesterbeek, and J. A. J. Metz (1990). "On the definition and the computation of the basic reproduction ratio R0 in models for infectious diseases in heterogeneous populations." In: *Journal of Mathematical Biology* 28.4, pp. 365–382.

Diekmann, O., J. A. P. Heesterbeek, and M. G. Roberts (2010). "The construction of next-generation matrices for compartmental epidemic models." In: *Journal of The Royal Society Interface* 7.47, pp. 873–885.

Diekmann, Odo and J.A.P. Heesterbeek (Jan. 2000). "Mathematical Epidemiology of Infectious Diseases: Model Building, Analysis and Interpretation." In: *Wiley Series in Mathematical and Computational Biology, Chichester, Wiley*.

Dohm, David J., Monica L. O'Guinn, and Michael J. Turell (2002). "Effect of Environmental Temperature on the Ability of Culex pipiens (Diptera: Culicidae) to Transmit West Nile Virus." In: *Journal of Medical Entomology* 39.1, pp. 221–225.

Donoso, Isabel et al. (2016-12-01). "Incorporating seed fate into plant-frugivore networks increases interaction diversity across plant regeneration stages.(Report)." In: *Oikos* 125.12, 1762(10).

Driessche, P. van den and James Watmough (2000). "A simple SIS epidemic model with a backward bifurcation." In: *Journal of Mathematical Biology* 40.6, pp. 525–540.

— (2002). "Reproduction numbers and sub-threshold endemic equilibria for compartmental models of disease transmission." In: *Mathematical Biosciences* 180.1, pp. 29 –48.

Driessche, Pauline van den (2017). "Reproduction numbers of infectious disease models." In: *Infectious Disease Modelling* 2.3, pp. 288 –303.

Dubé, Caroline et al. (Aug. 2011). "Inroduction to network analysis and its implications for animal disease modelling." In: *Revue scientifique et technique (International Office of Epizootics)* 30, pp. 425–36.

Duggal, Nisha K et al. (Sept. 2019). "On the Fly: Interactions Between Birds, Mosquitoes, and Environment That Have Molded West Nile Virus Genomic Structure Over Two Decades." In: *Journal of Medical Entomology* 56.6, pp. 1467–1474.

Durand, Benoit et al. (2010). "A metapopulation model to simulate West Nile virus circulation in Western Africa, Southern Europe and the Mediterranean basin." In: *Vet. Res.* 41.3, p. 32.

Eikenberry, Steffen E. and Abba B. Gumel (2018). "Mathematical modeling of climate change and malaria transmission dynamics: a historical review." In: *Journal of Mathematical Biology* 77.4, pp. 857–933.

Eldridge, Bruce F (1968). "The effect of temperature and photoperiod on blood-feeding and ovarian development in mosquitoes of the Culex pipiens complex." In: *The American journal of tropical medicine and hygiene* 17.1, pp. 133–140.

Emmerich, Petra et al. (Mar. 2018). "Sensitive and specific detection of Crimean–Congo Hemorrhagic Fever Virus (CCHFV)–Specific IgM and IgG antibodies in human sera using recombinant CCHFV nucleoprotein as antigen in μ-capture and IgG immune complex (IC) ELISA tests." In: *PLOS Neglected Tropical Diseases* 12.3, pp. 1–24.

Ergönül, Önder (2006). "Crimean-Congo haemorrhagic fever." In: *The Lancet Infectious Diseases* 6.4, pp. 203–214.

Ergonul, Onder and Ismet Battal (2014). "Potential Sexual Transmission of Crimean-Congo Hemorrhagic Fever Infection." In: *Japanese Journal of Infectious Diseases* 67.2, pp. 137–138.

Escribano-Romero, Estela et al. (2015). "West Nile virus serosurveillance in pigs, wild boars, and roe deer in Serbia." In: *Veterinary Microbiology* 176.3, pp. 365 –369.

Espíndola, Aquino L de et al. (2011). "An agent-based computational model of the spread of tuberculosis." In: *Journal of Statistical Mechanics: Theory and Experiment* 2011.05, P05003.

Ewing, D.A. et al. (2016). "Modelling the effect of temperature on the seasonal population dynamics of temperate mosquitoes." In: *Journal of Theoretical Biology* 400, pp. 65 –79.

Figuerola, Jordi et al. (2008). "Size matters: West Nile Virus neutralizing antibodies in resident and migratory birds in Spain." In: *Veterinary Microbiology* 132.1, pp. 39 –46.

Fitzgibbon, William E. et al. (2019). "Spatial models of vector-host epidemics with directed movement of vectors over long distances." In: *Mathematical Biosciences* 312, pp. 77–87.

FLI. *TSIS*. URL: https://tsis.fli.de/.

Fu, Shih and George Milne (Jan. 2003). "Epidemic Modelling Using Cellular Automata." In: *ACAL2003: The First Australian Conference on Artificial Life; Canberra, Australia*.

Gaff, Holly D. and Louis J. Gross (2007). "Modeling Tick-Borne Disease: A Metapopulation Model." In: *Bulletin of Mathematical Biology* 69.1, pp. 265–288.

Gamino, Virginia and Ursula Höfle (2013). "Pathology and tissue tropism of natural West Nile virus infection in birds: a review." In: *Veterinary Research* 44.1, p. 39.

Gargili, Aysen et al. (2017). "The role of ticks in the maintenance and transmission of Crimean-Congo hemorrhagic fever virus: A review of published field and laboratory studies." In: *Antiviral Research* 144, pp. 93–119.

Garrison, Aura R, Darci R Smith, and Joseph W Golden (June 2019). "Animal Models for Crimean-Congo Hemorrhagic Fever Human Disease." In: *Viruses* 11.7, p. 590.

Gilarranz, Luis J. (2020). "Generic Emergence of Modularity in Spatial Networks." In: *Scientific Reports* 10.1, p. 8708.

Gog, Julia, Rosie Woodroffe, and Jonathan Swinton (2002). "Disease in endangered metapopulations: the importance of alternative hosts." In: *Proceedings of the Royal Society of London. Series B: Biological Sciences* 269.1492, pp. 671–676.

Gonzalez, J.P. et al. (1992). "Sexual and transovarian transmission of Crimean-Congo haemorrhagic fever virus in Hyalomma truncatum ticks." In: *Research in Virology* 143, pp. 23 –28.

Grenfell, B T and J Harwood (1997). "(Meta)population dynamics of infectious diseases." In: *Trends. Ecol. Evol.* 12.10, pp. 395–399.

Gürbüz, Yunus et al. (2009). "A case of nosocomial transmission of Crimean–Congo hemorrhagic fever from patient to patient." In: *International Journal of Infectious Diseases* 13.3, e105–e107.

Hadfield, James et al. (Oct. 2019). "Twenty years of West Nile virus spread and evolution in the Americas visualized by Nextstrain." In: *PLOS Pathogens* 15.10, pp. 1–18.

Hamer, W. H. (1906). "The Milroy Lectures On Epidemic Disease In England—The Evidence Of Variability and Of Persistency Of Type." In: *The Lancet* 167.4305, pp. 569 –574.

Hansen, James et al. (2006). "Global temperature change." In: *Proc Natl Acad Sci U S A* 103.39, pp. 14288–14293.

Hansford, Kayleigh M. et al. (2019). "Hyalomma rufipes on an untraveled horse: Is this the first evidence of Hyalomma nymphs successfully moulting in the United Kingdom?" In: *Ticks and Tick-borne Diseases* 10.3, pp. 704 –708.

Hanski, I (1998). "Metapopulation dynamics." In: *Nature* 396.6706, pp. 41–49.

Harrigan, Ryan J. et al. (2014). "A continental risk assessment of West Nile virus under climate change." In: *Global Change Biology* 20.8, pp. 2417–2425.

Hartemink, N. A. et al. (2008). "The Basic Reproduction Number for Complex Disease Systems: Defining R0 for Tick-Borne Infections." In: *The American Naturalist* 171.6, pp. 743–754.

Hartley, David M. et al. (2012). "Effects of temperature on emergence and seasonality of West Nile virus in California." In: *Am J Trop Med Hyg* 86.5, pp. 884–894.

Hawman, David W and Heinz Feldmann (Oct. 2018). "Recent advances in understanding Crimean-Congo hemorrhagic fever virus." In: *F1000Research* 7, F1000 Faculty Rev–1715.

Heesterbeek, J.A.P. and M.G. Roberts (2007). "The type-reproduction number T in models for infectious disease control." In: *Mathematical Biosciences* 206.1, pp. 3 –10.

Heffernan, J.M, R.J Smith, and L.M Wahl (2005). "Perspectives on the basic reproductive ratio." In: *Journal of The Royal Society Interface* 2.4, pp. 281–293.

Herring, John (Jan. 1991). "The Mathematical Modeling of Spatial and Non-Spatial Information in Geographic Information Systems." In: *Mark D.M., Frank A.U. (eds) Cognitive and Linguistic Aspects of Geographic Space. NATO ASI Series (Series D: Behavioural and Social Sciences), vol 63. Springer, Dordrecht.*

Herrmann, John D. et al. (2016). "Connectivity from a different perspective: comparing seed dispersal kernels in connected vs. unfragmented landscapes." In: *Ecology* 97.5, pp. 1274–1282.

Hess, George (1996). "Disease in Metapopulation Models: Implications for Conservation." In: *Ecology* 77.5, pp. 1617–1632.

Hethcote, Herbert W. (2000). "The Mathematics of Infectious Diseases." In: *SIAM Review* 42.4, pp. 599–653.

Hoch, T. et al. (2016). "Identifying main drivers and testing control strategies for CCHFV spread." In: *Experimental and Applied Acarology* 68.3, pp. 347–359.

Hoch, Thierry, Eric Breton, and Zati Vatansever (Mar. 2018). "Dynamic Modeling of Crimean Congo Hemorrhagic Fever Virus (CCHFV) Spread to Test Control Strategies." In: *Journal of Medical Entomology* 55.5, pp. 1124–1132.

Hosack, Geoffrey R., Philippe A. Rossignol, and P. van den Driessche (2008). "The control of vector-borne disease epidemics." In: *Journal of Theoretical Biology* 255.1, pp. 16 –25.

House, James A., Michael J. Turell, and Charles A. Mebis (1992). "Rift Valley Fever: Present Status and Risk to the Western Hemisphere." In: *Annals of the New York Academy of Sciences* 653.1, pp. 233–242.

Hufnagel, Lars, Dirk Brockmann, and Theo Geisel (2004). "Forecast and control of epidemics in a globalized world." In: *Proc. Natl. Acad. Sci. U.S.A.* 101.42, p. 15124.

Iooss, Bertrand and Andrea Saltelli (2017). "Introduction to Sensitivity Analysis." In: Cham: Springer International Publishing. Chap. 26, pp. 1103–1122.

Janousek, William M., Peter P. Marra, and A. Marm Kilpatrick (2014). "Avian roosting behavior influences vector-host interactions for West Nile virus hosts." In: *Parasites & Vectors* 7.1, p. 399.

Juher, David, Jordi Ripoll, and Joan Saldaña (2009). "Analysis and Monte Carlo simulations of a model for the spread of infectious diseases in heterogeneous metapopulations." In: *Phys. Rev. E* 80, p. 041920.

Kao, R.R et al. (2006). "Demographic structure and pathogen dynamics on the network of livestock movements in Great Britain." In: *Proceedings of the Royal Society B: Biological Sciences* 273.1597, pp. 1999–2007.

Keeling, M. J and C. A Gilligan (2000). "Bubonic plague: a metapopulation model of a zoonosis." In: *Proceedings of the Royal Society of London. Series B: Biological Sciences* 267.1458, pp. 2219–2230.

Keeling, Matt (2005). "The implications of network structure for epidemic dynamics." In: *Theoretical Population Biology* 67.1, pp. 1 –8.

Keeling, Matt J and Ken T.D Eames (2005). "Networks and epidemic models." In: *Journal of The Royal Society Interface* 2.4, pp. 295–307.

Keeling, Matt J. and Pejman Rohani (2008). *Modeling Infectious Diseases in Humans and Animals*. Princeton University Press.

Keeling, Matt J and Pejman Rohani (2011). *Modeling infectious diseases in humans and animals*. Princeton University Press.

Keeling, Matt J. et al. (2010a). "Individual identity and movement networks for disease metapopulations." In: *Proceedings of the National Academy of Sciences* 107.19, pp. 8866–8870.

Keeling, Matt J et al. (2010b). "Individual identity and movement networks for disease metapopulations." In: *Proc. Natl. Acad. Sci. U.S.A.* 107.19, pp. 8866–8870.

Keeling, M.J. and B.T. Grenfell (1998). "Effect of variability in infection period on the persistence and spatial spread of infectious diseases." In: *Mathematical Biosciences* 147.2, pp. 207 –226.

Kermack, William Ogilvy, A. G. McKendrick, and Gilbert Thomas Walker (1927). "A contribution to the mathematical theory of epidemics." In: *Proceedings of the Royal Society of London. Series A, Containing Papers of a Mathematical and Physical Character* 115.772, pp. 700–721.

— (1932). "Contributions to the mathematical theory of epidemics. II - The problem of endemicity." In: *Proceedings of the Royal Society of London. Series A, Containing Papers of a Mathematical and Physical Character* 138.834, pp. 55–83.

— (1933). "Contributions to the mathematical theory of epidemics. III - Further studies of the problem of endemicity." In: *Proceedings of the Royal*

Society of London. Series A, Containing Papers of a Mathematical and Physical Character 141.843, pp. 94–122.

Kilpatrick, A. Marm et al. (June 2008). "Temperature, Viral Genetics, and the Transmission of West Nile Virus by Culex pipiens Mosquitoes." In: *PLOS Pathogens* 4.6, pp. 1–7.

Kioutsioukis, Ioannis and Nikolaos I. Stilianakis (2019). "Assessment of West nile virus transmission risk from a weather-dependent epidemiological model and a global sensitivity analysis framework." In: *Acta Tropica* 193, pp. 129 –141.

Kiss, István Z., Joel C. Miller, and Péter L. Simon (2017). "Disease spread in networks with large-scale structure." In: Cham: Springer International Publishing, pp. 367–379.

Kitching, R, Marcus Hutber, and M Thrusfield (Apr. 2005). "A review of foot-and-mouth disease with special consideration for the clinical and epidemiological factors relevant to predictive modeling of the disease." In: *Veterinary journal (London, England : 1997)* 169, pp. 197–209.

Kraay, Alicia N. M. et al. (2018). "Modeling environmentally mediated rotavirus transmission: The role of temperature and hydrologic factors." In: *Proceedings of the National Academy of Sciences* 115.12, E2782–E2790.

Kramer, Laura D., Jun Li, and Pei-Yong Shi (2007). "West Nile virus." In: *The Lancet Neurology* 6.2, pp. 171–181.

Krylova, Olga and David J. D. Earn (2013). "Effects of the infectious period distribution on predicted transitions in childhood disease dynamics." In: *Journal of The Royal Society Interface* 10.84, p. 20130098.

Kuby, M.J. et al. (2009). "Network Analysis." In: *International Encyclopedia of Human Geography*. Ed. by Rob Kitchin and Nigel Thrift. Oxford: Elsevier, pp. 391–398.

Lakshmikantham, Vangipuram, Srinivasa Leela, and Anatoly A Martynyuk (1989). *Stability analysis of nonlinear systems*. Springer.

Lalubin, Fabrice et al. (2013). "Temporal changes in mosquito abundance (Culex pipiens), avian malaria prevalence and lineage composition." In: *Parasites and Vectors* 6.1, p. 307.

Laperriere, Vincent, Katharina Brugger, and Franz Rubel (2011). "Simulation of the seasonal cycles of bird, equine and human West Nile virus cases." In: *Preventive Veterinary Medicine* 98.2, pp. 99–110.

Leblebicioglu, Hakan et al. (2015). "Consensus report: Preventive measures for Crimean-Congo Hemorrhagic Fever during Eid-al-Adha festival." In: *International Journal of Infectious Diseases* 38, pp. 9–15.

Lemaitre, Joseph et al. (2019). "Rainfall as a driver of epidemic cholera: Comparative model assessments of the effect of intra-seasonal precipitation events." In: *Acta Tropica* 190, pp. 235 –243.

Lentz, Hartmut H K, Thomas Selhorst, and Igor M Sokolov (June 2012). "Spread of infectious diseases in directed and modular metapopulation networks." In: *Phys. Rev. E* 85, p. 066111.

Lesnoff, M., P. Ezanno, and H. Caswell (2003). "Sensitivity analysis in periodic matrix models: A postscript to Caswell and Trevisan." In: *Mathematical and Computer Modelling* 37.9, pp. 945 –948.

Lessler, Justin and Derek A T Cummings (Mar. 2016). "Mechanistic Models of Infectious Disease and Their Impact on Public Health." In: *American journal of epidemiology* 183.5, pp. 415–422.

Levey, Douglas J., Joshua J. Tewksbury, and Benjamin M. Bolker (2008). "Modelling long-distance seed dispersal in heterogeneous landscapes." In: *Journal of Ecology* 96.4, pp. 599–608.

Liu, Wei-min, Herbert W. Hethcote, and Simon A. Levin (1987). "Dynamical behavior of epidemiological models with nonlinear incidence rates." In: *Journal of Mathematical Biology* 25.4, pp. 359–380.

Logan, Thomas M. et al. (1989). "Experimental Transmission of Crimean-Congo Hemorrhagic Fever Virus by Hyalomma Truncatum Koch." In: *The American Journal of Tropical Medicine and Hygiene* 40.2, pp. 207–212.

López, Guillermo et al. (2008). "Prevalence of West Nile Virus Neutralizing Antibodies in Spain Is Related to the Behavior of Migratory Birds." In: *Vector-Borne and Zoonotic Diseases* 8.5, pp. 615–622.

Lou, Yijun and Jianhong Wu (May 2017). "Modeling Lyme disease transmission." In: *Infectious Disease Modelling* 2.2, pp. 229–243.

Lou, Yijun and Xiao-Qiang Zhao (2010). "A Climate-Based Malaria Transmission Model with Structured Vector Population." In: *SIAM Journal on Applied Mathematics* 70.6, pp. 2023–2044.

Lowen, Anice C et al. (Oct. 2007). "Influenza virus transmission is dependent on relative humidity and temperature." In: *PLoS pathogens* 3.10, pp. 1470–1476.

M., Óscar, Júlio César Bicca-Marques, and Colin A. Chapman (Mar. 2018). "Quantity and quality of seed dispersal by a large arboreal frugivore in small and large Atlantic forest fragments." In: *PLOS ONE* 13.3, pp. 1–16.

Malkinson, Mertyn et al. (Apr. 2002). "Introduction of West Nile virus in the Middle East by migrating white storks." In: *Emerging infectious diseases* 8.4, pp. 392–397.

Marcati, Pierangelo and M. Assunta Pozio (1980). "Global asymptotic stability for a vector disease model with spatial spread." In: *Journal of Mathematical Biology* 9.2, pp. 179–187.

Marini, Giovanni et al. (2018). "West Nile virus transmission and human infection risk in Veneto (Italy): a modelling analysis." In: *Scientific Reports* 8.1, p. 14005.

Massaro, Emanuele, Daniel Kondor, and Carlo Ratti (2019). "Assessing the interplay between human mobility and mosquito borne diseases in urban environments." In: *Scientific Reports* 9.1, p. 16911.

MATLAB (2019). *version 9.6 (R2019a)*. Natick, Massachusetts: The MathWorks Inc.

Matser, Amy et al. (2009). "Elasticity analysis in epidemiology: an application to tick-borne infections." In: *Ecology Letters* 12.12, pp. 1298–1305.

McMichael, Anthony J, Rosalie E Woodruff, and Simon Hales (2006). "Climate change and human health: present and future risks." In: *The Lancet* 367.9513, pp. 859–869.

Messina, Jane P. et al. (July 2015). "The global distribution of Crimean-Congo hemorrhagic fever." In: *Transactions of The Royal Society of Tropical Medicine and Hygiene* 109.8, pp. 503–513.

Metcalf, C Jessica E et al. (Aug. 2017). "Identifying climate drivers of infectious disease dynamics: recent advances and challenges ahead." In: *Proceedings. Biological sciences* 284.1860, p. 20170901.

Meyer, Sebastian and Leonhard Held (Sept. 2014). "Power-law models for infectious disease spread." In: *Ann. Appl. Stat.* 8.3, pp. 1612–1639.

Michel, Friederike et al. (2018). "West Nile Virus and Usutu Virus Monitoring of Wild Birds in Germany." In: *International Journal of Environmental Research and Public Health* 15.1.

Mockus, Audris (1998). "Estimating Dependencies from Spatial Averages." In: *Journal of Computational and Graphical Statistics* 7.4, pp. 501–513.

Mondal, Mitun Kumar, Muhammad Hanif, and Md. Haider Ali Biswas (2017). "A mathematical analysis for controlling the spread of Nipah virus infection." In: *International Journal of Modelling and Simulation* 37.3, pp. 185–197.

Moon, Sifat A. et al. (Mar. 2019). "A spatio-temporal individual-based network framework for West Nile virus in the USA: Spreading pattern of West Nile virus." In: *PLOS Computational Biology* 15.3, pp. 1–24.

Moore, S et al. (Apr. 2011a). "Spatiotemporal Model of Barley and Cereal Yellow Dwarf Virus Transmission Dynamics with Seasonality and Plant Competition." In: *Bulletin of mathematical biology* 73, pp. 2707–30.

Moore, S. M. et al. (2011b). "Spatiotemporal Model of Barley and Cereal Yellow Dwarf Virus Transmission Dynamics with Seasonality and Plant Competition." In: *Bulletin of Mathematical Biology* 73.11, pp. 2707–2730.

Morand, Serge et al. (2013). "Climate variability and outbreaks of infectious diseases in Europe." In: *Scientific Reports* 3.1, p. 1774.

Mordecai, Erin A. et al. (Apr. 2017). "Detecting the impact of temperature on transmission of Zika, dengue, and chikungunya using mechanistic models." In: *PLOS Neglected Tropical Diseases* 11.4, pp. 1–18.

Morin, Cory W. and Andrew C. Comrie (2013). "Regional and seasonal response of a West Nile virus vector to climate change." In: *Proceedings of the National Academy of Sciences* 110.39, pp. 15620–15625.

Mossong, Joël et al. (Mar. 2008). "Social Contacts and Mixing Patterns Relevant to the Spread of Infectious Diseases." In: *PLOS Medicine* 5.3, pp. 1–1.

Mostafavi, Ehsan et al. (2013). "Temporal modeling of Crimean-Congo hemorrhagic fever in eastern Iran." In: *International Journal of Infectious Diseases* 17.7, e524 –e528.

Moulay, Djamila and Yoann Pigné (2013). "A metapopulation model for chikungunya including populations mobility on a large-scale network." In: *Journal of Theoretical Biology* 318, pp. 129 –139.

Mourya, Devendra T. et al. (2019). "Crimean Congo hemorrhagic fever serosurvey in humans for identifying high-risk populations and high-risk areas in the endemic state of Gujarat, India." In: *BMC Infectious Diseases* 19.1, p. 104.

Mpeshe, Saul C., Heikki Haario, and Jean M. Tchuenche (2011). "A Mathematical Model of Rift Valley Fever with Human Host." In: *Acta Biotheoretica* 59.3, pp. 231–250.

Mulatti, Paolo et al. (2014). "Determinants of the population growth of the West Nile virus mosquito vector Culex pipiens in a repeatedly affected area in Italy." In: *Parasites and Vectors* 7.1, p. 26.

Murray, James Dickson, E. A. Stanley, and D. L. Brown (1986). "On the spatial spread of rabies among foxes." In: *Proceedings of the Royal Society of London. Series B. Biological Sciences* 229.1255, pp. 111–150.

Murray, J.D. and W.L. Seward (1992). "On the spatial spread of rabies among foxes with immunity." In: *Journal of Theoretical Biology* 156.3, pp. 327 –348.

Myhre, E. A. and R. D. Akre (1994). "What Bit Me? Identifying Hawaii's Stinging and Biting Insects and Their Kin." In: *Journal of Medical Entomology* 31.3, p. 508.

Naderi, HamidReza et al. (2013). "Fatal Nosocomial Spread of Crimean-Congo Hemorrhagic Fever with Very Short Incubation Period." In: *The American Journal of Tropical Medicine and Hygiene* 88.3, pp. 469–471.

Nathan, Ran et al. (2008). "Mechanisms of long-distance seed dispersal." In: *Trends in Ecology & Evolution* 23.11, pp. 638 –647.

Newman, M. E. J. (2003). "The Structure and Function of Complex Networks." In: *SIAM Review* 45.2, pp. 167–256.

Newman, MEJ (2005). "Power laws, Pareto distributions and Zipf's law." In: *Contemporary Physics* 46.5, pp. 323–351.

Nguyen, Aileen, Joseph Mahaffy, and Naveen K. Vaidya (2019). "Modeling transmission dynamics of lyme disease: Multiple vectors, seasonality, and vector mobility." In: *Infectious Disease Modelling* 4, pp. 28 –43.

Noble, J. V. (1974). "Geographic and temporal development of plagues." In: *Nature* 250.5469, pp. 726–729.

Nogales, Manuel et al. (2012). "Evidence for overlooked mechanisms of long-distance seed dispersal to and between oceanic islands." In: *New Phytologist* 194.2, pp. 313–317.

Okely, Mohammed et al. (2019). "Mapping the environmental suitability of etiological agent and tick vectors of Crimean-Congo Hemorrhagic Fever." In: *Acta Tropica*, p. 105319.

Okuneye, Kamaldeen, Ahmed Abdelrazec, and Abba B. Gumel (2018). "Mathematical analysis of a weather-driven model for the population ecology of mosquitoes." In: *Mathematical Biosciences and Engineering* 15.1, pp. 57–93.

Papa, A. et al. (2002). "Crimean-Congo Hemorrhagic Fever in Albania, 2001." In: *European Journal of Clinical Microbiology and Infectious Diseases* 21.8, pp. 603–606.

Papa, Anna et al. (2017). "Crimean-Congo Hemorrhagic Fever: Tick-Host-Virus Interactions." In: *Frontiers in Cellular and Infection Microbiology* 7, p. 213.

Pastor-Satorras, Romualdo et al. (2015). "Epidemic processes in complex networks." In: *Rev. Mod. Phys.* 87, pp. 925–979.

Perez, Liliana and Suzana Dragicevic (2009). "An agent-based approach for modeling dynamics of contagious disease spread." In: *International Journal of Health Geographics* 8.1, p. 50.

Peterson, A. Townsend, David A. Vieglais, and James K. Andreasen (2003). "Migratory Birds Modeled as Critical Transport Agents for West Nile Virus in North America." In: *Vector-Borne and Zoonotic Diseases* 3.1, pp. 27–37.

"Plague in Ancient India" (Sept. 1899). In: *The Indian medical gazette* 34.9, pp. 347–347.

Polo, Gina, Marcelo B. Labruna, and Fernando Ferreira (2018). "Basic reproduction number for the Brazilian Spotted Fever." In: *Journal of Theoretical Biology* 458, pp. 119 –124.

Pshenichnaya, Natalia Yurievna and Svetlana Alexeevna Nenadskaya (2015). "Probable Crimean-Congo hemorrhagic fever virus transmission occurred after aerosol-generating medical procedures in Russia: nosocomial cluster." In: *International Journal of Infectious Diseases* 33, pp. 120–122.

Pshenichnaya, Natalia Yurievna et al. (2016). "Possible sexual transmission of Crimean-Congo hemorrhagic fever." In: *International Journal of Infectious Diseases* 45, pp. 109–111.

R Core Team (2018). R Foundation for Statistical Computing. Vienna, Austria.

Rappole, J H, S R Derrickson, and Z Hubálek (2000). "Migratory birds and spread of West Nile virus in the Western Hemisphere." In: *Emerging infectious diseases* 6.4, pp. 319–328.

Rappole, J.H. and Z. Hubálek (2003). "Migratory birds and West Nile virus." In: *Journal of Applied Microbiology* 94.s1, pp. 47–58.

Reed, Kurt D. et al. (2003a). "Birds, Migration and Emerging Zoonoses: West Nile Virus, Lyme Disease, Influenza A and Enteropathogens." In: *Clin Med Res* 1.1, pp. 5–12.

Reed, Kurt D et al. (Jan. 2003b). "Birds, migration and emerging zoonoses: west nile virus, lyme disease, influenza A and enteropathogens." In: *Clinical medicine & research* 1.1, pp. 5–12.

Reisen, William K., Ying Fang, and Vincent M. Martinez (2006). "Effects of Temperature on the Transmission of West Nile Virus by Culex tarsalis (Diptera: Culicidae)." In: *Journal of Medical Entomology* 43.2, pp. 309–317.

Reisen, William K. et al. (2006). "Overwintering of West Nile Virus in Southern California." In: *Journal of Medical Entomology* 43.2, pp. 344–355.

Riley, Steven et al. (Mar. 2015). "Five challenges for spatial epidemic models." In: *Epidemics* 10, pp. 68–71.

Rinaldo, Andrea et al. (2012). "Reassessment of the 2010–2011 Haiti cholera outbreak and rainfall-driven multiseason projections." In: *Proceedings of the National Academy of Sciences* 109.17, pp. 6602–6607.

Roberts, D. C. and D. L. Turcotte (1998). "Fractality and Self-Organized Criticality of Wars." In: *Fractals* 06.04, pp. 351–357.

Rogers, D.J. and S.E. Randolph (2006). "Climate Change and Vector-Borne Diseases." In: *Global Mapping of Infectious Diseases: Methods, Examples and Emerging Applications*. Ed. by Simon I. Hay, Alastair Graham, and David J. Rogers. Vol. 62. Advances in Parasitology. Academic Press, pp. 345 –381.

Rolle, M and A Mayr (May 2006). *Medizinische Mikrobiologie, Infektions- und Seuchenlehre*. 8. Enke, Stuttgart.

Rosà, Roberto and Andrea Pugliese (2007). "Effects of tick population dynamics and host densities on the persistence of tick-borne infections." In: *Mathematical Biosciences* 208.1, pp. 216 –240.

Ross, R. (1911). "The Prevention of Malaria." In: London: John Murray, London.

Ruan, Shigui and Wendi Wang (2003). "Dynamical behavior of an epidemic model with a nonlinear incidence rate." In: *Journal of Differential Equations* 188.1, pp. 135 –163.

Rubel, Franz et al. (2008). "Explaining Usutu virus dynamics in Austria: Model development and calibration." In: *Preventive Veterinary Medicine* 85.3, pp. 166 –186.

Rudolf, Ivo et al. (2017). "West Nile virus in overwintering mosquitoes, central Europe." In: *Parasites and Vectors* 10.1, p. 452.

Sas, Miriam A. et al. (2018). "A one-step multiplex real-time RT-PCR for the universal detection of all currently known CCHFV genotypes." In: *Journal of Virological Methods* 255, pp. 38 –43.

Schröder, Roland and Detlef Klöß (2004). "Einsatz von GIS-Technologien im Tierseuchennachrichtensystem." In: *GIL Jahrestagung*.

Schuster, Isolde et al. (2016). "Sheep and goats as indicator animals for the circulation of CCHFV in the environment." In: *Experimental and Applied Acarology* 68.3, pp. 337–346.

Semenza, Jan C. and Jonathan E. Suk (2018). "Vector-borne diseases and climate change: a European perspective." In: *FEMS Microbiol Lett* 365.2, fnx244.

Serfling, Robert E. (1952). "Historical Review of Epidemic Theory." In: *Human Biology* 24.3, pp. 145–166.

Shapiro, Lillian L. M., Shelley A. Whitehead, and Matthew B. Thomas (Oct. 2017). "Quantifying the effects of temperature on mosquito and parasite traits that determine the transmission potential of human malaria." In: *PLOS Biology* 15.10, pp. 1–21.

Shayan, Sara et al. (Aug. 2015). "Crimean-Congo Hemorrhagic Fever." In: *Laboratory Medicine* 46.3, pp. 180–189.

Shuai, Zhisheng, J. A. P. Heesterbeek, and P. van den Driessche (2013). "Extending the type reproduction number to infectious disease control targeting contacts between types." In: *Journal of Mathematical Biology* 67.5, pp. 1067–1082.

Siraj, Amir S. et al. (July 2017). "Temperature modulates dengue virus epidemic growth rates through its effects on reproduction numbers and generation intervals." In: *PLOS Neglected Tropical Diseases* 11.7, pp. 1–19.

Solla Price, Derek J. de (1965). "Networks of Scientific Papers." In: *Science* 149.3683, pp. 510–515.

Spanoudis, Christos G et al. (Dec. 2018). "Effect of Temperature on Biological Parameters of the West Nile Virus Vector Culex pipiens form ?molestus? (Diptera: Culicidae) in Greece: Constant vs Fluctuating Temperatures." In: *Journal of Medical Entomology* 56.3, pp. 641–650.

Spengler, Jessica R. and Agustin Estrada-Peña (Feb. 2018). "Host preferences support the prominent role of Hyalomma ticks in the ecology of Crimean-Congo hemorrhagic fever." In: *PLOS Neglected Tropical Diseases* 12.2, pp. 1–17.

Spielman, Andrew (2001). "Structure and Seasonality of Nearctic Culex pipiens Populations." In: *Annals of the New York Academy of Sciences* 951.1, pp. 220–234.

Stubben, Chris J. and Brook G. Milligan (2007). "Estimating and Analyzing Demographic Models Using the popbio Package in R." In: *Journal of Statistical Software* 22.11.

Swetnam, Daniele et al. (2018). "Terrestrial Bird Migration and West Nile Virus Circulation, United States." In: 24.12, p. 2184.

Switkes, J. et al. (2016). "A mathematical model for Crimean-Congo haemorrhagic fever: tick-borne dynamics with conferred host immunity." In: *Journal of Biological Dynamics* 10.1, pp. 59–70.

Team, Core Writing, R.K. Pachauri, and L.A. Meyer(eds.) (2014). *IPCC, 2014: Climate Change 2014 Synthesis Report. Contribution of Working*

Groups I, II and III to the Fifth Assessment Report of the Intergovernmental Panel on Climate Change. Climate Change 2014 Synthesis Report, Fifth Assessment Report 151 pp. Geneva, Switzerland: IPCC.

Thieme, H. R. (1977). "A model for the spatial spread of an epidemic." In: *Journal of Mathematical Biology* 4.4, pp. 337–351.

Tien, Joseph H. and David J. D. Earn (2010). "Multiple Transmission Pathways and Disease Dynamics in a Waterborne Pathogen Model." In: *Bulletin of Mathematical Biology* 72.6, pp. 1506–1533.

Tillett, H. E. (1992). "Infectious Diseases of Humans: Dynamics and Control. R. M. Anderson, R. M. May, Pp. 757. Oxford University Press; 1991." In: *Epidemiology and Infection* 108.1, pp. 211–211.

Tuite, Ashleigh et al. (2011). "Cholera Epidemic in Haiti, 2010: Using a Transmission Model to Explain Spatial Spread of Disease and Identify Optimal Control Interventions." In: *Annals of Internal Medicine* 154.9, pp. 593–601.

VanderWaal, Kimberly L. and Vanessa O. Ezenwa (2016). "Heterogeneity in pathogen transmission: mechanisms and methodology." In: *Functional Ecology* 30.10, pp. 1606–1622.

Verdonschot, Piet F.M. and Anna A. Besse-Lototskaya (2014). "Flight distance of mosquitoes (Culicidae): A metadata analysis to support the management of barrier zones around rewetted and newly constructed wetlands." In: *Limnologica* 45, pp. 69 –79.

Veronesi, Eva et al. (2018). "Experimental evaluation of infection, dissemination, and transmission rates for two West Nile virus strains in European Aedes japonicus under a fluctuating temperature regime." In: *Parasitol Res* 117.6, pp. 1925–1932.

Viboud, Cécile et al. (2006). "Synchrony, Waves, and Spatial Hierarchies in the Spread of Influenza." In: *Science* 312.5772, pp. 447–451.

Vinogradova, EB (2000). *Culex Pipiens Pipiens Mosquitoes: Taxonomy, Distribution, Ecology, Physiology, Genetics, Applied Importance and Control*. Pensoft Series Parasitologica, no. 2. ISBN 978-9546421036. Sofia : Pensoft, 2000.

Voitalov, Ivan et al. (Oct. 2019). "Scale-free networks well done." In: *Physical Review Research* 1.3, pp. 033034–.

Volz, Erik and Lauren Ancel Meyers (2009). "Epidemic thresholds in dynamic contact networks." In: *Journal of The Royal Society Interface* 6.32, pp. 233–241.

Vorou, R.M. (2009). "Crimean-Congo hemorrhagic fever in southeastern Europe." In: *International Journal of Infectious Diseases* 13.6, pp. 659 –662.

Wallace, John R. (2008). "Mosquito Overwintering Ecology." In: *Encyclopedia of Entomology*. Ed. by John L. Capinera. Dordrecht: Springer Netherlands, pp. 2470–2472.

Walt, Stéfan van der et al. (June 2014). "scikit-image: image processing in Python." In: *PeerJ* 2, e453.

Wang, Feng-Bin, Ruiwen Wu, and Xiao-Qiang Zhao (2019). "A West Nile Virus Transmission Model with Periodic Incubation Periods." In: *SIAM Journal on Applied Dynamical Systems* 18.3, pp. 1498–1535.

Wang, Xiunan and Xiao-Qiang Zhao (2017). "A Malaria Transmission Model with Temperature-Dependent Incubation Period." In: *Bulletin of Mathematical Biology* 79.5, pp. 1155–1182.

Wasserman, Stanley and Katherine Faust (1994). *Social Network Analysis: Methods and Applications*. Structural Analysis in the Social Sciences. Cambridge University Press.

Watts, Duncan J. et al. (2005). "Multiscale, resurgent epidemics in a hierarchical metapopulation model." In: *Proceedings of the National Academy of Sciences* 102.32, pp. 11157–11162.

White, Lauren A., James D. Forester, and Meggan E. Craft (2018). "Disease outbreak thresholds emerge from interactions between movement behavior, landscape structure, and epidemiology." In: *Proceedings of the National Academy of Sciences* 115.28, pp. 7374–7379.

Wikel, Stephen K. (2018). "Ticks and Tick-Borne Infections: Complex Ecology, Agents, and Host Interactions." In: *Veterinary Sciences* 5.2.

Wonham, Marjorie J., Tomás De-Camino-Beck, and Mark A. Lewis (2004). "An epidemiological model for West Nile virus: invasion analysis and control applications." In: *Proceedings of the Royal Society of London B: Biological Sciences* 271.1538, pp. 501–507.

Yadav, Pragya D. et al. (2016). "Nosocomial infection of CCHF among health care workers in Rajasthan, India." In: *BMC Infectious Diseases* 16.1, p. 624.

Yilmaz, Gul Ruhsar et al. (2009). "The epidemiology of Crimean-Congo hemorrhagic fever in Turkey, 2002–2007." In: *International Journal of Infectious Diseases* 13.3, pp. 380–386.

Yu, Don, Neal Madras, and Huaiping Zhu (2018). "Temperature-driven population abundance model for Culex pipiens and Culex restuans (Diptera: Culicidae)." In: *Journal of Theoretical Biology* 443, pp. 28 –38.

Zeller, H. G. and I. Schuffenecker (2004). "West Nile Virus: An Overview of Its Spread in Europe and the Mediterranean Basin in Contrast to Its Spread in the Americas." In: *European Journal of Clinical Microbiology and Infectious Diseases* 23.3, pp. 147–156.

Zhang, Yanfang et al. (2018). "Isolation, Characterization, and Phylogenetic Analysis of Two New Crimean-Congo Hemorrhagic Fever Virus Strains from the Northern Region of Xinjiang Province, China." In: *Virologica Sinica* 33.1, pp. 74–86.

Zhou Wang et al. (2004). "Image quality assessment: from error visibility to structural similarity." In: *IEEE Transactions on Image Processing* 13.4, pp. 600–612.

Zi, Z. (2011). "Sensitivity analysis approaches applied to systems biology models." In: *IET Systems Biology* 5.6, pp. 336–346.

Zias, Joseph (1991). "Current Archaeological Research in Israel: Death and Disease in Ancient Israel." In: *The Biblical Archaeologist* 54.3, pp. 147–159.

Ziegler, Ute et al. (2019). "West Nile virus epizootic in Germany, 2018." In: *Antiviral Research* 162, pp. 39 –43.

Ziegler, Ute et al. (Apr. 2020). "West Nile Virus Epidemic in Germany Triggered by Epizootic Emergence, 2019." In: *Viruses* 12.4, p. 448.

Zipf, George K. (1950). "Human behavior and the principle of least effort." In: *Journal of Clinical Psychology* 6.3, pp. 306–306.